

Efficient sparsity adaptive changepoint estimation

Per August Jarval Moen¹

Ingrid Kristine Glad¹

Martin Tveten²

¹Department of Mathematics, University of Oslo

²Norwegian Computing Center

Abstract

We propose a computationally efficient and sparsity adaptive procedure for estimating changes in unknown subsets of a high-dimensional data sequence. Assuming the data sequence is Gaussian, we prove that the new method successfully estimates the number and locations of changepoints with a given error rate and under minimal conditions, for all sparsities of the changing subset. Our method has computational complexity linear up to logarithmic factors in both the length and number of time series, making it applicable to large data sets. Through extensive numerical studies we show that the new methodology is highly competitive in terms of both estimation accuracy and computational cost. The practical usefulness of the method is illustrated by analysing sensor data from a hydro power plant, and an efficient R implementation is available.

1 Introduction

During the last decades, new technology has made it possible to gather data in larger quantities from an ever wider range of sources. Data can often display non-stationarities in the form of distributional changes over time, leading to incorrect statistical inferences if not accounted for. Inference on changepoints may also be of interest in itself. For instance, Cunen et al. (2020) search for changes in the number of battle deaths in interstate wars between 1816 and 2007, Gao et al. (2020) study monitoring of the temperature of transplant organs, and Tveten et al. (2022) use a changepoint detection algorithm for condition monitoring of a subsea pump.

In this paper, we study the problem of detection and estimation of an unknown number of changes in the mean of high-dimensional data. By *detection*, we refer to testing for the presence of one or more changepoints in the data. By *estimation*, we refer to estimation of the location(s) of the changepoint(s). This problem is well understood in the literature for univariate data. Several computationally efficient algorithms have been proposed during the last decade, including Pruned Exact Linear Time of Killick et al. (2012), Wild Binary Segmentation of Fryzlewicz (2014), Narrowest Over Threshold of Baranowski et al. (2019) and Seeded Binary Segmentation of Kovács et al. (2022). Notably, these methods have been shown to achieve near optimal performance, in a minimax sense, see Wang et al. (2020).

Several methods for the multivariate change in mean problem have also been proposed, although this problem is less studied than the univariate setting. The Inspect method of Wang and Samworth (2018) uses sparse projections of CUSUM statistics and a variant of Wild Binary Segmentation to detect and localize multiple sparse changes in the mean. Cho and Fryzlewicz (2015) propose the Sparsified Binary Segmentation algorithm based on thresholding and aggregating CUSUM statistics over coordinates, in combination with Binary Segmentation. The Double CUSUM method of Cho (2016) uses test statistics based on ordered CUSUMs, in combination with ordinary Binary Segmentation. The SUBSET method

of Tickle et al. (2021) uses a penalized likelihood approach, in combination with the Wild Binary Segmentation search procedure.

In this work, we present a novel multiple changepoint estimation algorithm, which we call ESAC (Efficient Sparsity Adaptive Changepoint estimator). The method is designed to detect and estimate the locations of an unknown number of changes in the mean of high-dimensional data sequences. An important feature of ESAC is that the subset of data components that undergo a change need not be known — it can be anything from a single changing component to a small subset to all components. We refer to the size of the changing subset as the *sparsity* of the change. ESAC comes with strong theoretical guarantees, and is in particular adaptive to all sparsities of changes and all distances between changepoints. Still, the worst-case computational cost of ESAC is linear in the number of observations, n , as well as the number of components, p , save for logarithmic factors. Via simulations, we demonstrate that ESAC is highly competitive in terms of statistical accuracy and running time.

The novelty of our work is threefold. Our first contribution is to modify a sparsity adaptive test statistic proposed by Liu et al. (2021) to make it suitable for testing for changepoints in a multiple changepoint setup. In particular, our proposed test facilitates control over its family-wise error rate, which is necessary in the multiple changepoint situation. Our second contribution is to propose a novel estimator for the location of a single changepoint. The estimator comes with strong theoretical guarantees, and may be of independent interest. Lastly and most importantly, we combine our proposed test statistic and changepoint estimator into a multiple changepoint estimation algorithm, ESAC, using a slight variant of Seeded Binary Segmentation (Kovács et al., 2022) and Narrowest-over-Threshold (Baranowski et al., 2019) selection of changepoints. ESAC is also efficiently implemented in an R package **HDCD** (Moen, 2023), available on The Comprehensive R Archive Network (cran.r-project.org). Efficient implementations of Inspect Wang and Samworth (2018) and the method of Pilliat et al. (2023) are also available in the package.

Most similar to ESAC is the multiple changepoint detection procedure of Pilliat et al. (2023) for Gaussian changes in mean. The theoretical guarantees, for instance, are the same for ESAC and the method of Pilliat et al. (2023). Still, there are important distinctions between the two methods, which we highlight here. As opposed to ESAC, the method proposed by Pilliat et al. (2023) is based on their novel "bottom up" search. Their approach segments the data into disjoint segments chosen as narrow as possible from a predefined grid, where for each interval, a test statistic must have detected a changepoint. To ensure a disjoint segmentation, they merge overlapping segments of equal length whenever a changepoint is detected in both. From this segmentation, changepoint locations are estimated by taking midpoints of the segments. Consequently, Pilliat et al.'s method only requires a test for a changepoint, and not a location estimator. In practice, this generality comes at a cost of changepoints being crudely estimated or not being detected at all, whenever the signal strength is low. This is illustrated in our simulation studies, which feature empirical comparisons between ESAC, the method of Pilliat et al. (2023) and other proposed methods.

The paper is organized as follows. In Section 2 we give a formal description of the model assumed throughout the paper. In Section 3.1 we present a test statistic for a single changepoint that facilitates control over its family-wise error rate. In Section 3.2 we propose an estimator for the location of a single changepoint, also stating its finite sample estimation error rate with comparisons to other methods. In Section 3.3 we propose ESAC, our proposed multiple changepoint estimation procedure. In Section 3.4 we present theoretical results regarding the statistical and computational properties of ESAC and compare these to other methods. In Section 4 we study the empirical performance of ESAC and other methods via simulations, including for misspecified models. In Section 5 we apply ESAC to sensor data from a Swedish hydro power plant. In Appendix A we prove our main theoretical results. In the remainder of the Appendix we discuss implementation of ESAC in practice, provide more simulation

results, and prove auxiliary lemmas for our main results.

We use the following notation throughout the paper. For any vector $y \in \mathbb{R}^d$ we let y_j denote its j -th component, $\|y\|_2$ denote its Euclidean norm and $\|y\|_0$ denote the number of non-zero entries in y . For any matrix $X \in \mathbb{R}^{p \times n}$ we let $X_{i,v}$ denote its (i, v) th element, $X_v \in \mathbb{R}^p$ denote its v th column, $X_{i,\cdot} \in \mathbb{R}^n$ denote its i th row, $\|X\|_F^2 = \sum_{i=1}^p \sum_{v=1}^n X_{i,v}^2$ denote the squared Frobenius norm of X , and $\|X\|_1 = \sum_{i=1}^p \sum_{v=1}^n |X_{i,v}|$ denote the entry-wise ℓ_1 norm of X . For any pair of matrices $X, Y \in \mathbb{R}^{p \times n}$, we let $\langle X, Y \rangle = \text{tr}(X^T Y)$ denote their trace inner product. For any positive integer I we define $[I] = \{1, \dots, I\}$. For any pair of real numbers x, y , we define $x \vee y = \max\{x, y\}$ and $x \wedge y = \min\{x, y\}$. For any pair of random variables X, Y , we let $X \leq_{\text{st}} Y$ mean that Y stochastically dominates X , i.e. $\mathbb{P}(X \leq t) \geq \mathbb{P}(Y \leq t)$ for all $t \in \mathbb{R}$. For any $x \in \mathbb{R}$, we let $\lfloor x \rfloor$ denote the largest integer no larger than x , and $\lceil x \rceil$ denote the smallest integer no smaller than x .

We find it useful to adopt the notation of Baranowski et al. (2019) to denote integer intervals. For any pair of integers s, e such that $s \leq e - 2$, we let (s, e) denote the open integer interval $\{s + 1, \dots, e - 1\}$ and let $(s, e]$ denote the left-open and right closed integer interval $\{s + 1, \dots, e\}$.

2 Problem description

To motivate our method and allow for theoretical analysis, we consider the following model for the remainder of the paper. In Section 4 we assess performance under various misspecified models. Suppose we observe $n \geq 2$ independent multivariate Gaussian variables

$$X_v = \mu_v + W_v, \tag{1}$$

where $\mu_v \in \mathbb{R}^p$ and $W_v \sim N_p(0, \sigma^2 I)$ for $v \in [n]$. Assume that there are $J \geq 0$ changepoints $0 < \eta_1 < \dots < \eta_J < n$ such that

$$\mu_v \neq \mu_{v+1} \text{ if and only if } v = \eta_j \text{ for some } j \in [J].$$

Let $\theta_j = \mu_{\eta_{j+1}} - \mu_{\eta_j}$ denote the change in mean occurring at the j th changepoint, and let $\varphi_j = \|\theta_j\|_2$ be the ℓ_2 -norm of the mean-change occurring at changepoint j . Further, let $k_j = \|\theta_j\|_0$ denote the *sparsity* of the j th changepoint, i.e. the number of non-zero components of θ_j . Lastly, let $\Delta_j = \min(\eta_j - \eta_{j-1}, \eta_{j+1} - \eta_j)$ denote the minimum distance between the j th changepoint and a neighboring changepoint (where we for convenience take $\eta_0 = 0$ and $\eta_{J+1} = n$). Our goal is to estimate J , the number of changepoints, and their locations $\eta_1 < \dots < \eta_J$.

In the theoretical analysis to follow, we take σ^2 to be known. For notational compactness, let $X, \mu \in \mathbb{R}^{p \times n}$ denote the matrices with X_v, μ_v as their v th columns, respectively, for $v \in [n]$.

3 Method and results

3.1 Single changepoint detection with family-wise error rate control

We begin by presenting a statistical test for a single change in mean in some arbitrary interval $(s, e) = \{s + 1, \dots, e - 1\}$, where $0 \leq s < e \leq n$, and $s \leq e - 2$. To simplify the exposition, assume for now that $\sigma = 1$, as the data can be normalized to satisfy this assumption. We seek a test statistic which facilitates control over the family-wise error rate when testing for changepoints over multiple intervals. This level of control is needed later on when we define a multiple changepoint algorithm in Section 3.3.

To construct a test statistic, we build upon the work of Liu et al. (2021). They propose an efficient and minimax rate optimal test statistic for testing for a single changepoint within an interval. Unfortunately,

this test does not allow for control of the family-wise error rate, and thus needs some modifications, presented next. For any candidate changepoint location v such that $0 \leq s < v < e \leq n$, we define the CUSUM transformation $T_{(s,e]}^v(y)$ of a vector $y \in \mathbb{R}^n$ as

$$T_{(s,e]}^v(y) = \left\{ \frac{e-v}{(e-s)(v-s)} \right\}^{1/2} \sum_{i=s+1}^v y_i - \left\{ \frac{v-s}{(e-s)(e-v)} \right\}^{1/2} \sum_{i=v+1}^e y_i, \quad (2)$$

To simplify notation, we use $C_{(s,e]}^v(i) = T_{(s,e]}^v(X_{i,\cdot})$ to denote the CUSUM of the i th component of the data within the integer interval $(s, e]$, evaluated at candidate changepoint position v .

Given a candidate sparsity level $t \in [p]$, and penalizing function $\gamma(t)$, both to be discussed later, define

$$S_{\gamma,(s,e]}^v(t) = \sum_{i=1}^p \left\{ C_{(s,e]}^v(i)^2 - \nu_{a(t)} \right\} \mathbb{1} \left\{ |C_{(s,e]}^v(i)| \geq a(t) \right\} - \gamma(t), \quad (3)$$

where the threshold value $a(t)$ is given by

$$a^2(t) = 4 \log \left(\frac{ep \log n}{t^2} \right) \mathbb{1} \left\{ t \leq (p \log n)^{1/2} \right\}, \quad (4)$$

and $\nu_{a(t)}$ is a mean-centering term defined by taking $\nu_a = \mathbb{E} (Z^2 \mid |Z| \geq a)$ for $Z \sim N(0, 1)$ and $a \geq 0$. In (4) we abuse notation slightly, writing $e = \exp(1)$ to mean Euler's number.

We refer to $S_{\gamma,(s,e]}^v(t)$ as a *sparsity-specific penalized score*, which heuristically measures the degree of evidence of a changepoint at $v \in (s, e)$ with sparsity t . To see this, we note that the CUSUM is a well known test statistic for a univariate change in mean, rejecting the null hypothesis of a constant mean for large values (see Wang et al., 2020). In the multivariate case, the statistic (3) aggregates CUSUM values in an effort to borrow information across coordinates. To prevent the noise drowning the signal, the CUSUMs are thresholded at level $a(t)$, tailored specifically for a given sparsity level t . The functional form of $a(t)$ is depicted in Figure 1, where one observes that $a(t)$ decreases with t . Hence, $S_{\gamma,(s,e]}^v(t)$ thresholds CUSUMs less harshly as t grows. More intuition on $a(t)$ is discussed in the end of this subsection. Also plotted in Figure 1 is $\nu_{a(t)}$, which serves as a mean-centering term for spuriously large CUSUMs, and satisfies $a^2(t) \leq \nu_{a(t)} \leq a^2(t) + 2$. Even after thresholding and mean-centering, however, the sum in (3) need not be small even when no changepoint is present. The role of the penalty function $\gamma(t)$ is therefore to ensure that $S_{\gamma,(s,e]}^v < 0$ with high probability whenever no changepoint is present.

The sparsity-specific penalized score $S_{\gamma,(s,e]}^v(t)$ is defined for a fixed sparsity t , while the true sparsity of a changepoint is taken to be unknown. To measure the overall degree of evidence of a changepoint at location v , we consider an exponentially increasing grid of candidate sparsity levels

$$\mathcal{T} = \{1, 2, 4, \dots, 2^{\lfloor \log_2 \lfloor \sqrt{p \log n} \rfloor \rfloor}\} \cup \{p\}. \quad (5)$$

This approach is also taken by Liu et al. (2021), where the grid \mathcal{T} is slightly smaller. This choice of grid is justified as follows. Whenever a changepoint has true sparsity $k < (p \log n)^{1/2}$, there always exists some $t \in \mathcal{T}$ such that $t/2 \leq k \leq t$, which turns out to be sufficient for detecting the changepoint. Conversely, when the true sparsity k satisfies $k \geq (p \log n)^{1/2}$, it is sufficient to consider $t = p$.

For a candidate changepoint position $s < v < e$, define the *penalized score* $S_{\gamma,(s,e]}^v$ as

$$S_{\gamma,(s,e]}^v = \max_{t \in \mathcal{T}} S_{\gamma,(s,e]}^v(t), \quad (6)$$

which heuristically measures the degree of evidence of a changepoint at location v , irregardless of the sparsity. As test statistic for a changepoint in the interval (s, e) , we take

$$S_{\gamma, (s, e]} = \mathbb{1} \left\{ \max_{s < v < e} S_{\gamma, (s, e]}^v > 0 \right\}. \quad (7)$$

As for the penalty function $\gamma(t)$, for $t \in [p]$ define

$$r(t) = r(t, n, p) = \begin{cases} (p \log n)^{1/2} & \text{if } t \geq (p \log n)^{1/2}, \\ t \log \left(\frac{ep \log n}{t^2} \right) \vee \log n & \text{otherwise.} \end{cases} \quad (8)$$

With penalty function $\gamma(t) = \gamma_0 r(t)$ for some suitably large constant $\gamma_0 > 0$, we obtain the following control over the family-wise error rate.

Proposition 3.1. *Consider the model in Section 2. For all s, e and v such that $0 \leq s < v < e \leq n$, assume that the quantity $S_{\gamma, (s, e]}$ is computed with variance-scaled input matrix $\tilde{X} = (1/\sigma)X$ and penalty function $\gamma(t) = \gamma_0 r(t)$ for some $\gamma_0 > 0$. Let I denote the set of all intervals $(s, e) \subseteq (0, n)$ containing no changepoint, i.e. satisfying $\eta_j \notin (s, e) \forall j \in [J]$. For any $\varepsilon > 0$, there exists a universal choice of $\gamma_0 > 0$ (depending only on ε) such that*

$$\mathbb{P} \left(\max_{(s, e) \in I} S_{\gamma, (s, e]} > 0 \right) \leq \varepsilon.$$

Some remarks are in order. Figure 1 displays plots of $a^2(t)$, $\nu_{a(t)}$ and $r(t)$ as functions of t , for $n = p = 500$. As our first remark, we observe that $a(t)$ and $\nu_{a(t)}$ are decreasing in t , while $r(t)$ is increasing for all $t \leq (p \log(n)/e)^{1/2}$, but with a bulk when t is close to $(p \log n)^{1/2}$. Several equivalent monotonic functions can be chosen in the place of $r(t)$, but we have chosen $r(t)$ due to its simple analytical form. The function $r(t)$ can be seen as the information theoretic detection boundary in terms of the signal-to-noise (SNR) ratio for multiple changes in mean of sparsity t in p -dimensional Gaussian vectors with sample size n (see Section 3.4 or Pilliat et al. 2023). When $p = 1$, we recover the standard penalty used in the univariate changepoint literature for Gaussian changes in mean (see e.g. Wang et al. 2020), as $r(1) = \log n$ in this case. As our second remark, the forms of the threshold $a(t)$ and penalty function $\gamma(t) \propto r(t)$ reflect the two sparsity regimes known in the statistical literature on multivariate mean change detection. In the sparse case where $t \leq (p \log n)^{1/2}$, the threshold $a(t)$ is non-zero and satisfies $a^2(t) \approx r(t)/t$, which is decreasing with t . Meanwhile, in the dense case where $t > (p \log n)^{1/2}$, the threshold satisfies $a(t) = 0$, in which case no thresholding takes place and all CUSUMs contribute to (3).

Lastly, we remark the following relation between our proposed test statistic and that of Liu et al. (2021). To facilitate control over the family-wise error rate, the threshold $a(t)$, the mean-centering term $\nu_{a(t)}$, and the penalty function $\gamma(t) = \gamma_0 r(t)$ grow faster with n than their equivalent counterparts in Liu et al. (2021). To recover the test statistic from Liu et al. (2021), one must replace $\log n$ by $\log \log(8n)$ in (3), (4), (5), (6), (7) and (8) and use the penalty function $\gamma(t) = \gamma_0 r(t)$ with the modified function $r(t)$.

3.2 Single changepoint estimation

We now consider the problem of estimating the location of a changepoint within some interval (s, e) , assuming the changepoint has already been detected or is known to be present. As before, we assume $\sigma = 1$, as the data can be normalized to satisfy this assumption. We further assume that the interval (s, e) contains only a single changepoint. Recalling the model defined in Section 1, this means that $J = 1$

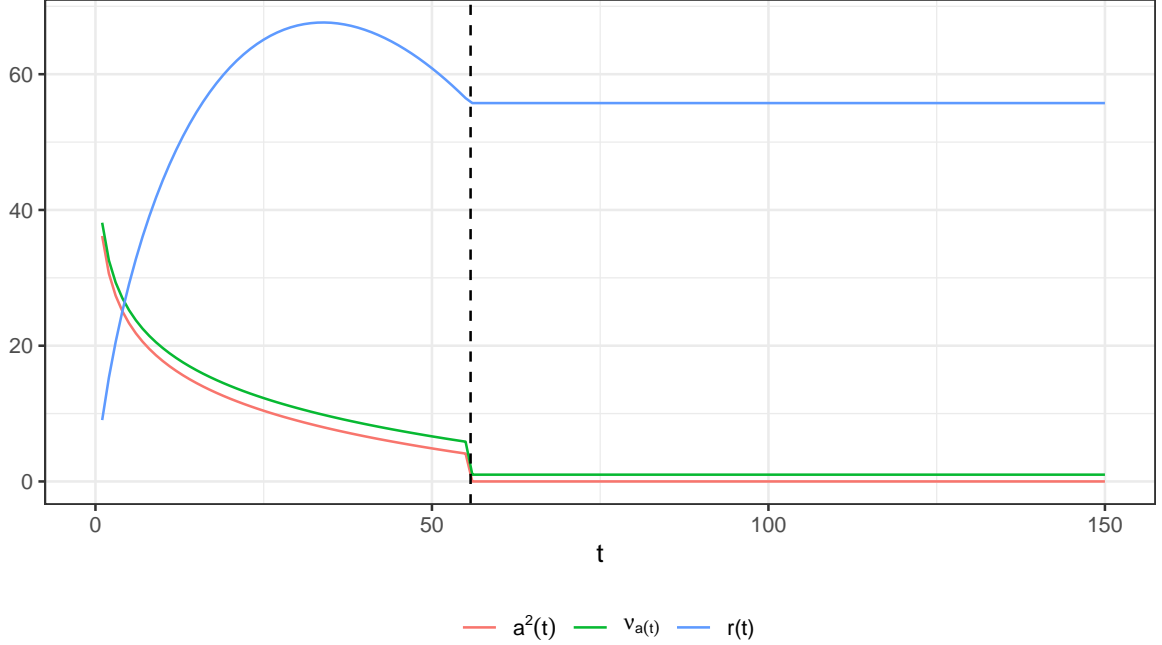


Figure 1: Plots of $a^2(t)$ (red), $\nu_{a(t)}$ (green), and $r(t)$ (red) for $n = p = 500$. The boundary between the dense and sparse regimes is given by a vertical dashed line at $k = (p \log n)^{1/2}$.

and $[s, e) = [0, n)$. The problem at hand is then to estimate the location $\eta = \eta_1$ of a single changepoint, taking the sparsity $k = k_1$ as unknown. As our estimator for η , we use the test statistic in (6) with a potentially separate penalty function $\lambda(t)$, and maximize it over all candidate changepoints. That is,

$$\hat{\eta}_\lambda = \arg \max_{0 < v < n} S_\lambda^v, \quad (9)$$

where we write S_λ^v shorthand for $S_{\lambda, (0, n]}^v$. The rationale behind this estimator is that $S^v(\lambda)$ measures the degree of evidence of a changepoint at location v . The maximizer is unique with high probability whenever the signal strength is reasonably large. Still, to ensure that $\hat{\eta}_\lambda$ is always well defined, we formally set $\hat{\eta}_\lambda$ be the smallest maximizer, although we suppress this from the notation.

The finite sample properties of $\hat{\eta}_\lambda$ are given in Theorem 3.2, which holds whenever $\lambda(t) = \lambda_0 r(t)$ for sufficiently large $\lambda_0 > 0$. Before stating the theorem, some remarks are in order. The threshold $a(t)$ is as before decreasing in t , while a penalty function of the form $\lambda(t) = \lambda_0 r(t)$ is increasing for most values of t . For such $\lambda(t)$, the penalized score S_λ^v involves an implicit model selection in terms of the sparsity. An inspection of the proof of Theorem 3.2 reveals the following intuition about the roles of $\lambda(t)$ and $a(t)$; whenever λ_0 is sufficiently large, the penalty function $\lambda(t) = \lambda_0 r(t)$ cancels all contributions to the sum in (3) from coordinates where there is no signal. Left are the contributions from the affected coordinates. For a changepoint with a moderate signal strength, these remaining contributions are maximized when t is close to the true sparsity k . To see this, note that when t is smaller than the true sparsity k , the thresholding is too strict, possibly cancelling the signal from the affected coordinates, either from the thresholding itself or from the mean-centering term. When t is greater k , the thresholding is less strict, but the penalty function $\lambda(t)$ may be larger than the signal strength from the affected coordinates.

The following finite sample result shows that the estimator $\hat{\eta}_\lambda$ is adaptive to the (unknown) sparsity and gives a high-probability upper bound on the estimation error.

Theorem 3.2. Consider the model in Section 2, with only one changepoint η , with sparsity k and ℓ_2 norm φ . Let $\Delta = \min(\eta, n - \eta)$. Let $\hat{\eta}_\lambda$ be as in (9), when the sparsity-specific score function $S_\lambda^v(t) = S_{\lambda, (0, n]}^v$ from (3) is computed with variance-scaled input matrix $\tilde{X} = (1/\sigma)X$ and penalty function $\lambda(t) = \lambda_0 r(t)$, where $\lambda_0 > 0$. Define

$$h(t) = h(t, n, p) = \begin{cases} [p \{\log n \vee \log \log(ep)\}]^{1/2} & \text{if } t \geq (p \log n)^{1/2}, \\ t \log\left(\frac{ep \log n}{t^2}\right) \vee \log n & \text{otherwise.} \end{cases} \quad (10)$$

There exist a universal choice of $\lambda_0 > 0$ and universal constants $C_0, C_1 > 0$ such that, if

$$\frac{\varphi^2 \Delta}{\sigma^2} \geq C_0 h(k), \quad (11)$$

we have that

$$\mathbb{P} \left\{ |\hat{\eta}_\lambda - \eta| \leq C_1 \frac{\sigma^2}{\varphi^2} h(k) \right\} \geq 1 - \frac{1}{n}.$$

The SNR requirement (11) implies that the absolute estimation error of $\hat{\eta}_\lambda$ satisfies $C_1 h(k) \sigma^2 / \varphi^2 \leq C_0 / C_1 \Delta < \Delta$ whenever the conditions of the Theorem holds. In particular, in an asymptotic regime where k, p, Δ and φ vary with n , the quantity $|\hat{\eta}_\lambda - \eta| / \Delta$ converges in probability to 0 as $n \rightarrow \infty$ whenever $(\varphi^2 \Delta) / \{\sigma^2 h(k)\}$ diverges with n . Similarly, if $\varphi^2 / \{\sigma^2 h(k)\}$ diverges with n , then $\hat{\eta}_\lambda$ converges in probability to η as $n \rightarrow \infty$. Note that Theorem 3.2 requires that the penalty function $\lambda(t)$ has a specific functional form. For practical choices of the penalty function $\lambda(t)$, we refer to Appendix B.

Some performance comparisons with related methods are in order. In comparison with Theorem 3.2, the SNR condition for the Inspect method (Wang and Samworth, 2018) in the single changepoint case is of the form $\varphi^2 \Delta / \sigma^2 \geq C v(k, n, p, \Delta)$ for some $C > 0$, where $v(k, n, p, \Delta) = (n/\Delta) k \log(p \log n)$. Ignoring constants, we see that the SNR condition of ESAC is weaker than that of Inspect whenever $k \geq \log n$ and for all values of k whenever $p \geq n / \log n$. Note also that $v(k, n, p, \Delta)$ consists of the factor n/Δ , which is not the case for ESAC. Once the SNR condition for Inspect is satisfied, its error rate is of order $(\sigma^2 / \varphi^2) \log \log n$, which is smaller than that of ESAC, and especially so whenever k is large. For the Double CUSUM algorithm of Cho (2016, Section 4) in the single changepoint case where $\sigma = 1$, the asymptotic SNR requirement for consistency implies that $\varphi^2 \Delta / (k \log^2 n) \rightarrow \infty$. By "consistency" we mean that $|\hat{\eta}_{\text{DC}} - \eta| / \Delta$ converges to 0 in probability, where $\hat{\eta}_{\text{DC}}$ is the Double CUSUM estimate of η . The (asymptotic) SNR requirement for the Double CUSUM algorithm is thus larger than that of ESAC by a factor of at least $k \log^2(n) / r(k)$, which grows with k and diverges with n . Note that theoretical results for the Double CUSUM algorithm only hold whenever p is of the same order as n^ω for some fixed $\omega > 0$. For an empirical comparison between the methods in the single changepoint case, we refer to Section 4.1.

The SNR requirement of ESAC grows much more slowly with k than Inspect and the DC algorithm, which implies that ESAC is able to reasonably estimate dense changepoints under much lower signal strength. Figure 2 displays the SNR requirement of ESAC, Inspect and DC as a function of k , when $n = p = 500$. On the left plot, the SNRs are plotted on linear scale, while on a log scale to the right. The boundary between the dense and sparse regimes is indicated by the vertical dashed line at $k = (p \log n)^{1/2}$. As the SNRs are only defined up to constants, each SNR requirement is normalized to have value 1 for sparsity $k = 1$. For ESAC, the normalized SNR ratio is $h(k) / h(1)$, while it is simply k for Inspect and DC. As we can see, the SNR condition of ESAC grows much more slowly with k than Inspect or DC. We remark that the apparent bulk in the SNR requirement of ESAC is a result of keeping the mathematical expression simple, as remarked in Section 3.1.

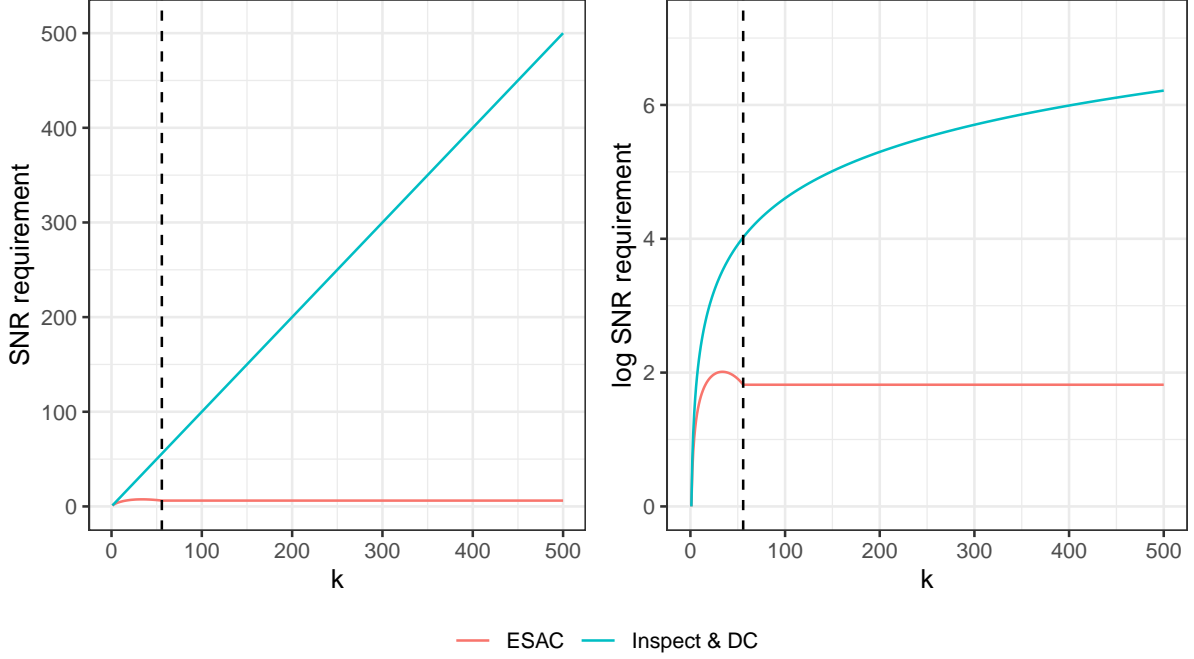


Figure 2: Normalized SNR conditions of ESAC (red) and Inspect and the Double CUSUM algorithm (blue), plotted as a function of the sparsity k , on a linear scale (left) and log scale (right). The boundary between the dense and sparse regimes is given by a vertical dashed line at $k = (p \log n)^{1/2}$.

Lastly, we remark the following. For fixed values of n and p , the function $h(k)$ is increasing for most values of k . Thus, the estimation error and the SNR condition of ESAC tend to grow with the sparsity k . As an example, the error rate for estimating a changepoint with sparsity $k = 1$ is $(\sigma^2/\varphi^2) (\log n \vee \log p)$, while the same error rate becomes $(\sigma^2/\varphi^2) [p \{\log n \vee \log \log(ep)\}]^{1/2}$ for $k = p$.

3.3 Detection and estimation of multiple changepoints

We now consider the combined problem of detecting and estimating an unknown number of changepoints in the data X_1, \dots, X_n . That is, our goal is to estimate J , the number of changepoints, and $(\eta_1, \dots, \eta_J)^\top$, the changepoint locations.

Our proposed test statistic from Section 3.1 and changepoint estimator from Section 3.2 are designed for segments with at most a single changepoint. Hence, a search procedure is needed to allow for multiple changepoint search. Our choice of search procedure is a slight variant of Seeded Binary Segmentation (Kovács et al., 2022). In essence, the Seeded Binary Segmentation search procedure generates a deterministic set of intervals (which they call seeded intervals), in which single changepoint candidates are searched for. As a single changepoint may be detected within several distinct intervals, a choice must be made regarding which of these intervals is to be used for estimating its location. We have opted for the Narrowest-Over-Threshold (Baranowski et al., 2019) choice of changepoints, using the narrowest interval in which a changepoint is detected to estimate its location. Our modification of Seeded Binary Segmentation is minor; in our variant, the generation of intervals is controlled by two parameters, α and K . The parameter K controls the distance between the centers of two consecutive intervals of the same length, and the parameter α controls the growth rate of the interval lengths. Our algorithm for generating seeded intervals is found in Appendix B (Algorithm 4).

Our proposed multiple changepoint estimation procedure, ESAC, is as follows. Let $\mathcal{M} = \{(s_m, e_m]; m \in$

$[M]$ denote an enumerated collection of candidate intervals. Let $\gamma(t), \lambda(t)$ denote the penalty functions used in the score statistic (3), for changepoint detection and estimation, respectively. Given data matrix X , our proposed procedure is initiated by calling the recursive algorithm $\text{ESAC}(X, (0, n], \mathcal{M}, \emptyset, \gamma, \lambda)$, defined by Algorithm 1.

For the theoretical analysis of ESAC given in Section 3.4, we find it necessary to consider a slightly modified variant of the algorithm, defined by Algorithm 2 in Appendix B. In this variant, candidate changepoint locations are trimmed away in the recursive step, discarding them from future use to detect or estimate further changepoints. The trimming of changepoints is introduced as a necessary technical step for the proof of Theorem 3.3 to go through, specifically to ensure that previously discovered changepoints are not re-discovered. In practice, we find trimming to be unnecessary and even degrading of performance. An even more modified variant of ESAC, given by Algorithm 3 defined in Appendix B, takes only the midpoint of an interval as the only candidate changepoint location when testing for a changepoint, in addition to interval trimming. This results in a substantial decrease in running time at the cost of reduced detection power, although the theoretical results in the next subsection hold for this variant as well. In practical application, we thus recommend using Algorithm 1 over Algorithms 2 and 3. A simulation study comparing the variants of ESAC is found in Appendix D.

Algorithm 1 $\text{ESAC}(X, (s, e], \mathcal{M}, \mathcal{B}, \gamma, \lambda)$

Input: A matrix of observations $X \in \mathbb{R}^{p \times n}$, an open integer interval (s, e) in which candidate changepoints are searched for, an enumerated collection $\mathcal{M} = \{(s_m, e_m] ; m \in [M]\}$ of M half open integer sub intervals of $(0, n]$, a set of already detected changepoints \mathcal{B} , and penalty functions $\gamma(t), \lambda(t)$.

Output: Set \mathcal{B} of already detected changepoints.

```

if  $e - s \leq 1$ 
  return  $\mathcal{B}$ 
set  $\mathcal{M}_{(s,e]} = \{m \in [M] : (s_m, e_m] \subset (s, e]\}$ 
set  $\mathcal{O}_{(s,e]} = \left\{ m \in \mathcal{M}_{(s,e]} : \max_{s_m < v < e_m} S_{\gamma, (s_m, e_m]}^v > 0 \right\}$ 
if  $\mathcal{O}_{(s,e]} = \emptyset$ 
  return  $\mathcal{B}$ 
set  $l^* = \min_{m \in \mathcal{O}_{(s,e]}} |e_m - s_m|$ 
set  $\mathcal{O}_{l^*} = \{m \in \mathcal{O}_{(s,e]} : |e_m - s_m| = l^*\}$ 
set  $m^* = \operatorname{argmax}_{m \in \mathcal{O}_{l^*}} \max_{s_m < v < e_m} S_{\lambda, (s_m, e_m]}^v$ 
set  $v^* = \operatorname{argmax}_{s_{m^*} < v < e_{m^*}} S_{\lambda, (s_{m^*}, e_{m^*}]}^v$ 
 $\mathcal{B} \leftarrow \mathcal{B} \cup \{v^*\}$ 
 $\mathcal{B} \leftarrow \text{ESAC}(X, (s, v^*], \mathcal{M}, \mathcal{B}, \gamma, \lambda)$ 
 $\mathcal{B} \leftarrow \text{ESAC}(X, (v^*, e], \mathcal{M}, \mathcal{B}, \gamma, \lambda)$ 
return  $\mathcal{B}$ 

```

3.4 Theoretical results for the multiple changepoint case

For the variants of ESAC defined by either Algorithm 2 or Algorithm 3 (both given in in Appendix B), we have the following finite-sample statistical result.

Theorem 3.3. *Let $X \in \mathbb{R}^{p \times n}$ follow the model in Section 2, and let $r(t)$ be defined as in (8). Let \mathcal{M} denote the set of candidate intervals generated from Algorithm 4 with parameters $\alpha \leq 2, K \geq 2$, and*

let the penalty function $\gamma(t)$ be defined as $\gamma(t) = \gamma_0 r(t)$. There exists a universal choice of $\gamma_0 > 0$, such that for some universal constants $C_0, C_1 > 0$, depending only on γ_0 , and for any choice of $\lambda(t)$, the following holds.

Let \hat{J} and $\hat{\eta}_1, \dots, \hat{\eta}_{\hat{J}}$ respectively be denote the estimated number of changepoints and sorted changepoint locations from Algorithm 2 or 3, using penalty functions $\gamma(t)$ and $\lambda(t)$, candidate intervals \mathcal{M} , and variance scaled input matrix $\tilde{X} = X/\sigma$. If the SNR condition

$$\frac{\varphi_j^2 \Delta_j}{\sigma^2} \geq C_0 r(k_j) \quad (12)$$

holds for all $j \in [J]$, we have that

$$\mathbb{P} \left\{ \hat{J} = J \cap |\hat{\eta}_j - \eta_j| \leq C_1 \frac{\sigma^2}{\varphi_j^2} r(k_j) \forall j \in [J] \right\} > 1 - \frac{1}{n}.$$

The explicit values of γ_0, C_0 and C_1 can be found in the proof of Theorem 3.3 in Appendix A. We remark that these constants have not been optimized. In practice, we recommend choosing the penalty functions $\gamma(t)$ via Monte Carlo simulation or setting $\lambda(t), \gamma(t)$ proportional to a slight variant of $r(t)$. In particular, when using $\lambda(t), \gamma(t) \propto r(t)$, our simulations suggest that the leading constants can be chosen independently of n and p , at least for the values of (n, p) we have considered. For further details and recommendations, we refer to Appendix B.

Note that, whenever the SNR condition (12) holds, the localization error of ESAC satisfies $C_1 \sigma^2 r(k_j) / \varphi_j < \Delta_j$. If the stronger condition $\varphi_j^2 / \{\sigma^2 r(k_j)\} \rightarrow \infty$ as $n \rightarrow \infty$ holds for all j (allowing all model parameters to vary with n), then $\max_{j \in [J]} |\hat{\eta}_j - \eta_j|$ converges to 0 in probability as $n \rightarrow \infty$. Note also that Theorem 3.3 holds for any choice of the penalty function $\lambda(t)$. This is because the bound on the estimation error in Theorem 3.3 relies upon the detection properties of penalized score $S_{\gamma, (s, e)}^v$ rather than the localization properties of our estimator $\hat{\eta}_\lambda$. Specifically, since ESAC uses Narrowest-over-Threshold selection of changepoints (Baranowski et al., 2019), it suffices to upper bound the minimum interval width required to detect a changepoint, which for each j is of the order of $\sigma^2 r(k_j) / \varphi_j^2$. This observation is due to Pilliat et al. (2023). In practice, we experience that using the estimator $\hat{\eta}_\lambda$ for changepoint localization improves performance compared to using e.g. the mid-point of an interval. For more details and a simulation study, see Appendix D.

Some performance comparisons to related methods are in order. Theorem 3.3 gives a very similar theoretical guarantee as the method of Pilliat et al. (2023, Corollary 3). When the probability of the desired event in the Corollary is the same as in Theorem 3.3, the method of Pilliat obtains the same error rate under an up to constants equal SNR requirement.

The Inspect method (Wang and Samworth 2018) requires a signal-to-noise condition of the form $\varphi^2 \Delta / \sigma^2 \geq C \log(np) \{(n/\Delta)^3 \vee k\} (n/\Delta)$, where $C > 0$ is some universal constant, $\Delta = \min_{j=1, \dots, J} \Delta_j$, $\varphi = \min_{j=1, \dots, J} \varphi_j$ and $k = \max_{j=1, \dots, J} k_j$. The SNR condition of Inspect is (up to constants) larger than (12) by factors of at least $n/\Delta \geq 1$ and $k \log(np) / r(k) \geq 1$. The former factor is only close to 1 whenever there are few changepoints with large spacing between, while the latter factor is only close to 1 whenever all changepoints are sparse. For the Double CUSUM algorithm (Cho, 2016) when $\sigma = 1$, its (asymptotic) SNR condition requires $\varphi_j^2 \Delta_j / (n^{3-5\beta/2} k_j \log^2 n) \rightarrow 0$ whenever $n^\beta = \mathcal{O}(\Delta_j)$ for all $j \in [J]$ for some $\beta \in (6/7, 1]$, as well as p being of the same order as n^ω for some fixed $\omega > 0$. The SNR requirement for the Double CUSUM algorithm is thus larger than that of ESAC by factors of at least \sqrt{n} and $k_j \log^2(n) / r(k_j)$. The latter factor diverges as $n \rightarrow \infty$ or $k_j \rightarrow \infty$.

Figure 3 displays the SNR requirements of ESAC (red), Inspect (green) and the Double CUSUM algorithm (blue) on a log scale as a function of the sparsity k , plotted for different values of n and p . Here we have removed the factor $(n/\Delta)^3 > 1$ from the SNR requirement of Inspect, as well as setting $\Delta = n/2$. To the left, we plot the requirements for $n = 10^2, 10^3, 10^4$, indicated by solid, dashed and dotted lines, respectively, keeping $p = 500$ fixed. Moreover, each SNR requirement is normalized to have value 1 for sparsity $k = 1$ at $n = 100$. To the right, we plot the requirements for $p = 500, 1000, 2000$, indicated by solid, dashed and dotted lines, respectively, keeping $n = 1000$ fixed. Here, each SNR requirement is normalized to have value 1 for sparsity $k = 1$ for $p = 500$. From Figure 3 we see that the SNR requirement of ESAC grows substantially slower with k than Inspect and the Double CUSUM. The SNR requirement of ESAC and Inspect grow substantially slower with n than the Double CUSUM, while the SNR requirement of ESAC grows faster with p than Inspect and the Double CUSUM. As before, the apparent bulk in the SNR requirement of ESAC is a result of keeping $r(t)$ mathematically simple, as remarked in Section 3.1.

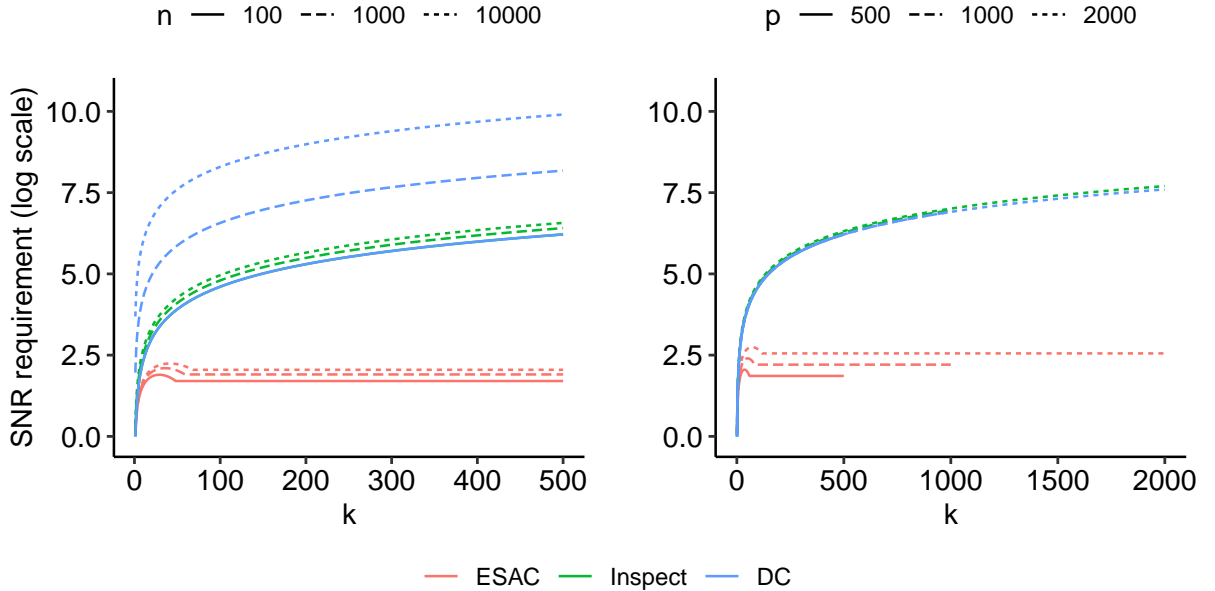


Figure 3: Normalized SNR conditions of ESAC (red) and Inspect (green) and the Double CUSUM algorithm (blue) on a log scale, plotted as a function of the sparsity k , and varying values of n (left) and p (right).

As for the changepoint location error rates, Inspect obtains a theoretical error rate of $\sigma^2(n/\Delta)^4 \log(np)/\varphi^2$ whenever its SNR condition is satisfied. In comparison, the theoretical error rate of ESAC is at most $\sigma^2 r(k_j)/\varphi_j^2 r(k_j)$, which is smaller than the error rate of Inspect whenever n/Δ is large (short distance between changepoints) or k is large. For the Double CUSUM algorithm, in the case where $\sigma = 1$, the theoretical error rate for each changepoint is at least of the order $\log^2(n)k_j/\varphi_j^2$. This is larger than the error rate of ESAC by a factor of at least $k_j \log^2(n)/r(k_j)$, which diverges with n and grows with k_j .

We now turn to optimality considerations. Observe first that the SNR condition (12) is up to constants minimal for identifying J , the number of changepoints. Indeed, for any n, p and $k \leq p$, an implication of Theorem 2 in Pilliat et al. (2023) is that

$$\sup_{P \in Q(n,p,k)} P(|\hat{\eta}| \neq J) \geq 1/4$$

for all estimators $\hat{\eta} = \hat{\eta}(X_1, \dots, X_n)$ of the changepoint vector $\eta = (\eta_1, \dots, \eta_J)$, where $Q(n, p, k)$ is the class of all probability distributions of X_1, \dots, X_n corresponding to the model given in Section 2 for which $k_j \leq k$ and $\varphi_j^2 \Delta_j / \sigma^2 \geq cr(k_j)$ for all $j \in [J]$, for some sufficiently small $c > 0$. As for the changepoint location error rate, the minimax rate has been shown by Wang and Samworth (2018) to be at least $\sigma^2 / (16\varphi^2)$ whenever $\Delta^{-1} \leq \varphi^2 / \sigma^2 \leq 1$. Hence, at least in this region of the parameter space, the estimator $\hat{\eta}$ from Section 3.2 and the full ESAC algorithm have minimax optimal error rates up to factors of $h(k)$ and $r(k)$, respectively, where k is the sparsity of the changepoint in question. Note that, while $r(k)$ and $h(k)$ are constant multiples of $\log n$ whenever $k = 1$, they grow substantially with k . Hence the error rate of ESAC is only close to minimax rate optimal for small values of the sparsity k .

Finally, we consider the computational cost of ESAC as a function of the size of the data. The following Proposition shows that ESAC has a log-linear computational cost.

Proposition 3.4. *Consider any input matrix $X \in \mathbb{R}^{p \times n}$, penalty functions $\gamma(t), \lambda(t)$ and seeded intervals generated by Algorithm 4 with fixed input parameters $\alpha > 1$ and $K \in \mathbb{N}$. Then the computational complexity of ESAC (either Algorithm 1, 2 or 3) measured in floating point operations is of order $\mathcal{O}\{np \log(p \log n)\}$ in the best case and $\mathcal{O}\{np \log n \log(p \log n)\}$ in the worst case.*

In comparison, the computational complexity of the Pilliat algorithm is $\mathcal{O}\{np \log(np)\}$, which is of slightly smaller order than the worst-case complexity of ESAC. For the other multiple changepoint methods like the Double CUSUM, Sparsified Binary Segmentation, SUBSET and Inspect, no specific forms of computational cost are provided in the respective articles. For an empirical comparison of running times, we refer to the next section.

4 Simulations

We now compare the empirical performance of ESAC with the following state-of-the-art methods for high-dimensional changepoint detection and estimation: a variant of the Inspect method by Wang and Samworth (2018), the method of Pilliat et al. (2023) hereby called Pilliat, Sparsified Binary Segmentation of Cho and Fryzlewicz (2015), the Double CUSUM algorithm of Cho (2016), and the SUBSET method by Tickle et al. (2021). We introduce a slightly modified variant of Inspect, based on Narrowest-over-Threshold search, mainly to reduce computational cost. The details of our modified Inspect algorithm can be found in Appendix C. To run the Sparsified Binary Segmentation and Double CUSUM algorithms, we use the R package **hdbinseg** (Cho and Fryzlewicz, 2018). To run SUBSET, we use the code from the Github repository of Tickle (2022). We have implemented the remaining methods ESAC, Pilliat and Inspect in the C programming language, which are found in the R package **HDCD** (Moen, 2023), available on CRAN. We remark that our implementations of Inspect and the method Pilliat et al. are orders of magnitude faster than their original implementations. Whenever running times are reported, they have been run using R (4.2.1) on a MacOS (12.3) computer with an (ARM) Apple M1 Pro CPU.

For each method in the simulation study, a choice of penalty parameters must be made, which is discussed in each subsection. In all simulations, changes in mean are taken to have magnitudes spread evenly across all affected coordinates. In Appendix E we run the same simulations with uneven and random magnitudes, giving similar results. In all simulations we assume $\sigma = 1$ is unknown. We estimate σ separately for each of the p coordinates of the observed time series, and use it to normalize the data before applying each changepoint detection method. As is commonly done in the changepoint literature, we estimate the noise level by the median absolute deviation of first-order differences with scaling factor 1.05 for the Gaussian distribution.

4.1 Single changepoint estimation

In this subsection we consider the algorithms' performance when estimating the location of a single changepoint, assuming that it has already been detected. Our simulations are run with parameters $n \in \{200, 500\}$, $p \in \{100, 1000, 5000\}$, $k \in \{1, \lceil p^{1/3} \rceil, \lceil \sqrt{p \log n} \rceil, p\}$. For each configuration of these parameters, we simulate 1000 data sets and apply the methods considered in the study. For each combination of n, p, k , the simulated data sets have a changepoint at $\eta = \lceil n/5 \rceil$ with change-vector $\theta \propto (I_1, \dots, I_k, 0, \dots, 0)^\top$, where I_1, \dots, I_k are drawn independently and uniformly from $\{-1, 1\}$. For each sample we scale θ such that $\Delta\varphi^2 = (n/5) \|\theta\|_2^2 = (5^2/2^2)r(k)$, where k is the sparsity of the change and $\Delta = \lceil n/5 \rceil$.

To keep the simulation study simple, we use the authors' recommended non-empirical choices of penalty parameters. We take ESAC to be the estimator given in (9), with penalty function $\tilde{\lambda}(t)$ as defined in Appendix B. As for Inspect, we use Algorithm 2 in Wang and Samworth (2018), with penalty parameter $\lambda = \{\log(p \log n)/2\}^{1/2}$. For the Double CUSUM algorithm we set $\varphi = -1$, corresponding to the version presented in Section 4.1 of Cho (2016). For Sparsified Binary Segmentation, a default choice of the threshold π_T is not available, so we take π_T to be the maximum value of the CUSUMs $|T_{[0,n]}^v(Z_{i,\cdot}/\hat{\sigma}_i)|$ over all values of $0 < v < n$ and $i \in [p]$, where $Z_{v,i} \sim N(0, 1)$ independently for $i \in [p]$, $v \in [n]$, and $\hat{\sigma}_i$ is the median absolute deviation of the noise level in the i th series, based on 1000 Monte Carlo samples. Whenever the Sparsified Binary Segmentation estimator is not defined, we set its output to be 1. For both the Double CUSUM and Sparsified Binary Segmentation algorithm, we have specified $height = 1$ when calling the respective functions to turn the methods into single changepoint estimators. The Pilliat algorithm is not included in this simulation as there is no straightforward way to modify it into a single changepoint estimator.

For each method and each configuration of parameters, Table 1 displays the average Mean Squared Error (MSE) and average running time in milliseconds. The Double CUSUM and Sparsified Binary Segmentation methods are abbreviated as DC and SBS, respectively. For each configuration of parameters, the minimum value of both the MSE and the running is indicated in boldface. In terms of statistical accuracy, Table 1 demonstrates that ESAC and SUBSET are the only methods with competitive accuracy across the sparsity regimes, although ESAC has a slight edge over SUBSET. ESAC has the lowest MSE in 14 out of the 24 different combinations of parameters (including both dense and sparse regimes), while SUBSET has the lowest MSE in 6 out of 24. When averaging the MSE over all the rows, ESAC is the clear winner, with SUBSET in second place. In comparison, the estimation accuracy of Inspect is excellent for $k = \lceil p^{1/3} \rceil$, but deteriorates for higher sparsity levels. The Double CUSUM algorithm displays excellent estimation accuracy when $k = 1$, but often not so for dense changepoints (although this seems to vary slightly with n and p). Sparsified Binary Segmentation has high estimation accuracy for sparse changepoints (especially when $k = 1$), but the accuracy deteriorates for dense changepoints.

In terms of running time, ESAC is the clear winner, with execution time around one fifth of SUBSET, the runner up, and down to 4% of the execution time of Inspect and Double CUSUM for large values of p . Note that SUBSET is the only method not implemented in C or C++, giving the other methods an advantage when comparing running times. We also remark that the running time of scaling the data by the median absolute deviations is not included in the running times of ESAC, Inspect and SUBSET, as it would otherwise dominate the running time. The running time of the scaling is included in the running times of the Double CUSUM and Sparsified Binary Segmentation algorithms, as the implementations of these algorithms do not offer an option to disable it.

Table 1: Single changepoint estimation

Parameters					MSE					Time in milliseconds					
n	p	k	η	φ	ESAC	Inspect	SBS	SUBSET	DC	ESAC	Inspect	SBS	SUBSET	DC	
200	100	1	40	1.40	10.4	25.3	83.0	54.2	9.8	0.4	2.1	9.7	1.7	12.9	
200	100	5	40	2.00	5.8	4.1	389.0	3.0	15.3	0.3	2.0	10.4	1.9	13.0	
200	100	24	40	1.90	96.5	139.6	1495.8	251.1	953.4	0.2	2.0	9.0	1.6	14.7	
200	100	100	40	1.90	95.1	425.9	1520.6	250.8	2807.6	0.2	2.0	9.1	1.6	11.7	
200	1000	1	40	1.52	6.9	105.8	29.5	33.1	6.5	2.0	40.8	84.5	12.0	120.6	
200	1000	10	40	2.93	5.1	0.8	130.6	1.2	10.4	1.9	40.8	84.0	12.6	122.2	
200	1000	73	40	3.37	4.6	64.5	1478.2	8.2	276.1	1.9	40.9	83.4	12.1	122.4	
200	1000	1000	40	3.37	3.5	796.2	1534.7	7.1	317.2	2.0	41.0	82.9	12.6	122.2	
200	5000	1	40	1.60	45.3	413.3	29.1	81.4	154.2	11.7	210.4	427.9	73.8	651.7	
200	5000	18	40	4.00	9.4	0.6	65.7	3.3	94.7	11.6	210.0	426.1	74.3	652.4	
200	5000	163	40	5.04	3.6	60.3	1466.2	3.6	7.2	11.8	210.1	422.3	75.0	654.0	
200	5000	5000	40	5.04	4.4	1453.9	1563.1	4.4	5.3	11.9	210.1	420.8	75.3	655.4	
500	100	1	100	0.92	55.4	97.9	120.8	216.4	54.6	0.7	5.4	16.2	3.9	26.3	
500	100	5	100	1.31	22.9	15.7	1060.2	12.6	108.0	0.6	5.3	15.5	3.7	24.9	
500	100	25	100	1.25	112.7	323.1	9560.3	2150.5	6850.1	0.6	5.3	16.0	3.6	25.3	
500	100	100	100	1.25	284.4	1845.9	9768.9	1959.7	18386.6	0.6	5.2	16.4	3.7	24.3	
500	1000	1	100	1.00	30.5	217.7	79.3	190.5	31.0	5.2	252.6	141.9	32.1	256.9	
500	1000	10	100	1.90	12.3	5.1	232.6	3.7	84.3	5.4	252.2	142.4	31.7	256.1	
500	1000	79	100	2.22	22.1	122.5	9547.8	66.4	1725.7	5.6	253.2	141.6	32.3	256.2	
500	1000	1000	100	2.22	15.4	3895.9	9790.4	82.9	2401.7	5.7	254.8	142.6	32.3	258.2	
500	5000	1	100	1.05	22.2	1322.6	51.6	95.9	192.0	31.0	1307.0	743.7	168.9	1536.6	
500	5000	18	100	2.58	7.9	1.8	102.9	3.2	505.5	30.1	1302.7	726.1	163.7	1434.2	
500	5000	177	100	3.32	11.2	175.0	9438.2	11.2	37.6	30.8	1300.5	720.1	158.6	1420.4	
500	5000	5000	100	3.32	20.2	8212.5	9799.4	33.7	27.2	31.0	1301.1	717.8	158.3	1415.7	
Average MSE					37.8	821.9	2889.1	230.3	1460.9						

4.2 Multiple changepoint estimation

In this subsection we consider the situation of an unknown number of changepoints. Our simulations are run with parameters $n = 200$, $p \in \{100, 1000, 5000\}$ and $J \in \{0, 2, 5\}$. For each simulated data set we take the changepoint locations η_1, \dots, η_J to be ordered and uniformly drawn samples from $\{1, \dots, n-1\}$ without replacement. For each combination of n, p and J , we consider three different sparsity regimes; *dense*, *sparse* and *mixed*. In the dense and sparse regimes, we sample k_1, \dots, k_J independently and uniformly from $\{\lceil \sqrt{(p \log n)} \rceil, \dots, p\}$ and $\{1, \dots, \lfloor \sqrt{(p \log n)} \rfloor\}$, respectively. In the mixed regime we sample each k_j independently from a mixture between the dense and sparse regimes, each with equal probability. For each combination of n, p, J and sparsity regime, each changepoint has change-vector $\theta_j \propto (I_{j,1}, \dots, I_{j,k}, 0, \dots, 0)^\top$, where $I_{j,1}, \dots, I_{j,k}$ are drawn independently and uniformly from $\{-1, 1\}$, scaled such that $\Delta_j \varphi_j^2 / \sigma_j^2 = (7/2)^2 r(k_j)$. Notice that we have increased the signal strength slightly in comparison with the single changepoint case, as multiple changepoint estimation is more challenging than estimating the position of a single changepoint whose existence is known. For each combination of n, p, J and sparsity regime we simulate 1000 data sets.

For both ESAC and the modified Inspect algorithm, we generate seeded intervals using Algorithm 4 with parameters $\alpha = 3/2$ and $K = 4$. For the Pilliat method we generate intervals using Algorithm 4 with parameters $\alpha = 3/2$ and $K = 2$, giving very similar intervals as the a -adic grid \mathcal{G}_a defined in Pilliat et al. (2023) for $a = 2/3$. Due to high computational cost, we run SUBSET with only 100 randomly drawn intervals in its Wild Binary Segmentation step. To ensure comparability with the remaining methods, we have modified the Pilliat algorithm so that its tests for a changepoint in an integer interval $(s, e]$ are performed by testing for a changepoint at each candidate position $s < v < e$, instead of only the mid-point. In our experience, testing only at the mid-point of an interval results in lower detection power.

We choose detection thresholds using either Monte Carlo simulations (using $N = 1000$ samples) or bootstrapping (using $B = 100$ samples). For the ESAC algorithm, we use the penalty functions $\tilde{\gamma}(t)$ and $\tilde{\lambda}(t)$ given in Appendix B, using a false positive rate $\varepsilon = 1/N$ to generate the former. For the Pilliat

algorithm we choose detection thresholds for the Partial Sum statistic and the dense statistic by Monte Carlo simulating the leading constant in the theoretical thresholds given in Pilliat et al. (2023), and apply a Bonferroni correction. For the modified version of Inspect we set $\lambda = \{\log(p \log n)/2\}^{1/2}$ and choose the detection threshold ξ to be the largest sparse projection over all seeded intervals and over $N = 1000$ data sets with no changepoints. For SUBSET we use the function for choosing thresholds provided by the author, which is based on Monte Carlo simulation. For Sparsified Binary Segmentation and Double CUSUM we use the default parameters when running the algorithms (except for setting $\varphi = -1$ for the Double CUSUM algorithm), and use the default bootstrap procedures to select detection thresholds.

For each method considered and each configuration of parameters and changepoint regimes, Table 2 displays the average Hausdorff distance and average absolute estimation error of J . The Double CUSUM and Sparsified Binary Segmentation methods are abbreviated as DC and SBS, respectively. For each configuration of parameters and changepoint regimes, the minimum value of each of the performance measures is indicated in boldface. In terms of average Hausdorff distance, Table 2 demonstrates that ESAC and SUBSET are the top performers across all sparsity regimes with comparable accuracy. SUBSET slightly outperforms ESAC when there are few changepoints ($J = 2$), while the opposite is true when there are $J = 5$ changepoints. Averaging the Hausdorff distance over all configurations, SUBSET is seen to slightly outperform ESAC. We believe this is due to ESAC using Narrowest-Over-Threshold choice of changepoints, which usually causes ESAC to use fewer observations to estimate changepoint locations. See Appendix D for a simulation where ESAC does not use Narrowest-Over-Threshold choice of changepoints locations, improving its performance. For estimating J , the number of changepoints, ESAC is the clear winner, with SUBSET in second place.

Figure 4 displays the natural logarithm of the running times (in milliseconds) of the methods as functions of n and p . For the left plot, we fix $p = 100$, and for the right plot we fix $n = 100$. When it comes to execution time, ESAC outperforms the competing methods by a significant margin for all considered values of n and p . The running time of ESAC is smaller than that of the competitors by a factor seemingly constant in n and p . When not applying a log transform to the running times (which is omitted for brevity), all methods are seen to have an approximately linear computational cost in both n and p .

Table 2: Multiple change-point estimation

Parameters				Hausdorff distance						$ \hat{J} - J $					
n	p	Sparsity	J	ESAC	Pilliat	Inspect	SBS	SUBSET	DC	ESAC	Pilliat	Inspect	SBS	SUBSET	DC
200	100	-	0	-	-	-	-	-	-	0.00	0.00	0.00	0.04	0.00	0.04
200	100	Dense	2	5.27	23.05	21.61	69.92	6.52	76.37	0.06	0.48	0.29	1.03	0.11	1.08
200	100	Sparse	2	1.43	12.54	7.92	49.19	1.67	14.92	0.01	0.25	0.10	0.70	0.04	0.26
200	100	Mixed	2	4.60	18.57	14.36	61.15	3.74	52.93	0.05	0.37	0.19	0.87	0.06	0.74
200	100	Dense	5	5.17	23.74	16.27	67.29	6.42	55.71	0.14	1.53	0.54	3.12	0.33	2.76
200	100	Sparse	5	1.36	13.99	6.38	57.18	2.42	23.19	0.02	0.78	0.23	2.79	0.20	1.36
200	100	Mixed	5	4.04	18.77	12.56	60.43	4.90	41.31	0.10	1.20	0.42	3.01	0.28	2.16
200	1000	-	0	-	-	-	-	-	-	0.00	0.00	0.00	0.34	0.02	0.02
200	1000	Dense	2	1.45	13.39	9.49	55.12	1.08	84.98	0.01	0.28	0.12	0.72	0.03	1.23
200	1000	Sparse	2	0.83	9.07	9.83	49.72	0.75	20.38	0.00	0.18	0.15	0.62	0.03	0.29
200	1000	Mixed	2	1.78	11.78	9.59	50.51	1.48	53.23	0.01	0.24	0.13	0.69	0.04	0.82
200	1000	Dense	5	1.52	15.81	9.33	57.33	1.56	60.79	0.03	1.02	0.26	2.96	0.17	3.06
200	1000	Sparse	5	0.69	11.34	9.16	54.20	1.52	25.80	0.00	0.64	0.36	2.68	0.17	1.43
200	1000	Mixed	5	1.19	13.93	9.45	58.26	1.72	45.16	0.02	0.81	0.33	2.86	0.19	2.38
200	5000	-	0	-	-	-	-	-	-	0.00	0.00	0.00	1.96	0.00	0.00
200	5000	Dense	2	0.97	12.99	13.25	54.75	0.60	124.34	0.00	0.29	0.17	0.53	0.02	1.68
200	5000	Sparse	2	0.76	9.66	15.81	58.96	0.51	70.83	0.00	0.20	0.24	0.56	0.03	1.04
200	5000	Mixed	2	0.98	11.36	13.76	55.92	0.78	96.95	0.00	0.25	0.21	0.50	0.03	1.36
200	5000	Dense	5	0.89	14.59	12.97	50.33	1.37	83.64	0.01	0.94	0.45	2.45	0.17	3.63
200	5000	Sparse	5	0.53	11.70	13.50	54.00	1.29	54.33	0.00	0.74	0.55	2.53	0.18	2.71
200	5000	Mixed	5	0.78	13.57	13.25	53.72	1.41	69.94	0.00	0.86	0.50	2.50	0.17	3.19
Average				1.90	14.43	12.13	56.55	2.21	58.60	0.02	0.61	0.29	1.73	0.12	1.73

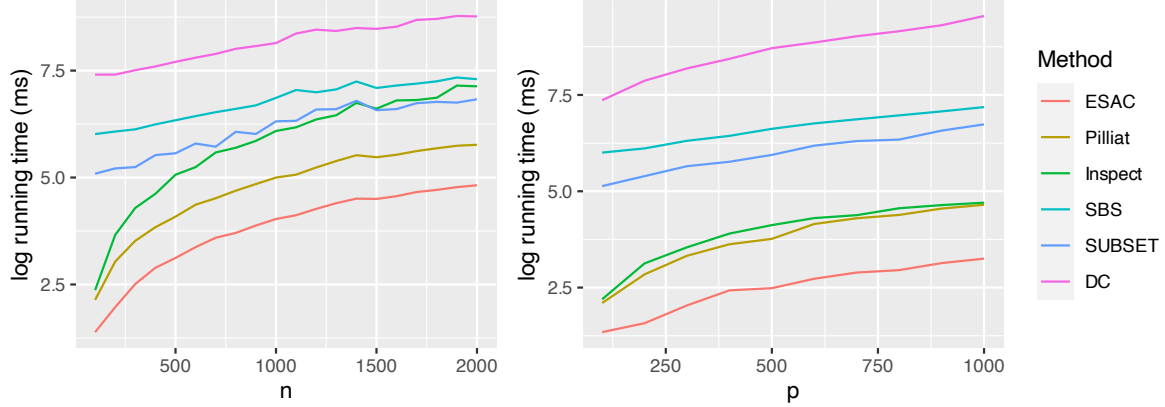


Figure 4: Running times as functions of n (left) and p (right) on a logarithmic scale.

4.3 Misspecified model

ESAC is designed for data with isotropic Gaussian noise, which can be an unrealistic assumption in practice. We now investigate the empirical performance of ESAC and the competing methods in the single changepoint setting under other data generating mechanism than the model described in Section 2. With the changepoint location fixed at $\eta = \lceil n/5 \rceil = 40$, we consider two sparsity regimes, *sparse* and *dense*. We sample k independently and uniformly from $\{1, \dots, \lfloor \sqrt{(p \log n)} \rfloor\}$ in the sparse regime, and from $\{\lceil \sqrt{(p \log n)} \rceil, \dots, p\}$ in the dense regime. In both regimes, we take the change-vector θ to satisfy $\theta \propto (I_1, \dots, I_k, 0, \dots, 0)^T$, where I_1, \dots, I_k are drawn independently and uniformly from $\{-1, 1\}$. Furthermore, we scale θ such that $\Delta\varphi^2 = (n/5) \|\theta\|_2^2 = 9r(k)$.

Similar to the simulation study in Wang and Samworth (2018), we consider the following data generating mechanisms. In model M_0 we take the noise vector W_v to satisfy $W_v \sim \mathcal{N}_p(0, I)$ independently for $v \in [n]$. In models M_{Unif} and M_{t_d} we take $W_{i,v} \sim \text{Unif}(-\sqrt{3}, \sqrt{3})$ and $\{d/(d-2)\}^{1/2} W_{i,v} \sim t_d$, respectively and independently for all $v \in [n]$ and $i \in [p]$, where t_d denotes the Student t distribution with d degrees of freedom. In model $M_{\text{cs,loc}}(\rho)$ we let the noise vectors W_1, \dots, W_n have short-ranged spatial correlation, taking $W_v \sim \mathcal{N}_p(0, \Sigma(\rho))$ independently for all $v \in [n]$, where $\Sigma(\rho)_{j,k} = \rho^{|j-k|}$ for each $j, k \in [p]$. In the model $M_{\text{cs}}(\rho)$ we let the noise vectors W_1, \dots, W_n have global spatial correlation by taking $W_v \sim \mathcal{N}_p(0, \Delta(\rho))$ independently for $v \in [n]$, where $\Delta(\rho) = (1-\rho)I_p + \rho/p I_p I_p^T$. In the model $M_{\text{temp}}(\rho)$ we allow for temporal dependence between the noise vectors W_1, \dots, W_n by letting $W_1 = \widetilde{W}_1$ and $W_v = \sqrt{\rho} \widetilde{W}_v + \sqrt{1-\rho} W_{v-1}$ for $v = 2, \dots, n$, where $\widetilde{W}_1, \dots, \widetilde{W}_n \sim \mathcal{N}_p(0, I_p)$, independently. In the models M_{async} and M_{gradual} we allow for changes in the mean to occur asynchronous and gradual in time, respectively, with noise vectors $W_v \sim \mathcal{N}_p(0, I_p)$ independently for $v \in [n]$. In M_{async} , for each changepoint η_j , we randomly shift the position (in time) of the change in mean in the i th coordinate, where the shifts are drawn independently from $\text{Unif}(\eta_j - \lfloor \Delta_j/2 \rfloor, \eta_j - \lfloor \Delta_j/2 \rfloor + 1, \dots, \eta_j + \lfloor \Delta_j/2 \rfloor)$. In M_{gradual} , for each changepoint η_j , any change in mean occurs linearly over time, starting at position $\eta_j - \lfloor \Delta_j/2 \rfloor + 1$ and ending at position $\eta_j + \lfloor \Delta_j/2 \rfloor + 1$. For both the single and multiple changepoint settings, we have set $n = p = 200$.

Table 3 displays the MSE of the competing methods using the same running parameters as in Section 4.1, based on $N = 1000$ runs. Table 3 indicates that ESAC (along with Inspect and SUBSET) is robust to model deviations in the form of light-tailed noise and short-ranged spatial correlation. With global spatial correlation, however, all methods degrade substantially in performance, with Inspect having a slight edge over the remaining methods. With autocorrelation, the performance of the methods also degrades

markedly, with ESAC and SUBSET having a slight edge over the remaining methods. Lastly, ESAC and SUBSET seem to be slightly more robust to asynchronous and gradual occurrence of changepoints than the remaining methods.

Table 3: Single changepoint estimation under misspecified models

Parameters		MSE				
Model	Sparsity	ESAC	Inspect	SBS	SUBSET	DC
M	Sparse	1.2	1.0	506.1	1.1	26.8
M	Dense	1.6	84.5	1507.9	1.6	1101.2
M_{Unif}	Sparse	1.0	1.2	666.7	0.9	17.7
M_{Unif}	Dense	7.5	141.3	1506.1	23.4	982.4
M_{t_3}	Sparse	1373.5	405.7	3014.5	1379.4	3342.1
M_{t_3}	Dense	1561.6	1184.0	12195.2	1642.9	8132.5
$M_{t_{10}}$	Sparse	2.3	1.5	649.5	1.4	64.3
$M_{t_{10}}$	Dense	2.1	54.6	2045.5	2.1	1256.2
$M_{\text{cs, loc}}(\rho = 0.1)$	Sparse	1.1	0.7	497.7	1.0	21.6
$M_{\text{cs, loc}}(\rho = 0.1)$	Dense	1.9	69.3	1501.3	1.9	1108.3
$M_{\text{cs, loc}}(\rho = 0.4)$	Sparse	1.3	1.2	508.0	1.2	17.9
$M_{\text{cs, loc}}(\rho = 0.4)$	Dense	2.7	116.6	1505.7	2.7	1347.6
$M_{\text{cs}}(\rho = 0.1)$	Sparse	126.7	2.0	524.3	82.2	20.9
$M_{\text{cs}}(\rho = 0.1)$	Dense	281.4	114.4	1516.1	281.4	1111.4
$M_{\text{cs}}(\rho = 0.4)$	Sparse	4087.5	66.2	540.1	3997.6	50.7
$M_{\text{cs}}(\rho = 0.4)$	Dense	5473.6	1296.8	1503.6	5473.6	2072.9
$M_{\text{AR}}(\rho = 0.1)$	Sparse	148.0	77.1	194.2	148.0	175.8
$M_{\text{AR}}(\rho = 0.1)$	Dense	40.6	461.7	3023.6	40.6	2557.8
$M_{\text{AR}}(\rho = 0.4)$	Sparse	979.9	1648.6	1270.0	979.9	2010.2
$M_{\text{AR}}(\rho = 0.4)$	Dense	1274.3	1994.0	2552.5	1274.3	4337.5
M_{async}	Sparse	83.1	99.0	603.8	81.2	233.3
M_{async}	Dense	75.8	288.3	1521.7	79.4	1644.7
M_{grad}	Sparse	50.3	54.5	794.5	49.2	223.8
M_{grad}	Dense	67.7	231.3	1524.4	92.2	2002.1
M_{grad}	Dense	67.7	231.3	1524.4	92.2	2002.1

5 Real data example

To illustrate how ESAC can be applied in practice, we examine raw sensor data from a Swedish hydro power plant. The data consists of measurements from 20 sensors taken every minute for 1800 minutes, so that $p = 20$ and $n = 1800$. The sensors measure the magnitude of movements and vibrations (the latter measured at 1-10 and 10-1000 Hz bands) at various locations along the shaft connecting the turbine and the generator. During the 1800 minutes we consider, the mode of operation changes several times, detailed in Table 4. We take these changes of operation mode as the ground truth regarding the number of changepoints and their locations.

Table 4: Operation modes of the hydro power plant

Time period	Operation mode
1 – 529	running
530 – 537	stopping
538 – 1307	off
1308 – 1310	starting
1311 – 2000	running

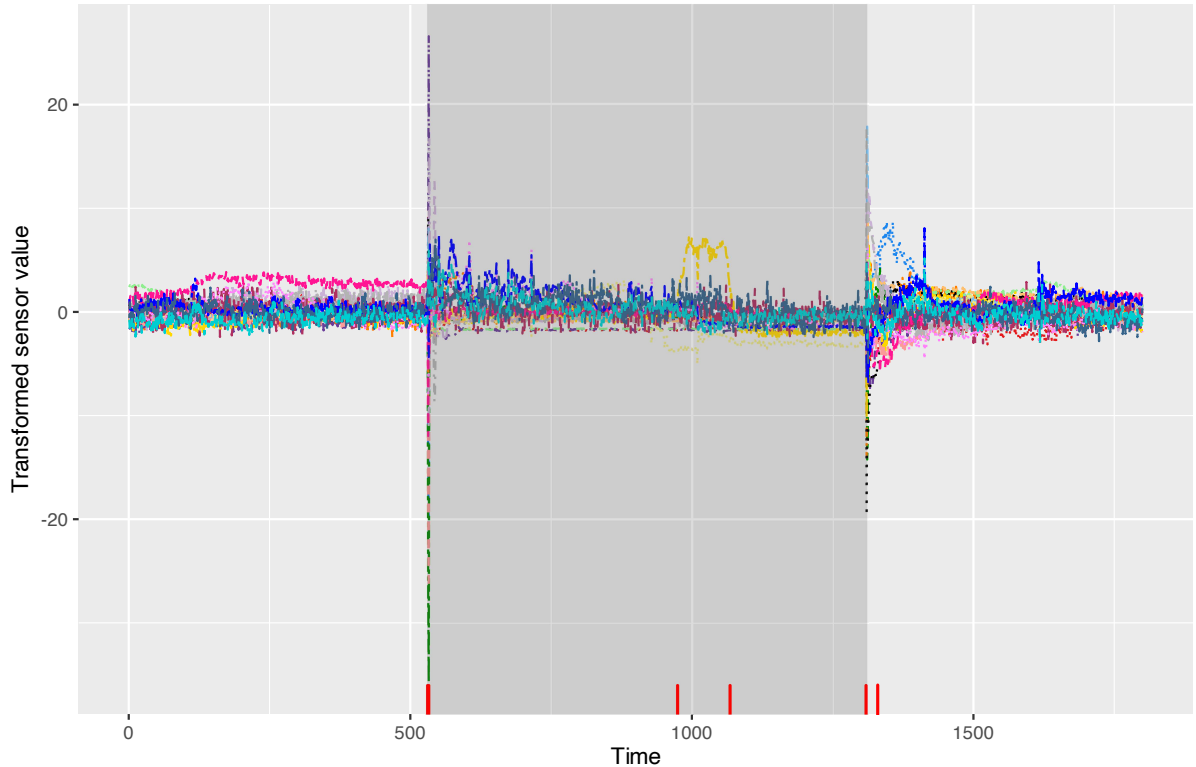


Figure 5: Vibration sensor measurements with detected changepoints indicated by red ticks. Grey areas indicate time intervals in which the plant is starting, stopping or off.

The data generating mechanism of the data is undeniably in violation of several underlying assumptions of ESAC. Importantly, the data are highly cross-correlated and auto-regressive. Moreover, the measurements in the data set are influenced by contextual variables such as power output, guide vane opening, and other (human controlled) running conditions in a complex manner. This dependence on contextual variables should ideally be modeled carefully, although such modeling is outside the scope of this paper. As a remedy, we instead transform the observed data by right multiplying each observed data point X_i by $\widehat{\Sigma}^{-1/2}$. Here, $\widehat{\Sigma}$ is the estimated variance-covariance matrix of X_i , estimated from an independent data set with 5992 observations, in which running conditions are stable (i.e. with no changes in operation mode). Moreover, we choose the penalty function $\gamma(t)$ empirically as described in Appendix B, using false probability rate $\varepsilon = 0.01$ and letting each of the $N = 1000$ Monte Carlo samples $X^{(j)}$ have independent entries following a t_5 distribution. This choice of penalty function ensures that ESAC is rather conservative in declaring changepoints.

The Monte Carlo simulation for generating the penalty function $\lambda(t)$ took 2 minutes and 2 seconds. Applying ESAC to the data took 0.035 seconds, resulting in six estimated changepoints, at locations 531, 533, 974, 1067, 1308, and 1330. Figure 5 displays the 20 transformed sensor measurements over the sampling period, with estimated changepoint locations indicated by red ticks on the x axis. The grey rectangle in the plot indicate the times at which the plant is either starting, stopping, or off. From the Figure, we clearly see that the first, second and fifth and sixth identified changepoint are associated with a change in operation mode of the plant. Interestingly, the other two changepoints, located at time points 974, 1067, are not associated with a change in running conditions. These changepoints are likely declared by ESAC due to the sudden shift in the yellow curves occurring at time 974 and reverting back again at time 1067.

Acknowledgement

We thank Idris Eckley, Arnaldo Frigessi and Nils Lid Hjort for constructive discussions and feedback. We also thank Camilla Feurst and Statkraft for providing the data used in our real-life example. This project has been partially funded by the centre BigInsight, Norwegian Research Council, project number 237718.

References

- Céline Cunen, Nils Lid Hjort, and Håvard Mogleiv Nygård. Statistical sightings of better angels: Analysing the distribution of battle-deaths in interstate conflict over time. *Journal of Peace Research*, 57(2):221–234, 2020.
- Zhenguo Gao, Pang Du, Ran Jin, and John L. Robertson. Surface temperature monitoring in liver procurement via functional variance change-point analysis. *The Annals of Applied Statistics*, 14(1): 143–159, 2020.
- Martin Tveten, Idris A. Eckley, and Paul Fearnhead. Scalable change-point and anomaly detection in cross-correlated data with an application to condition monitoring. *The Annals of Applied Statistics*, 16(2):721 – 743, 2022.
- R. Killick, P. Fearnhead, and I. A. Eckley. Optimal detection of changepoints with a linear computational cost. *Journal of the American Statistical Association*, 107(500):1590–1598, 2012.
- Piotr Fryzlewicz. Wild binary segmentation for multiple change-point detection. *The Annals of Statistics*, 42(6):2243–2281, 2014.
- Rafal Baranowski, Yining Chen, and Piotr Fryzlewicz. Narrowest-over-threshold detection of multiple change points and change-point-like features. *Journal of the Royal Statistical Society: Series B (Statistical Methodology)*, 81(3):649–672, 2019.
- S Kovács, P Bühlmann, H Li, and A Munk. Seeded binary segmentation: a general methodology for fast and optimal changepoint detection. *Biometrika*, 110(1):249–256, 2022.
- Daren Wang, Yi Yu, and Alessandro Rinaldo. Univariate mean change point detection: Penalization, CUSUM and optimality. *Electronic Journal of Statistics*, 14(1):1917 – 1961, 2020.
- Tengyao Wang and Richard J. Samworth. High dimensional change point estimation via sparse projection. *Journal of the Royal Statistical Society: Series B (Statistical Methodology)*, 80(1):57–83, 2018.
- Haeran Cho and Piotr Fryzlewicz. Multiple-change-point detection for high dimensional time series via sparsified binary segmentation. *Journal of the Royal Statistical Society. Series B (Statistical Methodology)*, 77(2):475–507, 2015.
- Haeran Cho. Change-point detection in panel data via double CUSUM statistic. *Electronic Journal of Statistics*, 10(2):2000–2038, 2016.
- S. O. Tickle, I. A. Eckley, and P. Fearnhead. A computationally efficient, high-dimensional multiple changepoint procedure with application to global terrorism incidence. *Journal of the Royal Statistical Society: Series A (Statistics in Society)*, 184(4):1303–1325, 2021.
- Haoyang Liu, Chao Gao, and Richard J. Samworth. Minimax rates in sparse, high-dimensional change point detection. *The Annals of Statistics*, 49(2):1081–1112, 2021.

Per August Jarval Moen. *HDCD: High-Dimensional Changepoint Detection*, 2023. URL <https://CRAN.R-project.org/package=HDCD>. R package version 1.0.

Emmanuel Pilliat, Alexandra Carpentier, and Nicolas Verzelen. Optimal multiple change-point detection for high-dimensional data. *Electronic Journal of Statistics*, 17(1):1240 – 1315, 2023.

Haeran Cho and Piotr Fryzlewicz. *hdbinseg: Change-Point Analysis of High-Dimensional Time Series via Binary Segmentation*. Github, 2018. URL <https://CRAN.R-project.org/package=hdbinseg>.

Sam Tickle. Subset. <https://github.com/SOTickle/SUBSET>, 2022. URL <https://github.com/SOTickle/SUBSET>. Github repository. Downloaded 2022-08-24.

M. R. Sampford. Some Inequalities on Mill’s Ratio and Related Functions. *The Annals of Mathematical Statistics*, 24(1):130–132, 1953.

Lucien Birgé. An alternative point of view on Lepski’s method. *State of the art in probability and statistics*, 36:113–134, January 2001.

Moshe Shaked and J. George Shanthikumar. *Stochastic Orders*. Springer Series in Statistics. Springer-Verlag New York, 1st edition edition, 2007. ISBN 978-0-387-34675-5.

Appendices

A Proofs of main results

Proof of Proposition 3.1. Set $c_1 = 6 + 2 \log(8/\varepsilon)/\log(2)$, $c_2 = 12 + 2(\log(1/\varepsilon))^{1/2} + 2 \log(1/\varepsilon)$ and $\gamma_0 = 9(c_1 + c_1^{1/2} \exp(-1)) + c_2$. Note first that I has cardinality no larger than n^3 . By a union bound, it thus suffices to show that $\mathbb{P}(S_{\gamma, (s, e]} > 0) \leq \varepsilon n^{-3}$ for any $(s, e) \subseteq I$.

So fix any $(s, e) \subseteq I$. Let $t \in \mathcal{T} \setminus \{p\}$ (the case $t = p$ is handled later), and fix $x_t > 0$ (to be specified shortly). Since (s, e) does not contain any changepoint, we must have $C_{(s, e]}^v(i) \stackrel{\text{i.i.d.}}{\sim} \mathcal{N}(0, 1)$ for all $i \in [p]$. By Lemma 5.2 we have that

$$\sum_{i=1}^p \left\{ C_{(s, e]}^v(i)^2 - \nu_{a(t)} \right\} \mathbb{1} \left\{ \left| C_{(s, e]}^v(i) \right| > a(t) \right\} \geq 9 \left[\left\{ p e^{-a(t)^2/2} x_t \right\}^{1/2} + x_t \right]$$

with probability at most e^{-x_t} . Now set $x_t = c_1 \left\{ \frac{p \log^2(n)}{t^2} \wedge r(t) \right\}$ for all t . Then,

$$\sum_{t \in \mathcal{T} \setminus \{p\}} e^{-x_t} \leq \sum_{t \in \mathcal{T} \setminus \{p\}} \exp \left\{ -c_1 \frac{p \log^2(n)}{t^2} \right\} + \sum_{t \in \mathcal{T} \setminus \{p\}} \exp \{-c_1 r(t)\}.$$

For the first sum, we have

$$\begin{aligned}
\sum_{t \in \mathcal{T} \setminus \{p\}} \exp \left\{ -c_1 \frac{p \log^2(n)}{t^2} \right\} &\leq \sum_{k=0}^{\infty} \exp \left\{ -c_1 \log(n) 4^k \right\} \\
&= \sum_{k=0}^{\infty} \left(\frac{1}{n^{c_1}} \right)^{4^k} \\
&\leq n^{-c_1} + n^{-c_1} \sum_{k=1}^{\infty} \left(\frac{1}{n^{c_1}} \right)^{3k} \\
&= 2n^{-c_1}.
\end{aligned}$$

For the second sum, noting that $c_1 r(t) = c_1 \left\{ t \log \left(\frac{ep \log n}{t^2} \right) \vee \log n \right\} \geq (c_1/2)t \log \left(\frac{ep \log n}{t^2} \right) + (c_1/2) \log n$, we have

$$\begin{aligned}
\sum_{t \in \mathcal{T} \setminus \{p\}} \exp \{-c_1 r(t)\} &\leq n^{-c_1/2} \exp(-c_1/2) \sum_{t \in \mathcal{T} \setminus \{p\}} \left(\frac{t^2}{ep \log n} \right)^{c_1 t/2} \\
&\leq n^{-c_1/2} \exp(-c_1/2) \left(1 + \sum_{k=1}^{\infty} 4^{-c_1 k/2} \right) \\
&\leq 2n^{-c_1/2}.
\end{aligned}$$

With this choice of x_t , we thus have that

$$\sum_{t \in \mathcal{T} \setminus \{p\}} e^{-x_t} \leq 4n^{-c_1/2},$$

using that $c_1 > 1$. Moreover, using that $a^2(t) = 4 \log \left(\frac{ep \log n}{t^2} \right)$, we have that

$$\begin{aligned}
9 \left[\left\{ p e^{-a^2(t)/2} x_t \right\}^{1/2} + x_t \right] &= 9 \left[\left\{ p \frac{t^4}{e^2 p^2 \log^2 n} x_t \right\}^{1/2} + x_t \right] \\
&\leq 9 \left\{ \frac{t c_1^{1/2}}{e} + c_1 r(t) \right\} \\
&\leq 9 \left(c_1^{1/2} \exp(-1) + c_1 \right) r(t),
\end{aligned}$$

where we used that $x_t \leq c_1 r(t)$ and $x_t \leq c_1 p \log^2(n)/t^2$, as well as the fact that $t \leq r(t)$ whenever $t \leq (p \log n)^{1/2}$. Recalling that $\gamma(t) = \gamma_0 r(t)$, since $\gamma_0 > 9 \left(c_1 + c_1^{1/2} \exp(-1) \right)$, a union bound gives

$$\begin{aligned}
&\mathbb{P}(\exists t \in \mathcal{T} \setminus \{p\}; S_{\gamma, (s, e]}(t) \geq 0) \\
&= \mathbb{P} \left[\exists t \in \mathcal{T} \setminus \{p\}; \sum_{i=1}^p \left\{ C_{(s, e]}^v(i)^2 - \nu_{a(t)} \right\} \mathbb{1} \left\{ |C_{(s, e]}^v(i)| > a(t) \right\} \geq \gamma_0 r(t) \right] \\
&\leq 4n^{-c_1/2} \\
&\leq 4n^{-3 - \log(8/\varepsilon)/\log(2)} \\
&\leq 4n^{-3} \exp(-\log(8/\varepsilon) \log(n)/\log(2)) \\
&\leq n^{-3} \varepsilon/2,
\end{aligned}$$

where we in the last inequality used that $n \geq 2$.

Now consider the case where $t = p$. If $p \leq (p \log n)^{1/2}$, then similarly as above we have that

$$\mathbb{P} (S_{\gamma, (s, e]}(p) \geq 0) \leq n^{-3} \varepsilon / 2.$$

If we instead have $p > (p \log n)^{1/2}$ (in which case $a(p) = 0$ and $\nu_{a(p)} = 1$), then

$$\sum_{i=1}^p \left\{ C_{(s, e]}^v(i)^2 - \nu_{a(p)} \right\} \mathbb{1} \left\{ |C_{(s, e]}^v(i)| > a(p) \right\} = \sum_{i=1}^p C_{(s, e]}^v(i)^2 - p.$$

As $\sum_{i=1}^p C_{(s, e]}^v(i)^2 \sim \chi_p^2$, we obtain from Lemma 5.4 that

$$\mathbb{P} \left\{ \sum_{i=1}^p C_{(s, e]}^v(i)^2 - p > 2(p \log(2n^3/\varepsilon))^{1/2} + 2 \log(2n^3/\varepsilon) \right\} \leq n^{-3} \varepsilon / 2.$$

Now,

$$\begin{aligned} 2(p \log(2n^3/\varepsilon))^{1/2} + 2 \log(2n^3/\varepsilon) &\leq 2(p \log(n^4/\varepsilon))^{1/2} + 2 \log(n^4/\varepsilon) \\ &\leq 4(p \log n)^{1/2} + 2(p \log(1/\varepsilon))^{1/2} + 8 \log n - 2 \log(\varepsilon) \\ &\leq r(p) \left(12 + 2(\log(1/\varepsilon))^{1/2} + 2 \log(1/\varepsilon) \right) \\ &= c_2 r(p) \\ &< \gamma_0 r(p), \end{aligned}$$

using that $n \geq 2$, $r(p) \geq 1$, and $r(p) = (p \log n)^{1/2} \geq \log n$ whenever $p \geq (p \log n)^{1/2}$. Hence,

$$\mathbb{P} \left\{ \sum_{i=1}^p C_{(s, e]}^v(i)^2 - p > \gamma_0 r(p) \right\} \leq n^{-3} \varepsilon / 2.$$

We conclude that

$$\begin{aligned} \mathbb{P} \left(\max_{(s, e) \in I} S_{\gamma, (s, e]} > 0 \right) &\leq n^3 \mathbb{P} (\exists t \in \mathcal{T} ; S_{\gamma, (s, e]}(t) \geq 0) \\ &\leq n^3 (n^{-3} \varepsilon / 2 + n^{-3} \varepsilon / 2) \\ &= \varepsilon, \end{aligned}$$

and we are done. \square

Proof of Theorem 3.2. Let $\lambda_0 \geq 63$, $\lambda(t) = \lambda_0 r(t)$, $C_1 = 2 \left\{ 2(4\lambda_0 + 242)^{1/2} + 2\lambda_0 + 123 \right\}$ and $C_0 > C_1$. Let $\hat{\eta} \in \arg \max_{0 < v < n} S_{\lambda}^v$, where S_{λ}^v is defined as in (6), and let $S^v(t)$ be defined as in (3). Let the CUSUM transformation $T_{(s, e]}^v(\cdot)$ be defined as in (2), and for ease of notation, let $T^v(\cdot) = T_{(0, n]}^v(\cdot)$. Let $\mathcal{K} = \{i ; \mu_{i, \eta+1} - \mu_{i, \eta} \neq 0\}$ denote the set of coordinates for which there is a change in mean, and for any $0 < v < n$ let $\beta_v = \sum_{i \in \mathcal{K}} \{T^v(\mu_{i, \cdot})^2 - T^v(\mu_{i, \cdot})\}$. Let \bar{k} denote the smallest element in \mathcal{T} such that $\bar{k} \geq k$. We may without loss of generality take $\sigma = 1$, as we can otherwise normalize the data matrix X and replace the squared norm of the change in mean φ^2 by φ^2/σ^2 .

Consider the event $\mathcal{E} = \mathcal{E}_1 \cap \mathcal{E}_2 \cap \mathcal{E}_3 \cap \mathcal{E}_4$ as defined in Lemma 5.5, for which we know that $\mathbb{P}(\mathcal{E}) \geq 1 - \frac{1}{n}$. On the event \mathcal{E} , we will show that any $0 < v < n$ such that $|v - \eta| > C_1 h(k)/\varphi^2$ must satisfy $S_{\lambda}^{\eta} > S_{\lambda}^v$, which implies that $|\hat{\eta}_{\lambda} - \eta| \leq C_1 h(k)/\varphi^2$.

Fix some $0 < v < n$ and let $t^* \in \arg \max_{t \in \mathcal{T}} S_\lambda^v(t)$, so that $S_\lambda^v = S_\lambda^v(t^*)$. We claim that

$$S_\lambda^\eta - S_\lambda^v \geq \beta_v - 2 \{2\beta_v h(k)\}^{1/2} - (119 + 2\lambda_0)h(k). \quad (13)$$

To see this, suppose first that $k \leq (p \log n)^{1/2}$. We have that

$$\begin{aligned} S_\lambda^\eta - S_\lambda^v &\geq S_\lambda^\eta(\bar{k}) - S_\lambda^v(t^*) \\ &= \sum_{i=1}^p \left[\left(C^\eta(i)^2 - \nu_{a(\bar{k})} \right) \mathbb{1}\{|C^\eta(i)| > a(\bar{k})\} - \left(C^v(i)^2 - \nu_{a(t^*)} \right) \mathbb{1}\{|C^v(i)| > a(t^*)\} \right] \\ &\quad - \lambda_0 r(\bar{k}) + \lambda_0 r(t^*). \end{aligned}$$

For any $x \in \mathbb{R}$ and any $t \in \mathcal{T}$, we have $x^2 - \nu_{a(t)} \leq (x^2 - \nu_{a(t)}) \mathbb{1}\{|x| > a(t)\} \leq x^2$, and so

$$\begin{aligned} S_\lambda^\eta - S_\lambda^v &\geq \sum_{i \in \mathcal{K}} [C^\eta(i)^2 - C^v(i)^2] - k\nu_{a(\bar{k})} \\ &\quad + \sum_{i \in [p] \setminus \mathcal{K}} \left[\left(C^\eta(i)^2 - \nu_{a(\bar{k})} \right) \mathbb{1}\{|C^\eta(i)| > a(\bar{k})\} - \left(C^v(i)^2 - \nu_{a(t^*)} \right) \mathbb{1}\{|C^v(i)| > a(t^*)\} \right] \\ &\quad - \lambda_0 r(\bar{k}) + \lambda_0 r(t^*). \end{aligned}$$

On the event $\mathcal{E}_1 \cap \mathcal{E}_2 \cap \mathcal{E}_3 \supseteq \mathcal{E}$ we therefore have that

$$\begin{aligned} S_\lambda^\eta - S_\lambda^v &\geq \beta_v - 2 \{2\beta_v \log n\}^{1/2} - 16r(k) - 35r(\bar{k}) \\ &\quad - (63 - \lambda_0)r(t^*) - \lambda_0 r(\bar{k}) - k\nu_{a(\bar{k})} \\ &\geq \beta_v - 2 \{2\beta_v r(k)\}^{1/2} - (92 + 2\lambda_0)r(k), \end{aligned}$$

where we have used that $\lambda_0 \geq 63$, $\log n \leq r(k)$, $r(\bar{k}) \leq 2r(k)$, and for $k \leq (p \log n)^{1/2}$, we have $k\nu_{a(\bar{k})} \leq k(2 + a^2(\bar{k})) \leq 2k + ka^2(k) \leq 6r(k)$. Since $r(k) \leq h(k)$ for all $k \in [p]$, the claim (13) holds whenever $k \leq (p \log n)^{1/2}$.

Now suppose $k > (p \log n)^{1/2}$. By the definition of \mathcal{E}_4 , we have that $S_\lambda^v(t^*) - S_\lambda^v(p) \leq 5h(p) + 63r(t^*) - \lambda_0 r(t^*) + \lambda_0 r(p)$. Hence,

$$\begin{aligned} S_\lambda^\eta - S_\lambda^v &\geq S_\lambda^\eta(p) - S_\lambda^v(t^*) \\ &= S_\lambda^\eta(p) - S_\lambda^v(p) + S_\lambda^v(p) - S_\lambda^v(t^*) \\ &\geq S_\lambda^\eta(p) - S_\lambda^v(p) - 5h(p) - 63r(t^*) + \lambda_0 r(t^*) - \lambda_0 r(p) \\ &= \sum_{i=1}^p \{C^\eta(i)^2 - C^v(i)^2\} - 5h(p) - 63r(t^*) + \lambda_0 r(t^*) - \lambda_0 r(p). \end{aligned}$$

On the event \mathcal{E} we thus have that

$$\begin{aligned} S_\lambda^\eta - S_\lambda^v &\geq \beta_v - 2 \{2\beta_v \log n\}^{1/2} - 16r(p) - 63r(p) - 35r(p) - 5h(p) \\ &\quad - 63r(t^*) + \lambda_0 r(t^*) - \lambda_0 r(p) \\ &\geq \beta_v - 2 \{\beta_v h(p)\}^{1/2} - (119 + \lambda_0)h(p), \end{aligned}$$

where we in the last inequality used that $r(k) \leq h(k)$ for all k and $\lambda_0 \geq 63$. Hence (13) holds whenever $k > (p \log n)^{1/2}$. Solving the quadratic inequality (13) with respect to β_v , we obtain that $S_\lambda^\eta - S_\lambda^v > 0$ if

$$\beta_v > \left\{ 2(4\lambda_0 + 242)^{1/2} + 2\lambda_0 + 123 \right\} h(k). \quad (14)$$

Without loss of generality we may assume $v \geq \eta$ (the converse case is similar). By Lemma 5.11 we have that

$$\begin{aligned}\beta_v &= \sum_{i \in \mathcal{K}} \{T^\eta(\mu_{i,\cdot})^2 - T^v(\mu_{i,\cdot})^2\} \\ &= \frac{|v - \eta|\eta}{|v - \eta| + \eta} \varphi^2 \\ &\geq \frac{1}{2} \min(|v - \eta|, \eta) \varphi^2,\end{aligned}$$

and therefore (14) is satisfied if

$$\begin{aligned}\min(|v - \eta|, \eta) &> 2 \left\{ 2(4\lambda_0 + 242)^{1/2} + 2\lambda_0 + 123 \right\} \frac{h(k)}{\varphi^2} \\ &= C_1 \frac{h(k)}{\varphi^2}.\end{aligned}\tag{15}$$

By the assumption $C_0 > C_1$, η is strictly larger than the right hand side of (15). Therefore (14) is satisfied if

$$|v - \eta| > C_1 \frac{h(k)}{\varphi^2}.$$

Hence, if $|\eta - v| > C_1 h(k)/\varphi^2$, we must have $S_\lambda^\eta > S_\lambda^v$, and the proof is complete. \square

Proof of Theorem 3.3. Let $\gamma_0 \geq 82$, $\gamma(t) = \gamma_0 r(t)$ and define $C_1 = 32 \left\{ \gamma_0 + 170 + 8(2\gamma_0 + 276)^{1/2} \right\}$ and $C_0 = 2C_1$. We may without loss of generality take $\sigma = 1$, as we can otherwise normalize the data matrix X and replace the squared norm of the change in mean φ^2 by φ^2/σ^2 . Let $\mathcal{M} = \{(s_m, e_m); m \in [M]\}$ denote the (enumerated) collection of seeded intervals generated by Algorithm 4. In the following, we will use the name ESAC to refer to either Algorithm 2 or 3. We work on the event $\mathcal{E} = \mathcal{E}_5 \cap \mathcal{E}_6$ as defined in Lemma 5.6, for which we know that $\mathbb{P}(\mathcal{E}) \geq 1 - 1/n$. The proof goes as follows. In step 1 we show that each changepoint η_j will be detected using a seeded interval with certain properties. In step 2, by an inductive argument, we show that ESAC detects all changepoints within the given error-rate.

Step 1. We first claim that, for each $j \in [J]$, there exists a seeded interval $(s_{\tilde{m}}, e_{\tilde{m}}] = (v - l, v + l] \in \mathcal{M}$ such that the following holds

- (P1) $C_1 r(k_j)/(4\varphi_j^2) \leq l \leq C_1 r(k_j)/(2\varphi_j^2) \vee 1$;
- (P2) $|\eta_j - v| \leq l/2$;
- (P3) $s_{\tilde{m}} \geq \eta_j - (\Delta_j/2 \vee 1)$;
- (P4) $e_{\tilde{m}} \leq \eta_j + (\Delta_j/2 \vee 1)$;
- (P5) $S_{\gamma, (s_{\tilde{m}}, e_{\tilde{m}}]}^v \geq 0$.

To see this, fix any $j \in [J]$, and let $h = C_1 r(k_j)/(2\varphi_j^2)$. Now let $(s_{\tilde{m}}, e_{\tilde{m}}] = (v - l, v + l]$ denote the seeded interval from Lemma 5.7. Then properties (P1) and (P2) follow immediately. Moreover, as $\varphi_j^2 \Delta_j \geq C_0 r(k_j)$ (by the signal-to-noise ratio assumption (12) in Theorem 3.3) and $C_0 \geq 2C_1$, we have

$h \leq \Delta_j/4$. The properties (P3) and (P4) then follow from Lemma 5.7. To show the last property (P5), observe first that

$$S_{\gamma, (s_{\tilde{m}}, e_{\tilde{m}}]}^v \geq \beta_{(s_{\tilde{m}}, e_{\tilde{m}}]}^v - 8 \left\{ 2\beta_{(s_{\tilde{m}}, e_{\tilde{m}}]}^v r(k_j) \right\}^{1/2} - (\gamma_0 + 106) r(k_j),$$

on the event \mathcal{E} , where $\beta_{(s_{\tilde{m}}, e_{\tilde{m}}]}^v = \sum_{i=1}^p T_{(s_{\tilde{m}}, e_{\tilde{m}}]}^v(\mu_{i,\cdot})^2$. By solving the quadratic inequality, we obtain that $S_{\gamma, (s_{\tilde{m}}, e_{\tilde{m}}]}^v \geq 0$ whenever

$$\begin{aligned} \beta_{(s_{\tilde{m}}, e_{\tilde{m}}]}^v &\geq \left\{ \gamma_0 + 170 + 8(2\gamma_0 + 276)^{1/2} \right\} r(k_j) \\ &= C_1/32r(k_j). \end{aligned}$$

Assume without loss of generality that $\eta_j \leq v$ (the converse case is similar). By the definition of the CUSUM, and using that $|\eta_j - v| \leq l/2$, we get that

$$\begin{aligned} \beta_{(s_{\tilde{m}}, e_{\tilde{m}}]}^v &= \frac{v - s_{\tilde{m}}}{(e_{\tilde{m}} - s)(e_{\tilde{m}} - v)} (e_{\tilde{m}} - \eta_j)^2 \varphi_j^2 \\ &\geq \frac{1}{2l} (l/2)^2 \varphi_j^2 \\ &= l\varphi_j^2/8. \end{aligned}$$

Since $l \geq C_1 r(k_j)/(4\varphi_j^2)$, we must have that $\beta_{(s_{\tilde{m}}, e_{\tilde{m}}]}^v \geq C_1/32r(k_j)$, which implies (P5).

Step 2. We continue the proof as follows. By induction, with some slight abuse of notation, it suffices to consider any integer interval $(s, e] \subseteq (0, n]$ such that

$$\eta_{h-1} \leq s < \eta_h < \dots < \eta_{h+q} < e \leq \eta_{q+h+1},$$

for some $q \geq -1$, and, whenever $q > -1$,

$$\begin{aligned} s &\leq \eta_h - \Delta_h/2; \\ e &\geq \eta_{h+q} + \Delta_{h+q}/2. \end{aligned}$$

Note that $q = -1$ corresponds to there being no changepoint in the open integer interval (s, e) . We consider this case first. For any seeded interval $(s_m, e_m] \subseteq (s, e]$ and any $s_m < v < e_m$, we will have that $S_{\gamma, (s_m, e_m]}^v < 0$, due to the definition of the event \mathcal{E} . Hence no changepoint will be declared by ESAC in this case.

Now consider the case where $q > -1$. Note first that a changepoint will be declared by the ESAC algorithm. Indeed, for the h th changepoint we may take $(s_{\tilde{m}}, e_{\tilde{m}}]$ as in step 1, for which the properties (P3) and (P4) imply that $(s_{\tilde{m}}, e_{\tilde{m}}] \subseteq (s, e]$, due to the inductive hypothesis. By property (P5), we know that $S_{\gamma, (s_{\tilde{m}}, e_{\tilde{m}}]}^v \geq 0$, and hence a changepoint will be detected in (s, e) . This implies that $\mathcal{O}_{(s, e]}$, as defined in the ESAC algorithm, satisfies $\mathcal{O}_{(s, e]} \neq \emptyset$. Now let m^* , v^* and l^* be as defined in the ESAC algorithm. Note that (s_{m^*}, e_{m^*}) must contain a changepoint, say η_j , as we by the definition of \mathcal{E} otherwise would have had $S_{\gamma, (s_{m^*}, e_{m^*})}^v < 0$ for any $s_{m^*} < v < e_{m^*}$. Further, since ESAC uses the narrowest possible seeded interval to estimate a changepoint, we must have that $l^* = (e_{m^*} - s_{m^*})$ satisfies $l^* \leq e_{\tilde{m}} - s_{\tilde{m}} \leq C_1 r(k_j)/(\varphi_j^2) \vee 2$, where $(s_{\tilde{m}}, e_{\tilde{m}}]$ is the seeded interval as in the claim for η_j . Since $s_{m^*} < v^* < e_{m^*}$, it then follows that

$$|v^* - \eta_j| \leq \left\{ C_1 r(k_j)/\varphi_j^2 \vee 2 \right\} - 2 \leq C_1 \frac{r(k_j)}{\varphi_j^2}.$$

It remains to show that the two new segments in the recursive step, $(s, s_{m^*} + 1]$ and $(e_{m^*} - 1, e]$ satisfy the inductive hypothesis. Without loss of generality consider $(s, s_{m^*} + 1]$ (the argument for the other interval is similar), and suppose that $j \geq h + 1$ (otherwise there is nothing to show). To show that the inductive hypothesis holds for $(s, s_{m^*} + 1]$, it suffices to show that $s_{m^*} + 1 \geq \eta_{j-1} + \Delta_{j-1}/2$. As $\eta_j \in (s_{m^*}, e_{m^*})$, we must have $e_{m^*} \geq \eta_j + 1$. Hence

$$\begin{aligned}
s_{m^*} + 1 &= e_{m^*} + 1 - l^* \\
&\geq \eta_j + 2 - \{C_1 r(k_j)/\varphi_j^2 \vee 2\} \\
&= \eta_{j-1} + (\eta_j - \eta_{j-1}) - \{C_1 r(k_j)/\varphi_j^2 - 2 \vee 0\} \\
&\geq \eta_{j-1} + (\eta_j - \eta_{j-1}) - \Delta_j/2 \\
&\geq \eta_{j-1} + (\eta_j - \eta_{j-1})/2 \\
&\geq \eta_{j-1} + \Delta_{j-1}/2,
\end{aligned}$$

where we in the first inequality used that $l^* = (e_{m^*} - s_{m^*}) \leq C_1 r(k_j)/\varphi_j^2 \vee 2$ and in the second inequality used that the signal-to-noise ratio condition (12) implies $C_1 r(k_j)/\varphi_j^2 \leq \Delta_j/2$. Hence the inductive hypothesis holds for $(s, s_{m^*} + 1]$. \square

Proof of Proposition 3.4. Let \mathcal{M} denote the set of seeded intervals generated from Algorithm 4. Note first that computing and storing the cumulative sum of all rows of X requires $\mathcal{O}(np)$ FLOPs. Once these are stored, the number of FLOPs required to compute $C_{(s,e]}^v(j)$ as in (2) for some $(s, e] \in \mathcal{M}$ and some $s < v < e$ is of order $\mathcal{O}(p)$. Hence, the number of FLOPs required to compute $S_{\lambda, (s,e]}^v$ is of order $p|\mathcal{T}| = \mathcal{O}\{p \log(p \log n)\}$. In the best case there are $n - 1$ changepoints detected by the ESAC algorithm using all $n - 1$ intervals $(s, e] \in \mathcal{M}$ such that $e - s = 2$. In this case, the total number of FLOPs executed before ESAC terminates is of order $\mathcal{O}\{np + np \log(p \log n)\} = \mathcal{O}\{np \log(p \log n)\}$. In the worst case there are no changepoints detected by ESAC, in which case $S_{\lambda, (s,e]}^v$ has to be computed over each triple of integers s, v, e such that $s < v < e$ and $(s, e] \in \mathcal{M}$. By Lemma 5.9, there are at most $\mathcal{O}(n \log n)$ distinct such triples. Hence the number of FLOPs executed before ESAC terminates in this case is of order $\mathcal{O}\{np \log n \log(p \log n)\}$. \square

B Implementation details

To apply ESAC in practice, a choice must be made regarding the penalty functions λ, γ , estimation of σ , as well as the parameters α and K controlling the generation of seeded intervals. In this subsection we discuss these issues in turn, but first, we define two variants of ESAC as well as our algorithm for generating seeded intervals.

B.1 Slight modifications to ESAC

Algorithm 2 constitutes the variant of the ESAC algorithm that features interval trimming. Here, the recursive step in the algorithm (the third and second last lines) differ from those found in 1. When Algorithm 2 declares a changepoint at location v^* , detected in the interval (s^*, e^*) , the remaining elements in interval (s^*, e^*) are never again used to detect or estimate changepoints.

A faster variant of Algorithm 2 is given by Algorithm 3. Algorithm 3 reduces the execution time by modifying step 3 in Algorithm 2 to only evaluate $S_{\gamma, (s_m, e_m]}^v$ at the mid-point $v_m = (s_m + e_m)/2$ of any seeded interval. Interestingly, the theoretical guarantees given by Theorem 3.3 also hold for this variant of ESAC, unlike Algorithm 1. Note that the same modification can naturally be made to Algorithm 1 as well. In practice, we have experienced that Algorithm 3 has much lower power for detecting changepoints compared to 1. We therefore only recommend using Algorithm 3 when the consequent reduction in computational cost is necessary.

Algorithm 2 ESAC'(X, (s, e], M, B, γ, λ).

Input: Matrix of observations $X \in \mathbb{R}^{p \times n}$, left open and right closed integer interval $(s, e]$ in which candidate changepoints are searched for, an enumerated collection $\mathcal{M} = \{(s_m, e_m] ; m \in [M]\}$ of M half open integer sub intervals of $\{0, \dots, n\}$, a set of already detected changepoints \mathcal{B} , and penalty functions $\gamma(t), \lambda(t)$.

Output: Set \mathcal{B} of detected changepoints.

```
if  $e - s \leq 1$ :
    stop
set  $\mathcal{M}_{(s,e]} = \{m \in [M] : (s_m, e_m] \subset (s, e]\}$ 
set  $\mathcal{O}_{(s,e]} = \left\{ m \in \mathcal{M}_{(s,e]} : \max_{s_m < v < e_m} S_{\gamma, (s_m, e_m]}^v > 0 \right\}$ 
if  $\mathcal{O}_{(s,e]} = \emptyset$ 
    stop
set  $l^* = \min_{m \in \mathcal{O}_{(s,e]}} |e_m - s_m|$ 
set  $\mathcal{O}_{l^*} = \{m \in \mathcal{O}_{(s,e]} : |e_m - s_m| = l^*\}$ 
set  $m^* = \operatorname{argmax}_{m \in \mathcal{O}_{l^*}} \max_{s_m < v < e_m} S_{\lambda, (s_m, e_m]}^v$ 
set  $v^* = \operatorname{argmax}_{s_{m^*} < v < e_{m^*}} S_{\lambda, (s_{m^*}, e_{m^*})}^v$ 
 $\mathcal{B} \leftarrow \mathcal{B} \cup \{v^*\}$ 
 $\mathcal{B} \leftarrow \text{ESAC}'(X, (s, s_{m^*} + 1], \mathcal{M}, \mathcal{B}, \gamma, \lambda)$ 
 $\mathcal{B} \leftarrow \text{ESAC}'(X, (e_{m^*} - 1, e], \mathcal{M}, \mathcal{B}, \gamma, \lambda)$ 
return  $\mathcal{B}$ 
```

Algorithm 3 ESAC''(X, (s, e], M, B, γ, λ)

Input: Matrix of observations $X \in \mathbb{R}^{p \times n}$, left open and right closed integer interval $(s, e]$ in which candidate changepoints are searched for, an enumerated collection $\mathcal{M} = \{(s_m, e_m] ; m \in [M]\}$ of M half open integer sub intervals of $\{0, \dots, n\}$, a set of already detected changepoints \mathcal{B} , and penalty parameters γ, λ .

Output: Set \mathcal{B} of detected changepoints.

```
if  $e - s \leq 1$ 
    stop
set  $\mathcal{M}_{(s,e]} = \{m \in [M] : (s_m, e_m] \subset (s, e]\}$ 
set  $v_m = \lfloor \frac{s_m + e_m}{2} \rfloor$  for all  $m = 1, \dots, M$ 
set  $\mathcal{O}_{(s,e]} = \left\{ m \in \mathcal{M}_{(s,e]} : S_{\gamma, (s_m, e_m]}^{v_m} > 0 \right\}$ 
if  $\mathcal{O}_{(s,e]} = \emptyset$ 
    stop
set  $l^* = \min_{m \in \mathcal{O}_{(s,e]}} |e_m - s_m|$ 
set  $\mathcal{O}_{l^*} = \{m \in \mathcal{O}_{(s,e]} : |e_m - s_m| = l^*\}$ 
set  $m^* = \operatorname{argmax}_{m \in \mathcal{O}_{l^*}} \max_{s_m < v < e_m} S_{\lambda, (s_m, e_m]}^v$ 
set  $v^* = \operatorname{argmax}_{s_{m^*} < v < e_{m^*}} S_{\lambda, (s_{m^*}, e_{m^*})}^v$ 
 $\mathcal{B} \leftarrow \mathcal{B} \cup \{v^*\}$ 
 $\mathcal{B} \leftarrow \text{ESAC}''(X, (s, s_{m^*} + 1], \mathcal{M}, \mathcal{B}, \gamma, \lambda)$ 
 $\mathcal{B} \leftarrow \text{ESAC}''(X, (e_{m^*} - 1, e], \mathcal{M}, \mathcal{B}, \gamma, \lambda)$ 
return  $\mathcal{B}$ 
```

B.2 Efficient implementation of ESAC

The ESAC Algorithms 1, 2 and 3 are based on Narrowest-Over-Threshold selection of changepoints. Once a changepoint is detected in some seeded interval, say of length l^* , the changepoint location is estimated based only on intervals of length l^* . To minimize running time, any version of ESAC should therefore iterate through the seeded intervals $\{(s_m, e_m] : m \in [M]\}$ in the (increasing) order of their width. This computational trick gives significant speed improvements whenever changepoints can be detected by short seeded intervals.

B.3 Choice of α and K

The choice of α and K entails a trade-off between computational cost and statistical performance. As either α^{-1} or K increase, more seeded intervals are generated from Algorithm 4, increasing both the chance of detecting a changepoint and the running time of ESAC. After some experimentation, we have experienced that $\alpha = 3/2$ and $K = 4$ give a decent balance between running time and statistical accuracy.

B.4 Variance re-scaling

In the theoretical analysis of this paper, the noise level σ of each time series is assumed known and common across all p time series. In practice, this is an unrealistic assumption. As is common in the changepoint literature, we suggest estimating the noise level separately for each time series by the (scaled) Median Absolute Deviation (MAD) of first-order differences, as in e.g. Wang and Samworth (2018). If it is reasonable to assume that each time series has approximately the same noise level, the common noise level σ can be estimated for instance by taking a mean or median of the MAD estimates for each time series. Once estimates of the noise levels are obtained, the time series need only to be re-scaled by their estimated noise levels before applying ESAC.

B.5 Analytical choice of penalty functions

Recall that $\lambda(t)$ and $\gamma(t)$ are the penalty functions used in the penalized score statistic for changepoint localization and detection, respectively. The proofs of Theorems 3.2 and 3.3 provide suggestions for analytical choices of these penalty functions. However, we believe the leading constants are overly conservative. To obtain more practical choices of analytical penalizing functions, we have run simulations for combinations of n up to 1000 and p up to 5000. We have experienced that replacing n with n^4 in $a(t)$ (4) and $r(t)$ (8) gives a slightly better balance between the two terms $t \log \left(\frac{ep \log n}{t^2} \right)$ and $\log n$ in $r(t)$. As default values in our R package, as well as in the simulation study, we have replaced n with n^4 in $a(t)$ and $r(t)$. For changepoint estimation, we recommend using the penalty function

$$\tilde{\lambda}(t) = \begin{cases} \frac{3}{2} \left\{ (p \log n^4)^{1/2} + \log n^4 \right\} & \text{if } t \geq (p \log n)^{1/2}, \\ t \log \left(\frac{ep \log n^4}{t^2} \right) + \log n^4 & \text{otherwise.} \end{cases}$$

This recommendation is independent of whether each time series is re-scaled by Median Absolute Deviation (MAD) estimates. The choice of the two leading constants in $\tilde{\lambda}$ are the result of minimizing the Mean Squared Error (MSE) of the estimator (9) over a rough grid of n , p , η and k , where n has ranged from 200 to 1000 and p has ranged from 100 to 5000. For changepoint detection one can also use $\gamma(t) = \tilde{\lambda}(t)$, which in our experience gives a false positive rate of less than $1/n$. If the variance of each time series is re-scaled by MAD estimates, however, we recommend choosing the penalty function $\gamma(t)$ for changepoint detection using Monte Carlo simulation.

B.6 Empirical choice of penalty functions

To obtain exact control over the probability of a false changepoint being detected by ESAC, one can choose the penalty function $\gamma(t)$ by Monte Carlo simulation. Consider any false positive probability $\varepsilon > 0$ and Monte Carlo sample size N . A naive choice of empirical penalty function, denoted by $\hat{\gamma}_\varepsilon(t)$, is given by the following. Let \mathcal{M} denote the collection of seeded intervals to be used by ESAC. Simulate N data sets $(X^{(j)})_{j=1}^N$ following model (1) with no changepoints, in which each row is rescaled by MAD estimates if applicable. For each $t \in \mathcal{T}$, let $\hat{\gamma}_\varepsilon(t)$ denote the $\lceil N(1 - \varepsilon) \rceil$ largest value of $\max_{(s,e] \in \mathcal{M}} \max_{s < v < e} S_{0,(s,e]}^v(X^{(j)})(t)$ over $j = 1, \dots, N$, where $S_{0,(s,e]}^v(X^{(j)})(t)$ is the sparsity-specific score statistic from (3) computed over the seeded interval $(s, e]$ with input matrix $X^{(j)}$ and with penalty function 0.

Due to multiple testing, the approximate false positive probability when using the naive penalty function $\hat{\gamma}_\varepsilon$ can only be upper bounded by $|\mathcal{T}|\varepsilon$. To adjust for multiple testing, a Bonferroni correction can easily be applied by replacing ε by $\varepsilon/|\mathcal{T}|$ in the definition of $\hat{\gamma}_\varepsilon(t)$. In our experience, though, such a Bonferroni correction is too conservative. An alternative approach to handle the multiple testing is to use the empirical penalty function $\hat{\gamma}^*(t) = r(t) \max_{s \in \mathcal{T}} \hat{\gamma}_\varepsilon(s)/r(s)$, in which the functional form is specified and only the leading constant is chosen by Monte Carlo simulation. In our experience, this approach also leads to an overly conservative penalty function, as the functional form of $\hat{\gamma}_\varepsilon(t)$ does not match the theoretical counterpart $r(t)$ exactly. We therefore recommend to use the following penalty function $\tilde{\gamma}(t)$, in which we introduce three separate leading constants for different segments of \mathcal{T} (and consequently a Bonferroni correction) for slightly more flexibility. Let $\tilde{\gamma}(t)$ be defined by

$$\tilde{\gamma}(t) = \begin{cases} \tilde{\gamma}_1 r(t), & \text{for } t \leq \log n \wedge (p \log n)^{1/2} \\ \tilde{\gamma}_2 r(t), & \text{for } \log n < t \leq (p \log n)^{1/2} \\ \hat{\gamma}_{\varepsilon/3}(p), & \text{for } t = p, \end{cases}$$

where $\tilde{\gamma}_1$ and $\tilde{\gamma}_2$ are defined by

$$\tilde{\gamma}_1 = \max_{t \in \mathcal{T}; t \leq \log n} \hat{\gamma}_{\varepsilon/3}(t)/r(t),$$

$$\tilde{\gamma}_2 = \max_{t \in \mathcal{T}; \log n < t \leq \sqrt{p \log n}} \hat{\gamma}_{\varepsilon/3}(t)/r(t).$$

The penalty function $\tilde{\gamma}(t)$ ensures that the approximate probability of a false positive using ESAC is at most ε . We remark that the upper boundary of the first segment ($\log n$) is chosen somewhat ad hoc, while the second segment is the remaining region of the sparse regime, and the last segment is the dense regime. The empirical penalty function $\tilde{\gamma}(t)$ can also be used for changepoint estimation, i.e. setting $\lambda(t) = \tilde{\gamma}(t)$, although we have experienced that the analytical penalty function $\tilde{\lambda}(t)$ gives better performance in terms of MSE for Gaussian data.

B.7 Generation of seeded intervals

Given some sample size $n \geq 2$ and parameters $\alpha > 1$ and $K > 1$, Algorithm 4 generates a set of seeded intervals.

C A Narrowest-over-Threshold variant of Inspect

We have modified the Inspect algorithm given by Algorithm 4 in Wang and Samworth (2018) in the following fashion. Instead of using Wild Binary Segmentation as search procedure, the methodology of Kovács et al. (2022) is used. More specifically, the collection of integer sub-intervals is generated

Algorithm 4 Seeded Interval Generation(α, K)

Input: Parameters α and K controlling the number of generated intervals

Output: Set of seeded intervals

```
Intervals  $\leftarrow \{\}$ 
 $l \leftarrow 1$ 
while  $l \leq \frac{n}{2}$ :
    set  $s = \max\{1, \lfloor \frac{l}{K} \rfloor\}$ 
    for  $i = 0, \dots, \frac{n-2l}{s}$ :
        Intervals  $\leftarrow$  Intervals  $\cup \{(is, is + 2l)\}$ 
    Intervals  $\leftarrow$  Intervals  $\cup \{(n - 2l, n)\}$ 
     $l \leftarrow \max\{l + 1, \lfloor \alpha l \rfloor\}$ 
Return Intervals.
```

by Algorithm 4 instead of the random draws. Moreover, the location of any detected changepoint is determined using only the narrowest intervals in which a changepoint is detected. We have given this modified version of Inspect the name NOTInspect, which is short for Narrowest-Over-Threshold Inspect. Formally, NOTInspect is defined as follows. For any $0 \leq s < e \leq n$, let $H^{(s,e]}$ denote the $p \times (e - s - 1)$ matrix in which the (i, j) th element is given by

$$H_{i,j}^{(s,e]} = T_{(s,e]}^{s+j}(X_{i,\cdot}),$$

i.e. the CUSUM of the i th row of X computed over the interval $(s, e]$ and evaluated at position $s + j$. For ease of notation, let $H_v^{(s,e]}$ denote the $(v - s)$ th column of $H^{(s,e]}$. Given $\lambda > 0$, let $\widehat{v}_\lambda^{(s,e]}$ denote the leading left singular vector of the matrix

$$\widehat{M}_\lambda = \arg \max_{M \in \mathcal{S}_2} \left(\langle H^{(s,e]}, M \rangle - \lambda \|M\|_1 \right),$$

where $\mathcal{S}_2 = \{M \in \mathbb{R}^{p \times (e-s-1)} : \|M\|_F \leq 1\}$.

Given an enumerated set $\mathcal{M} = \{(s_m, e_m]\}_{m=1}^M$ of M half open integer sub intervals of $0, \dots, n$, observations $X \in \mathbb{R}^{p \times n}$, and tuning parameters $\lambda, \xi > 0$, the NOTInspect algorithm is initiated by calling NOTInspect($X, (s, e], \mathcal{M}, \emptyset, \lambda, \xi$), and defined by Algorithm 5.

D Empirical comparison between different variants of ESAC

In the following we compare the empirical performance of different variants of the ESAC algorithm. In all versions, seeded intervals are generated using Algorithm 4 with parameters α and K specified. The variants and configurations considered are:

ESAC A: Algorithm 3 *without interval trimming* and with $\alpha = 2, K = 4$;

ESAC B: Algorithm 1 with $\alpha = 2, K = 4$;

ESAC C: Algorithm 1 with $\alpha = 3/2, K = 4$;

ESAC D: Algorithm 2 with $\alpha = 3/2, K = 4$;

ESAC E: Algorithm 1 without Narrowest-Over-Threshold choice of changepoint location and $\alpha = 3/2, K = 4$;

ESAC F: Algorithm 1 with mid-point estimation and $\alpha = 3/2, K = 4$.

ESAC A is a mix of Algorithm 3 and Algorithm 1, in the sense that it tests for a changepoint at the midpoint of each seeded interval, but does not trim away intervals once a changepoint is detected. With

Algorithm 5 NOTInspect($X, (s, e], \mathcal{M}, \mathcal{B}, \lambda, \xi$)

Input: Matrix of observations $X \in \mathbb{R}^{p \times n}$, left open and right closed integer interval $(s, e]$ in which candidate changepoints are searched for, an enumerated collection $\mathcal{M} = \{(s_m, e_m] ; m \in [M]\}$ of M half open integer sub intervals of $\{0, \dots, n\}$, a set of already detected changepoints \mathcal{B} , and penalization parameters $\lambda, \xi > 0$.

Output: A set \mathcal{B} of detected changepoints.

```
if  $e - s \leq 1$ :
    stop
set  $\mathcal{M}_{(s,e]} = \{m : (s_m, e_m] \subset (s, e]\}$ 
set  $\mathcal{O}_{(s,e]} = \left\{ m \in \mathcal{M}_{(s,e]} : \max_{s_m < b < e_m} \left( \widehat{v}_\lambda^{(s_m, e_m]} \right)^\top H_{b_m}^{(s_m, e_m]} > \xi \right\}$ 
if  $\mathcal{O}_{(s,e]} = \emptyset$ :
    stop
set  $l^* = \min_{m \in \mathcal{O}_{(s,e]}} |e_m - s_m|$ 
set  $\mathcal{O}_{l^*} = \mathcal{O}_{(s,e]} \cap \{m : |e_m - s_m| = l^*\}$ 
set  $m^* = \operatorname{argmax}_{m \in \mathcal{O}_{l^*}} \max_{s_m < b < e_m} \left( \widehat{v}_\lambda^{(s_m, e_m]} \right)^\top H_b^{(s_m, e_m]}$ 
set  $b^* = \operatorname{argmax}_{s_{m^*} < b < e_{m^*}} \left( \widehat{v}_\lambda^{(s_{m^*}, e_{m^*}]} \right)^\top H_b^{(s_{m^*}, e_{m^*}]}$ 
 $\mathcal{B} \leftarrow \mathcal{B} \cup \{b^*\}$ 
 $\mathcal{B} \leftarrow \text{NOTInspect}(X, (s, b^*], \mathcal{M}, \mathcal{B}, \lambda, \xi)$ 
 $\mathcal{B} \leftarrow \text{NOTInspect}(X, (b^*, e], \mathcal{M}, \mathcal{B}, \lambda, \xi)$ 
return  $\mathcal{B}$ 
```

ESAC E, a changepoint location is estimated by considering all seeded intervals in which a changepoint is detected, and not only the narrowest seeded intervals. This is achieved by replacing \mathcal{O}_{l^*} by $\mathcal{O}_{(s,e]}$ in Algorithm 1. In ESAC F, the estimated changepoint location v^* is replaced by $v^* = \lfloor (e_{m^*} + s_{m^*})/2 \rfloor$.

We have run a simulation with the exact same configuration as in Section 4.2 in the main text. For changepoint detection, we have chosen the empirical penalty function $\widetilde{\lambda}(t)$ as in Section B separately for each variant of ESAC. For changepoint estimation we have used the analytical penalty function $\widetilde{\lambda}(t)$ as given in Section B. For each variant of ESAC and each configuration of parameters and changepoint regimes, Table 5 displays the average Hausdorff distance, average absolute estimation error of J and average running time in milliseconds. For each configuration of parameters and changepoint regimes, the minimum (and best) value of each of the performance measures is indicated in boldface.

Comparing ESAC A and B, one observes that testing only for a changepoint at the midpoint of a seeded interval results in a substantial improvement of running time but with a cost to statistical accuracy. The running time of ESAC B is roughly three to four times that of ESAC A, while the average Hausdorff distance and absolute estimation error of K of ESAC B are generally significantly larger than those of ESAC A, independently of the model configuration. This is likely due to ESAC A having lower power in detecting changepoints than ESAC B, as is indicated by ESAC A having higher estimation error of K . Comparing ESAC B and C, one observes a similar effect of decreasing α from 2 to 3/2. ESAC C has a running time almost twice that of ESAC B, while the average Hausdorff distance over all simulation setups is around half that of ESAC B. Comparing ESAC C and D, one observes that interval trimming substantially reduces statistical performance, with virtually no gain in terms of computational cost. Importantly, the estimation error of K is markedly higher for ESAC D, which indicates that interval trimming reduces power in detecting changepoints.

Comparing ESAC C and E, one observes that using a Narrowest-over-Threshold method to estimate changepoints (as opposed to considering seeded intervals of all widths) has a mixed effect on statistical performance and a positive effect on the computational cost. In terms of Hausdorff distance, ESAC E tends to slightly outperform ESAC C, while the converse is true when considering estimation error of K . In terms of running time, ESAC C slightly outperforms ESAC E, especially when there are many changepoints. Lastly, comparing ESAC C and F, one observes that estimating changepoints using the penalized score statistic improves estimation accuracy compared to estimating changepoints by taking a mid-point of a seeded interval. For ESAC C, The average Hausdorff distance over all simulations is around one third that of ESAC F. Somewhat less pronounced is the difference in estimation error of K , where ESAC C also outperforms ESAC F.

Table 5: Multiple changepoint estimation with different variants of ESAC

Parameters				Hausdorff distance						$ \hat{J} - J $						Time in milliseconds						
n	p	Sparsity	K	A	B	C	D	E	F	A	B	C	D	E	F	A	B	C	D	E	F	
200	100	-	0	-	-	-	-	-	-	0.000	0.000	0.000	0.000	0.000	0.000	2.494	8.122	13.202	13.291	13.429	13.254	
200	100	Dense	2	29.557	7.248	7.197	19.046	7.046	12.934	0.453	0.104	0.088	0.414	0.093	0.110	2.720	8.088	12.539	12.329	13.826	12.549	
200	100	Sparse	2	5.172	1.615	1.658	6.885	1.525	5.886	0.085	0.020	0.012	0.150	0.019	0.025	2.822	7.838	12.347	12.036	13.794	12.580	
200	100	Mixed	2	17.593	5.016	5.006	13.105	5.087	9.727	0.274	0.065	0.054	0.280	0.067	0.068	2.615	7.857	12.385	12.130	13.766	12.474	
200	100	Mixed	5	24.954	10.901	6.476	20.446	6.747	10.947	1.107	0.345	0.194	1.246	0.225	0.254	2.695	7.133	11.089	10.747	14.609	11.043	
200	100	Sparse	5	7.042	3.584	1.585	9.954	1.748	5.156	0.236	0.088	0.028	0.483	0.058	0.052	2.699	7.056	10.710	10.719	14.382	10.906	
200	100	Mixed	5	17.453	8.030	4.609	16.320	4.565	8.727	0.734	0.231	0.128	0.882	0.137	0.157	2.774	7.083	10.964	10.580	14.536	10.942	
200	1000	-	0	-	-	-	-	-	-	0.002	0.001	0.000	0.000	0.000	0.000	21.873	80.721	132.741	132.657	132.787	132.845	
200	1000	Dense	2	8.523	2.200	1.731	11.782	1.482	6.582	0.144	0.029	0.016	0.285	0.021	0.025	23.498	75.455	121.002	118.612	134.114	121.129	
200	1000	Sparse	2	1.772	1.166	0.972	4.981	0.751	4.916	0.024	0.011	0.004	0.121	0.009	0.008	23.417	73.991	119.314	116.363	133.431	118.794	
200	1000	Mixed	2	4.570	2.151	1.779	9.092	1.564	6.183	0.081	0.024	0.015	0.210	0.019	0.021	23.233	74.204	119.315	116.722	133.449	119.462	
200	1000	Dense	5	11.205	3.319	2.201	16.493	1.929	6.409	0.412	0.090	0.043	0.919	0.059	0.053	23.379	65.516	103.870	100.549	139.538	103.803	
200	1000	Sparse	5	3.561	1.982	0.933	9.515	0.736	4.507	0.092	0.045	0.011	0.429	0.025	0.021	23.647	65.101	101.906	98.008	136.001	101.782	
200	1000	Mixed	5	8.422	3.099	1.754	14.095	1.373	5.419	0.274	0.072	0.033	0.682	0.040	0.052	23.416	65.203	102.504	99.180	138.009	102.491	
200	5000	-	0	-	-	-	-	-	-	0.000	0.002	0.003	0.003	0.003	0.003	110.148	425.285	700.419	700.541	698.719	702.664	
200	5000	Dense	2	6.299	1.293	1.150	5.607	0.747	5.082	0.107	0.010	0.005	0.130	0.009	0.007	118.414	385.540	619.304	599.710	702.220	619.071	
200	5000	Sparse	2	1.586	0.909	0.812	2.787	0.406	4.261	0.022	0.005	0.001	0.049	0.003	0.009	117.881	380.432	607.773	591.900	702.059	608.943	
200	5000	Mixed	2	5.353	1.105	1.081	5.124	0.668	5.067	0.085	0.007	0.005	0.115	0.007	0.016	119.099	382.842	615.231	595.623	698.241	613.451	
200	5000	Dense	5	8.858	2.516	0.836	9.285	0.544	4.386	0.290	0.054	0.006	0.448	0.016	0.021	118.777	334.106	516.330	498.218	712.661	517.062	
200	5000	Sparse	5	3.073	1.200	0.680	4.043	0.341	3.737	0.080	0.019	0.001	0.160	0.007	0.015	118.780	328.529	507.473	486.259	703.117	507.189	
200	5000	Mixed	5	6.073	1.582	0.706	7.221	0.453	4.124	0.190	0.032	0.004	0.321	0.014	0.019	118.770	330.622	511.869	489.977	705.463	511.883	
500	100	-	0	-	-	-	-	-	-	0.001	0.000	0.001	0.001	0.001	0.001	6.205	24.287	40.742	40.820	40.817	40.840	
500	100	Dense	2	67.900	29.573	10.152	42.356	10.293	22.459	0.384	0.148	0.047	0.379	0.062	0.053	6.580	23.749	38.286	37.800	41.399	38.353	
500	100	Sparse	2	21.915	8.268	2.361	9.141	2.005	11.876	0.119	0.035	0.001	0.075	0.007	0.008	6.589	23.215	37.525	36.811	41.112	37.503	
500	100	Mixed	2	49.745	17.831	5.829	27.407	6.041	17.856	0.277	0.087	0.021	0.240	0.032	0.036	6.526	23.268	37.893	37.271	41.240	37.939	
500	100	Dense	5	48.052	21.964	11.901	50.218	12.038	22.616	0.820	0.272	0.125	1.265	0.148	0.176	6.665	21.533	34.640	33.852	43.034	34.689	
500	100	Sparse	5	18.105	7.235	2.312	17.084	2.506	10.364	0.266	0.071	0.007	0.334	0.046	0.032	6.652	21.166	33.671	32.940	42.543	33.844	
500	100	Mixed	5	34.329	14.720	6.449	33.383	6.254	15.993	0.567	0.174	0.056	0.755	0.086	0.086	6.708	21.385	34.159	33.330	43.037	34.114	
500	1000	-	0	-	-	-	-	-	-	0.000	0.003	0.000	0.000	0.000	0.000	58.259	241.550	408.466	410.328	408.340	411.164	
500	1000	Dense	2	35.257	6.585	4.104	24.037	3.594	14.977	0.203	0.026	0.014	0.254	0.018	0.021	62.356	231.143	378.515	371.903	410.607	379.165	
500	1000	Sparse	2	6.619	2.473	1.603	7.812	1.050	10.553	0.034	0.004	0.000	0.078	0.006	0.001	62.345	227.051	372.265	363.301	411.828	371.272	
500	1000	Mixed	2	21.890	6.052	2.034	15.490	1.473	12.472	0.117	0.023	0.002	0.150	0.008	0.006	62.723	228.743	372.856	366.669	410.545	374.385	
500	1000	Dense	5	28.396	7.049	2.960	39.687	2.806	12.167	0.438	0.066	0.017	0.912	0.040	0.025	63.259	207.844	336.695	327.587	427.493	335.335	
500	1000	Sparse	5	8.535	3.037	1.769	14.935	1.211	9.094	0.096	0.020	0.003	0.278	0.025	0.011	63.527	204.245	328.075	317.877	416.863	326.975	
500	1000	Mixed	5	17.612	4.813	3.147	26.652	2.371	11.192	0.274	0.034	0.017	0.572	0.033	0.025	63.396	205.635	333.017	323.492	423.150	332.866	
500	5000	-	0	-	-	-	-	-	-	0.000	0.000	0.000	0.000	0.000	0.000	316.528	1328.522	2242.270	2245.298	2249.252	2236.030	
500	5000	Dense	2	16.733	5.984	2.294	13.965	1.390	11.295	0.088	0.023	0.002	0.132	0.007	0.003	336.784	1262.177	2023.982	1994.241	2267.927	2031.555	
500	5000	Sparse	2	4.798	1.625	1.951	3.990	0.859	10.402	0.024	0.001	0.002	0.022	0.003	0.008	334.060	1241.024	2009.202	1957.339	2269.248	1999.724	
500	5000	Mixed	2	14.071	5.259	1.946	8.262	1.092	11.044	0.068	0.018	0.002	0.068	0.009	0.009	331.958	1250.821	2026.691	1978.321	2270.342	2019.991	
500	5000	Dense	5	13.681	5.718	2.015	20.418	1.283	10.137	0.182	0.054	0.003	0.408	0.029	0.018	335.042	1118.323	1771.210	1701.822	2302.847	1761.599	
500	5000	Sparse	5	3.990	2.460	1.726	6.917	0.877	8.494	0.038	0.012	0.006	0.098	0.019	0.020	334.404	1085.380	1720.665	1656.142	2260.874	1714.863	
500	5000	Mixed	5	9.622	4.317	1.925	14.145	0.908	9.686	0.120	0.036	0.001	0.255	0.021	0.021	331.365	1095.025	1731.004	1666.874	2258.874	1733.001	
Average				16.453	5.941	2.990	15.602	2.660	9.631	0.210	0.056	0.023	0.324	0.034	0.036							

E Some more simulations

E.1 Extended table from Section 4.2

For each method considered and each configuration of parameters (now $n \in \{200, 500\}$) and changepoint regimes, Table 6 displays the average Hausdorff distance and average absolute estimation error of J .

E.2 Simulations with randomly drawn changes in mean

Tables 7 and 8 respectively display the results of re-running the simulations in Sections 4.1 and 4.2 with the modification that changes in the mean-vector drawn randomly. More specifically, for each changepoint we have taken the change in mean θ to satisfy $\theta_{1:k} \propto \left(Z^T, 0_{p-k}^T \right)$ where $Z \sim N_k(0, 1)$. Apart from this single modification, the simulation setups are identical to the ones in Sections 4.1 and 4.2, including the norms of the changes in mean.

Table 6: Multiple changepoint estimation

Parameters				Hausdorff distance						$ \hat{J} - J $					
n	p	Sparsity	J	ESAC	Pilliat	Inspect	SBS	SUBSET	DC	ESAC	Pilliat	Inspect	SBS	SUBSET	DC
200	100	-	0	-	-	-	-	-	-	0.000	0.000	0.000	0.035	0.001	0.043
200	100	Dense	2	5.273	23.045	21.610	69.918	6.516	76.367	0.059	0.477	0.286	1.028	0.108	1.076
200	100	Sparse	2	1.427	12.539	7.920	49.193	1.667	14.918	0.009	0.245	0.103	0.695	0.035	0.260
200	100	Mixed	2	4.598	18.566	14.355	61.153	3.741	52.926	0.051	0.356	0.188	0.867	0.062	0.742
200	100	Dense	5	5.172	23.738	16.271	67.285	6.424	55.707	0.137	1.530	0.540	3.198	0.330	2.759
200	100	Sparse	5	1.359	13.986	6.378	57.178	2.424	23.193	0.023	0.799	0.228	2.786	0.204	1.361
200	100	Mixed	5	4.042	18.768	12.559	60.433	4.901	41.305	0.098	1.197	0.421	3.008	0.281	2.164
200	1000	-	0	-	-	-	-	-	-	0.000	0.000	0.000	0.340	0.024	0.017
200	1000	Dense	2	1.452	13.393	9.490	55.116	1.079	84.983	0.008	0.279	0.119	0.721	0.031	1.232
200	1000	Sparse	2	0.830	9.074	9.830	49.716	0.751	20.376	0.003	0.182	0.151	0.621	0.029	0.291
200	1000	Mixed	2	1.776	11.782	9.585	50.506	1.480	53.226	0.013	0.243	0.125	0.690	0.041	0.817
200	1000	Dense	5	1.524	15.808	9.328	57.330	1.558	60.791	0.025	1.018	0.261	2.960	0.173	3.057
200	1000	Sparse	5	0.685	11.342	9.161	54.198	1.520	25.800	0.002	0.639	0.357	2.684	0.167	1.428
200	1000	Mixed	5	1.189	13.932	9.446	58.255	1.720	45.158	0.017	0.813	0.332	2.864	0.191	2.377
200	5000	-	0	-	-	-	-	-	-	0.000	0.000	0.002	1.957	0.000	0.000
200	5000	Dense	2	0.965	12.988	13.254	54.753	0.600	124.337	0.003	0.294	0.170	0.534	0.019	1.679
200	5000	Sparse	2	0.763	9.655	15.806	58.961	0.512	70.825	0.001	0.203	0.235	0.562	0.028	1.039
200	5000	Mixed	2	0.977	11.364	13.762	55.915	0.782	96.945	0.003	0.254	0.212	0.500	0.027	1.361
200	5000	Dense	5	0.891	14.586	12.967	50.328	1.373	83.639	0.009	0.942	0.449	2.448	0.173	3.635
200	5000	Sparse	5	0.534	11.697	13.501	53.998	1.291	54.328	0.000	0.735	0.548	2.529	0.176	2.712
200	5000	Mixed	5	0.776	13.568	13.252	53.718	1.413	69.941	0.004	0.855	0.501	2.503	0.174	3.191
500	100	-	0	-	-	-	-	-	-	0.000	0.000	0.000	0.057	0.004	0.046
500	100	Dense	2	15.310	71.171	50.125	130.610	7.423	140.433	0.078	0.612	0.299	0.784	0.048	0.838
500	100	Sparse	2	2.739	30.053	15.911	66.668	3.201	21.826	0.003	0.284	0.096	0.363	0.035	0.161
500	100	Mixed	2	11.309	54.753	35.821	93.890	5.418	88.264	0.063	0.464	0.208	0.533	0.038	0.530
500	100	Dense	5	20.245	66.890	50.548	120.816	8.226	102.263	0.229	1.939	0.726	2.543	0.207	1.988
500	100	Sparse	5	3.591	36.375	20.258	70.980	4.767	19.457	0.021	0.923	0.301	1.605	0.191	0.513
500	100	Mixed	5	12.290	53.954	39.507	104.507	6.803	77.078	0.150	1.489	0.582	2.138	0.193	1.441
500	1000	-	0	-	-	-	-	-	-	0.000	0.002	0.000	0.471	0.000	0.025
500	1000	Dense	2	2.217	30.635	18.859	102.138	2.790	99.626	0.002	0.295	0.094	0.531	0.044	0.591
500	1000	Sparse	2	2.052	17.323	23.773	71.741	1.325	18.185	0.002	0.148	0.135	0.382	0.023	0.116
500	1000	Mixed	2	2.181	25.431	21.361	92.648	1.907	68.446	0.002	0.223	0.114	0.496	0.061	0.426
500	1000	Dense	5	2.893	36.449	25.510	97.098	3.660	86.127	0.015	0.964	0.282	2.143	0.174	1.717
500	1000	Sparse	5	1.808	22.483	22.461	66.221	4.089	20.893	0.001	0.547	0.363	1.493	0.191	0.498
500	1000	Mixed	5	2.526	31.025	24.077	90.958	4.682	60.749	0.011	0.768	0.315	1.847	0.213	1.216
500	5000	-	0	-	-	-	-	-	-	0.000	0.002	0.006	2.508	0.025	0.000
500	5000	Dense	2	2.011	34.047	21.082	139.285	1.647	282.956	0.002	0.329	0.105	1.106	0.030	1.562
500	5000	Sparse	2	2.033	16.974	32.140	144.237	1.408	132.128	0.002	0.148	0.188	1.159	0.083	0.778
500	5000	Mixed	2	2.277	26.553	24.275	141.006	1.990	207.933	0.003	0.241	0.133	1.146	0.027	1.184
500	5000	Dense	5	1.937	42.354	24.293	84.334	3.570	187.785	0.006	1.182	0.292	1.133	0.186	3.405
500	5000	Sparse	5	1.671	21.168	29.794	79.665	2.654	104.455	0.002	0.560	0.500	1.073	0.150	2.029
500	5000	Mixed	5	1.957	31.474	25.265	84.857	3.864	143.185	0.006	0.860	0.380	1.154	0.190	2.772
Average				3.480	25.248	20.098	77.767	3.033	81.015	0.025	0.549	0.246	1.385	0.104	1.263

In the single changepoint case, ESAC displays a slightly larger variability in performance compared to the simulation where changes in mean are evenly spread across the affected coordinates. Averaging over all values of n , p and k , one observes that the MSE of ESAC has increased slightly in comparison with table 1. Meanwhile, the opposite is true for the competing methods. Still, Tables 1 and 7 are quite similar, and ESAC has highly competitive performance in both.

E.3 Single changepoint detection

Here we investigate the power of each method when testing for the presence of a single changepoint. It is assumed known that there is at most one changepoint in the simulated data, and thus no multiple changepoint search method like Binary Segmentation or Seeded Binary Segmentation is used for any of the methods. Instead, we have for each method computed the corresponding test statistic for a single changepoint on the whole generated data set X , using e.g. $S_{\gamma, (0, n)}^v$ in (3) for ESAC. Our simulations are run with the same setup as in Section 4.1, with the exception of a slightly lower signal strength to avoid 0% testing error. We adjust φ such that $\Delta\varphi^2 = n \|\theta\|_2^2 / 5 = 1.8^2 r(k)$ for each combination of n , p and k .

Table 7: Single changepoint estimation with changes in mean randomly drawn

Parameters					MSE					Time in milliseconds					
n	p	k	η	φ	ESAC	Inspect	SBS	SUBSET	DC	ESAC	Inspect	SBS	SUBSET	DC	
200	100	1	40	1.40	10.1	25.7	70.4	39.2	9.4	0.3	2.2	11.0	2.1	13.8	
200	100	5	40	2.00	4.6	2.4	40.0	2.6	6.6	0.4	2.2	11.2	2.4	14.5	
200	100	24	40	1.90	46.6	20.3	977.3	125.1	168.4	0.3	2.1	10.6	1.8	17.5	
200	100	100	40	1.90	53.0	147.2	1507.2	307.4	1614.6	0.3	2.2	10.5	1.9	13.4	
200	1000	1	40	1.52	5.1	95.2	34.9	27.5	5.2	2.1	44.3	96.1	13.4	136.0	
200	1000	10	40	2.93	1.4	0.6	2.5	0.5	3.4	2.2	44.2	96.0	13.9	138.2	
200	1000	73	40	3.37	6.1	2.0	510.3	4.9	15.0	2.2	44.3	95.4	13.7	137.7	
200	1000	1000	40	3.37	3.7	544.8	1546.1	3.7	357.0	2.1	44.5	94.8	13.4	138.9	
200	5000	1	40	1.60	38.9	481.5	19.3	47.6	165.3	12.4	226.8	486.2	80.6	730.1	
200	5000	18	40	4.00	1.1	0.5	0.9	0.6	1.4	12.6	226.8	483.2	81.7	731.0	
200	5000	163	40	5.04	3.4	0.7	281.0	3.4	18.2	12.6	226.4	479.2	82.3	733.8	
200	5000	5000	40	5.04	3.8	1299.5	1548.5	3.8	6.0	13.0	226.6	478.3	83.1	734.2	
500	100	1	100	0.92	48.8	86.9	130.1	242.1	48.9	0.6	6.0	17.9	4.6	29.7	
500	100	5	100	1.31	14.2	13.3	49.7	12.5	37.2	0.6	6.0	17.9	5.1	29.0	
500	100	25	100	1.25	223.3	63.7	5044.6	746.3	671.9	0.6	6.0	17.7	4.1	28.4	
500	100	100	100	1.25	446.9	727.1	9526.7	1953.2	8663.5	0.6	6.0	18.6	3.9	28.1	
500	1000	1	100	1.00	30.1	200.6	30.0	125.3	29.3	5.7	275.3	160.7	35.7	288.9	
500	1000	10	100	1.90	4.7	4.3	11.6	2.7	13.9	5.7	274.5	161.5	35.2	288.5	
500	1000	79	100	2.22	14.6	10.5	1854.5	13.3	168.5	5.8	275.2	161.1	35.4	288.2	
500	1000	1000	100	2.22	22.4	2083.8	9755.1	63.5	2677.1	6.0	277.1	160.6	35.4	289.5	
500	5000	1	100	1.05	26.4	1290.1	36.0	75.3	265.8	32.8	1401.2	812.4	178.8	1634.8	
500	5000	18	100	2.58	2.2	1.4	7.0	1.2	9.3	31.7	1399.8	804.8	178.9	1564.4	
500	5000	177	100	3.32	13.9	1.9	812.9	13.9	111.0	32.8	1399.2	803.7	177.0	1563.2	
500	5000	5000	100	3.32	14.9	6546.6	9921.2	14.9	25.2	33.6	1400.3	800.8	175.1	1560.7	
Average MSE					43.331	568.765	1821.581	159.599	628.846						

Similar to the version of ESAC given in Algorithm 3, the Pilliat method only tests for a changepoint in the midpoint of any seeded interval (s, e) . This time saving trick does not affect the theoretical guarantees of neither ESAC nor Pilliat in the multiple changepoint situation because intervals for both methods are generated such that any changepoint will be close to a midpoint of some interval (s, e) . In this section, however, we are concerned with testing for a changepoint over a single interval (i.e. $(s, e) = (0, n)$), in which case testing only for a changepoint in the midpoint can lead to great efficiency losses whenever the true changepoint is far from the midpoint. To obtain fair and meaningful power comparisons with the remaining methods in the simulation study, we have modified the test statistic from the Pilliat algorithm to test for a changepoint in all time points $v = 1, \dots, n - 1$.

For any testing procedure, there is a trade-off between Type I and Type II errors. In order to have precise control over the Type I error of each method, we have run the competing methods with empirically chosen penalty parameters. Each method is calibrated to have Type I error at most 1% based on $N = 1000$ Monte Carlo simulations. The methods ESAC and Pilliat, unlike the remaining methods, combine several test statistics to test for a changepoint, resulting in a multiple testing situation. For ESAC we have adjusted for the multiple testing by using the empirical penalty function $\tilde{\gamma}$ as defined in Section B. Similarly, we have for the Pilliat algorithm chosen thresholds for two of its three constituent tests by Monte Carlo simulating the leading constant in the theoretical thresholds and applied a Bonferroni correction. For the last test statistic used in the Pilliat algorithm (the Berk Jones statistic), we have used the theoretical threshold provided in the paper. For Inspect, we have chosen the detection threshold ξ to be the 10th largest sparse projection $\max_{0 < b < n} \left(\hat{v}_\lambda^{(0, n]} \right)^T T_b^{(0, n]}$, where $\lambda = \{\log(p \log n) / 2\}^{1/2}$ (see Appendix C), over $N = 1000$ data sets with no changepoints. For SUBSET we have used the function for choosing the penalty parameter β provided by the author, with the remaining penalty parameters at their recommended values, also using the 10th largest value out of $N = 1000$ Monte Carlo samples. For Sparsified Binary Segmentation we have chosen the threshold π_T in the same way as in Section 4.1, also using the 10th largest among $N = 1000$ Monte Carlo samples. For the Double CUSUM algorithm we have used the input parameter $\varphi = -1$ and chosen the threshold value to be the 10th largest double

Table 8: Multiple changepoint estimation with randomly drawn changes in mean

Parameters			Hausdorff distance						$ \hat{J} - J $						Time in milliseconds							
n	p	Sparsity	K	ESAC	Pilliat	Inspect	SBS	SUBSET	DC	ESAC	Pilliat	Inspect	SBS	SUBSET	DC	ESAC	Pilliat	Inspect	SBS	SUBSET	DC	
200	100	Dense	2	6.343	24.101	16.779	54.275	5.489	40.699	0.000	0.000	0.000	0.036	0.001	0.056	12.966	30.647	74.424	216.435	210.336	267.195	
200	100	Dense	2	6.343	24.101	16.779	54.275	5.489	40.699	0.068	0.494	0.217	0.811	0.087	0.595	13.286	27.903	63.091	215.905	369.398	283.611	
200	100	Sparse	2	1.041	9.866	9.135	51.509	1.341	13.402	0.005	0.168	0.121	0.688	0.041	0.185	12.863	26.726	59.260	217.011	376.712	285.572	
200	100	Mixed	2	4.530	18.165	12.471	49.626	3.579	29.501	0.044	0.350	0.156	0.712	0.056	0.403	12.998	27.244	60.739	215.607	368.155	281.791	
200	100	Dense	5	5.051	23.400	13.704	60.773	7.000	36.150	0.134	1.571	0.446	2.984	0.372	1.990	11.560	23.256	44.433	218.781	406.915	286.411	
200	100	Sparse	5	1.144	11.798	7.383	54.875	2.197	21.282	0.014	0.628	0.272	2.793	0.215	1.227	11.062	21.775	40.321	216.358	405.685	286.231	
200	100	Mixed	5	3.868	19.370	11.640	57.086	4.795	32.205	0.102	1.135	0.390	2.825	0.259	1.687	11.252	22.338	42.175	218.172	398.624	287.708	
200	1000	Dense	2	-	-	-	-	-	-	0.001	0.002	0.001	0.334	0.049	0.011	133.635	417.508	676.153	1383.229	1644.789	1541.410	
200	1000	Dense	2	1.621	13.373	7.469	46.956	0.914	65.967	0.010	0.288	0.085	0.652	0.025	0.966	123.439	349.062	504.772	1396.731	2937.718	1620.628	
200	1000	Sparse	2	0.580	5.056	9.926	45.467	0.580	9.819	0.001	0.061	0.150	0.601	0.025	0.160	112.348	332.217	493.877	1405.696	2935.402	1680.447	
200	1000	Mixed	2	1.160	9.583	9.511	48.964	1.000	44.287	0.007	0.171	0.118	0.625	0.034	0.629	113.235	340.377	500.685	1395.207	2947.915	1646.245	
200	1000	Dense	5	1.676	15.654	6.579	52.049	2.015	52.562	0.025	0.967	0.181	2.737	0.184	2.694	98.949	283.893	339.906	1403.437	3137.914	1689.102	
200	1000	Sparse	5	0.654	6.088	10.978	56.695	1.380	20.461	0.004	0.261	0.409	2.797	0.180	1.196	92.722	266.748	332.063	1406.943	3189.067	1704.795	
200	1000	Mixed	5	0.972	11.230	7.933	54.369	1.532	40.742	0.014	0.587	0.283	2.757	0.181	2.090	94.930	274.330	336.437	1396.920	3164.231	1693.709	
200	5000	Dense	2	-	-	-	-	-	-	0.001	0.000	0.003	2.045	0.000	0.000	691.022	2483.067	3438.853	6474.674	7839.738	45460.281	
200	5000	Dense	2	0.833	12.928	9.419	53.485	0.881	125.673	0.002	0.253	0.113	0.503	0.029	1.675	608.734	2068.055	2597.533	6476.473	13875.649	46029.927	
200	5000	Sparse	2	0.680	5.005	21.564	56.211	0.372	20.694	0.002	0.078	0.311	0.544	0.021	0.288	576.760	1980.902	2657.543	6486.496	13803.731	45776.696	
200	5000	Mixed	2	0.819	8.515	17.548	54.106	0.476	76.468	0.005	0.142	0.233	0.533	0.021	1.027	588.131	2024.048	2643.031	6478.838	14013.301	46452.491	
200	5000	Dense	5	0.838	14.882	10.696	51.242	1.505	82.618	0.006	0.965	0.332	2.432	0.191	3.589	503.523	1679.471	1755.036	6466.005	14882.984	44220.589	
200	5000	Sparse	5	0.564	5.720	17.985	52.833	1.438	28.486	0.004	0.268	0.716	2.542	0.167	1.557	469.414	1583.551	1810.660	6480.760	14912.785	45156.719	
200	5000	Mixed	5	0.915	10.379	13.680	51.268	1.290	55.573	0.011	0.549	0.531	2.485	0.173	2.667	483.432	1628.287	1787.464	6447.313	14864.080	43521.559	
500	100	Dense	2	-	-	-	-	-	-	0.001	0.000	0.000	0.046	0.001	0.035	38.700	94.066	304.918	246.704	357.170	358.181	
500	100	Dense	2	14.852	71.176	36.840	76.220	7.096	50.032	0.072	0.598	0.209	0.443	0.043	0.298	40.440	88.531	270.099	256.006	638.682	396.802	
500	100	Sparse	2	2.493	18.588	19.554	59.445	3.716	16.005	0.003	0.122	0.117	0.340	0.043	0.110	38.181	83.009	253.752	255.744	636.948	398.321	
500	100	Mixed	2	11.450	49.265	31.611	74.956	6.349	38.182	0.054	0.390	0.183	0.422	0.046	0.230	39.096	85.391	260.994	254.795	641.740	396.331	
500	100	Dense	5	19.669	65.912	41.700	86.378	8.573	50.159	0.235	1.918	0.552	1.913	0.245	0.936	36.228	76.931	206.456	258.670	679.120	419.395	
500	100	Sparse	5	2.497	23.396	20.207	70.891	5.215	14.485	0.009	0.518	0.296	1.595	0.217	0.325	34.096	71.251	188.874	260.845	681.193	423.444	
500	100	Mixed	5	12.201	48.611	32.186	78.728	7.454	36.218	0.148	1.241	0.460	1.762	0.238	0.754	34.799	73.492	198.098	257.864	690.167	418.055	
500	1000	Dense	2	-	-	-	-	-	-	0.000	0.000	0.000	0.492	0.016	0.017	398.208	1285.509	3847.094	1662.366	2824.899	3863.389	
500	1000	Dense	2	2.771	31.180	13.583	78.957	2.315	74.251	0.006	0.276	0.062	0.399	0.038	0.461	369.555	1118.043	2773.639	1698.756	5014.257	2678.245	
500	1000	Sparse	2	1.666	9.834	25.831	73.875	1.250	8.877	0.001	0.041	0.168	0.383	0.027	0.072	345.645	1072.310	2701.346	1699.812	5020.515	2720.316	
500	1000	Mixed	2	2.211	20.015	19.778	78.736	2.062	45.206	0.003	0.152	0.107	0.392	0.039	0.286	352.894	1094.544	2712.138	1698.072	4973.244	2699.230	
500	1000	Dense	5	3.369	36.761	17.330	80.512	4.553	64.838	0.021	1.004	0.200	1.751	0.221	1.272	318.164	964.578	1829.702	1719.044	5337.658	2886.657	
500	1000	Sparse	5	1.404	9.821	25.099	74.378	3.735	12.836	0.001	0.135	0.397	1.512	0.209	0.314	300.161	905.299	1768.004	1727.178	5324.184	2912.666	
500	1000	Mixed	5	2.193	24.535	19.081	74.682	3.797	47.089	0.009	0.511	0.280	1.585	0.184	0.971	308.808	933.998	1801.129	1717.245	5316.684	2874.535	
500	5000	Dense	2	-	-	-	-	-	-	0.001	0.001	0.005	2.548	0.001	0.000	2190.188	7671.521	21419.785	9984.972	13603.143	80867.898	
500	5000	Dense	2	2.521	32.488	15.256	138.242	1.923	276.838	0.004	0.319	0.066	1.124	0.025	1.536	1986.577	6730.429	14858.876	7973.077	23855.000	73071.458	
500	5000	Sparse	2	1.292	5.778	44.258	130.900	0.847	19.421	0.001	0.010	0.273	1.030	0.019	0.110	1871.097	6313.414	15406.145	7977.799	23782.197	77183.655	
500	5000	Mixed	2	2.227	18.370	26.340	142.507	1.243	155.575	0.003	0.132	0.153	1.089	0.019	0.917	1934.793	6529.652	15159.541	7965.174	23783.834	75432.805	
500	5000	Dense	5	1.854	39.501	16.271	80.997	3.996	176.776	0.004	1.178	0.185	1.091	0.221	3.332	1720.410	5776.899	9325.082	7991.455	24947.670	73536.119	
500	5000	Sparse	5	1.299	5.986	37.767	78.567	3.635	22.392	0.002	0.045	0.621	1.127	0.203	0.596	1590.057	5281.750	9756.378	8003.694	25304.561	71966.096	
500	5000	Mixed	5	2.164	22.478	27.356	81.147	3.183	116.785	0.005	0.438	0.407	1.092	0.166	2.236	1646.648	5509.990	9507.831	8003.054	24760.199	69574.033	
Average				3.374	21.078	19.012	69.775	3.020	56.182	0.025	0.428	0.234	1.299	0.108	0.940							

CUSUM statistic over $N = 1000$ Monte Carlo simulated data sets without any changepoints.

For each method considered and each configuration of parameters, Table 9 displays the average detection rate and average running time in milliseconds. For each configuration of parameters, the best value of the detection rate and the running time is indicated in boldface (when there are no changepoints, boldface indicates the detection rate closest to 1% from below). In terms of statistical power, Table 9 demonstrates that ESAC, Pilliat and SUBSET are the only methods with competitive power across all sparsity regimes and combinations of n and p . Pilliat has the highest power in seven out of the 24 different combinations of parameters with a changepoint, while the same number is three for ESAC and one for SUBSET. Averaging over the 24 combinations of parameters, Pilliat and ESAC have the highest over-all power. The Pilliat algorithm has a slight edge over ESAC, and SUBSET in third place. In comparison, Inspect has high detection power only for $k = \lceil p^{1/3} \rceil$, and with performance seemingly deteriorating when p grows. Double CUSUM has excellent power for detecting dense changepoints, but fails to detect sparse changepoints, especially when $k = 1$ or p is large. Sparsified Binary Segmentation has high power for sparse changepoints (especially when $k = 1$), but fails completely to detect dense changepoints. In terms of running time, ESAC is again the clear winner, with Pilliat as the runner-up. We remark again that SUBSET is the only method not implemented in C or C++, giving the other methods an advantage when comparing running times. We also remark that the running time of the noise level scaling by MAD estimates is not included in the running times of ESAC, Inspect, Pilliat and SUBSET, as the running time of the scaling dominates the running time of ESAC, SUBSET and Pilliat. The running time of the MAD scaling is however included in the running times of the Double CUSUM and Sparsified Binary Segmentation algorithms, as the implementations of these algorithms do not offer an option to disable the MAD scaling.

It is interesting to note that the power of ESAC, Pilliat and SUBSET seems to grow with n . This might be due to the Signal-to-Noise ratio of the simulated changepoints being proportional to the detection boundary for multiple changepoints, which grows faster with n than the minimax testing rate for a

single changepoint, see Liu et al. (2021).

Table 9: Single changepoint detection

Parameters					Detection rate						Time in milliseconds					
n	p	k	η	φ	ESAC	Pilliat	Inspect	SBS	SUBSET	DC	ESAC	Pilliat	Inspect	SBS	SUBSET	DC
200	100	-	-	-	0.016	0.013	0.008	0.015	0.017	0.007	0.2	0.8	2.2	11.2	2.1	9.5
200	100	1	$n/5$	1.12	0.849	0.815	0.232	0.892	0.886	0.082	0.1	0.3	2.1	9.8	1.7	8.6
200	100	5	$n/5$	1.60	0.952	0.965	0.911	0.690	0.962	0.775	0.1	0.2	2.0	9.4	1.6	8.6
200	100	24	$n/5$	1.52	0.696	0.749	0.666	0.075	0.567	0.813	0.1	0.4	2.0	12.6	1.6	8.5
200	100	100	$n/5$	1.52	0.675	0.740	0.550	0.038	0.543	0.819	0.1	0.4	2.1	9.4	1.7	8.8
200	1000	-	-	-	0.008	0.009	0.010	0.006	0.010	0.008	1.8	10.6	42.8	88.2	12.5	87.5
200	1000	1	$n/5$	1.22	0.809	0.796	0.003	0.853	0.841	0.018	1.1	4.0	42.5	88.4	13.8	89.0
200	1000	10	$n/5$	2.35	0.994	0.995	0.498	0.649	0.987	0.299	0.9	2.2	42.4	88.1	12.7	90.3
200	1000	73	$n/5$	2.70	0.823	0.880	0.645	0.046	0.788	0.900	1.1	3.3	42.4	88.0	13.0	89.6
200	1000	1000	$n/5$	2.70	0.805	0.868	0.390	0.014	0.783	0.918	1.1	3.4	42.5	87.7	13.3	89.1
200	5000	-	-	-	0.007	0.008	0.003	0.012	0.012	0.012	11.6	65.4	216.7	449.8	78.0	458.9
200	5000	1	$n/5$	1.28	0.782	0.775	0.000	0.856	0.797	0.018	7.1	26.0	215.9	447.3	77.7	455.9
200	5000	18	$n/5$	3.20	0.996	1.000	0.011	0.698	0.997	0.182	5.6	17.4	215.0	446.0	78.0	454.6
200	5000	163	$n/5$	4.03	0.911	0.925	0.249	0.038	0.898	0.911	6.7	18.5	214.9	441.5	79.1	457.1
200	5000	5000	$n/5$	4.03	0.897	0.893	0.119	0.013	0.868	0.934	8.8	20.8	214.2	440.8	78.6	457.9
500	100	-	-	-	0.007	0.005	0.007	0.015	0.015	0.008	0.5	2.1	5.6	16.0	4.2	16.0
500	100	1	$n/5$	0.74	0.944	0.897	0.288	0.973	0.968	0.069	0.2	0.6	5.4	16.5	3.8	15.7
500	100	5	$n/5$	1.04	0.978	0.988	0.973	0.882	0.987	0.821	0.2	0.5	5.4	16.7	3.6	15.5
500	100	25	$n/5$	1.00	0.809	0.785	0.755	0.120	0.718	0.852	0.3	0.8	5.4	15.9	3.6	15.5
500	100	100	$n/5$	1.00	0.796	0.776	0.627	0.062	0.699	0.853	0.3	0.8	5.4	16.0	3.7	15.8
500	1000	-	-	-	0.004	0.004	0.005	0.014	0.010	0.008	4.4	26.4	261.9	147.0	32.8	163.2
500	1000	1	$n/5$	0.80	0.924	0.876	0.000	0.963	0.942	0.026	2.5	8.8	259.7	147.4	32.4	163.4
500	1000	10	$n/5$	1.52	0.994	0.998	0.551	0.860	0.994	0.357	2.3	5.7	259.0	148.1	32.4	164.7
500	1000	79	$n/5$	1.78	0.936	0.926	0.711	0.073	0.868	0.925	2.8	7.6	260.5	148.6	32.5	165.2
500	1000	1000	$n/5$	1.78	0.927	0.920	0.466	0.023	0.877	0.965	2.5	8.1	260.4	149.1	32.3	165.6
500	5000	-	-	-	0.006	0.002	0.010	0.008	0.006	0.011	25.9	158.2	1343.5	769.4	182.0	955.7
500	5000	1	$n/5$	0.84	0.939	0.890	0.000	0.958	0.947	0.017	13.7	46.6	1341.9	762.7	184.3	908.5
500	5000	18	$n/5$	2.06	1.000	1.000	0.010	0.907	1.000	0.204	12.0	28.3	1341.4	763.1	185.4	908.1
500	5000	177	$n/5$	2.66	0.964	0.959	0.455	0.045	0.951	0.956	12.8	37.7	1342.3	762.1	184.1	908.7
500	5000	5000	$n/5$	2.66	0.953	0.956	0.243	0.009	0.956	0.982	13.0	37.5	1342.8	757.8	179.5	907.7
Average detection rate					0.890	0.891	0.390	0.447	0.868	0.571						

F Auxiliary Lemmas

Lemma 5.1. For any $a \geq 0$, define $\nu_a = \mathbb{E}(Z^2 \mid |Z| \geq a)$ where $Z \sim N(0, 1)$. Then

$$a^2 + 1 \leq \nu_a \leq a^2 + 2.$$

Proof. The second inequality follows from Lemma 4 in Liu et al. (2021). For the first inequality, let $\bar{\Phi}(x) = \int_x^\infty \varphi(t)dt$, where $\varphi(\cdot)$ denotes the density function of a standard normal distribution. If $a > 0$, we have that

$$\begin{aligned} \nu_a - 1 - a^2 &= a \frac{\varphi(a)}{\bar{\Phi}(a)} - a^2 \\ &= a \left\{ \frac{\varphi(a)}{\bar{\Phi}(a)} - a \right\} \\ &\geq 0, \end{aligned}$$

using that $\varphi(a)/\bar{\Phi}(a) > a$ for all $a > 0$ (see e.g. Sampford, 1953). For $a = 0$, we have that $\nu_a = \mathbb{E}(Z^2) = 1$, and the claim follows. \square

The following Lemma is due to Liu et al. (2021).

Lemma 5.2 (Liu et al. 2021, Lemma 5). Let $Z_i \stackrel{i.i.d.}{\sim} N(0, 1)$ for $i \in [p]$, where $p \in \mathbb{N}$. Let $a \geq 0$ and define $\nu_a = \mathbb{E}(Z^2 \mid |Z| \geq a)$. Then for all $x > 0$,

$$\mathbb{P} \left[\sum_{i=1}^p (Z_i^2 - \nu_a) \mathbb{1}(|Z_i| \geq a) \geq 9 \left\{ \left(p e^{-a^2/2} x \right)^{1/2} + x \right\} \right] \leq e^{-x}.$$

The following Lemma is analogous to Lemma 5.2, and gives a corresponding lower bound.

Lemma 5.3. Let $Z_i \stackrel{i.i.d.}{\sim} N(0, 1)$ for $i \in [p]$, where $p \in \mathbb{N}$. Let $a \geq 1$ and define $\nu_a = \mathbb{E}(Z_1^2 \mid |Z_1| \geq a)$. Then for all $x > 0$,

$$\mathbb{P} \left[\sum_{i=1}^p (Z_i^2 - \nu_a) \mathbb{1}(|Z_i| \geq a) \leq -5 \left\{ \left(p e^{-a^2/2} x \right)^{1/2} + x \right\} \right] \leq e^{-x}.$$

Proof. The proof is similar to the proof of Lemma 5 in Liu et al. (2021). Let $X = (Z^2 - \nu_a) \mathbb{1}(|Z| \geq a)$, where $Z \sim N(0, 1)$. Let $\lambda \in (0, \frac{1}{2}]$. Then, as $\mathbb{E}(X) = 0$, we have that

$$\mathbb{E} \left(e^{-\lambda X} \right) = 1 + \mathbb{E} \left(e^{-\lambda X} - 1 + \lambda X \right),$$

By the deterministic bound

$$e^{-y} - 1 + y \leq \begin{cases} y^2, & \text{if } y > 0, \\ y^2, & \text{if } -1 \leq y \leq 0, \\ e^{-y}, & \text{if } y \leq -1, \end{cases}$$

we obtain that

$$\begin{aligned} \mathbb{E} \left(e^{-\lambda X} \right) &\leq 1 + \lambda^2 \mathbb{E} \left\{ X^2 \mathbb{1}(X > 0) \right\} + \lambda^2 \mathbb{E} \left\{ X^2 \mathbb{1} \left(-\frac{1}{\lambda} \leq X \leq 0 \right) \right\} \\ &\quad + \mathbb{E} \left\{ e^{-\lambda X} \mathbb{1} \left(X < -\frac{1}{\lambda} \right) \right\}. \end{aligned}$$

We bound each term separately. Let $p(x)$ denote the density function of the χ_1^2 distribution. For the second term, we have that

$$\begin{aligned} \mathbb{E} \left\{ X^2 \mathbb{1}(X > 0) \right\} &= \int_{\nu_a}^{\infty} (x - \nu_a)^2 p(x) dx \\ &= \int_{\nu_a}^{\infty} (x - \nu_a)^2 \frac{1}{(2\pi x)^{1/2}} e^{-x/2} dx \\ &\leq \frac{16}{(2\pi\nu_a)^{1/2}} e^{-\nu_a/2}, \end{aligned}$$

using that $1+a^2 \leq \nu_a \leq a^2+2$ (Lemma 5.1) and $a \geq 1$. For the third term, using that $X \geq a^2 - \nu_a \geq -2$ whenever $X \leq 0$, we have that

$$\begin{aligned} \mathbb{E} \left\{ X^2 \mathbb{1} \left(-\frac{1}{\lambda} \leq X \leq 0 \right) \right\} &\leq \mathbb{E} \left\{ 2^2 \mathbb{1} \left(-\frac{1}{\lambda} \leq X \leq 0 \right) \right\} \\ &\leq 4 \mathbb{E} \left\{ \mathbb{1}(|Z| \geq a) \right\} \\ &\leq 8 e^{-a^2/2} / (2\pi a^2)^{1/2} \\ &\leq 8 e^{-a^2/2} / (2\pi)^{1/2}, \end{aligned}$$

where we in the penultimate step used the standard bound $\mathbb{P}(Z > a) \leq e^{-a^2/2}/(2\pi a^2)^{1/2}$ for all $a > 0$. For the last term, as $\lambda \leq 1/2$, we have that $\mathbb{P}(X < -\frac{1}{\lambda}) \leq \mathbb{P}(X < -2) = 0$, because $X \geq a^2 - \nu_a \geq -2$. Therefore, $\mathbb{E}\{e^{-\lambda X} \mathbb{1}(X < -1/\lambda)\} = 0$. Hence,

$$\begin{aligned} \mathbb{E}\left(e^{-\lambda X}\right) &\leq 1 + \lambda^2 \left\{ \frac{8}{(2\pi)^{1/2}} + \frac{16e^{-\frac{1}{2}}}{2\sqrt{\pi}} \right\} e^{-a^2/2} \\ &\leq 1 + 6\lambda^2 e^{-a^2/2} \\ &\leq \exp\left(6\lambda^2 e^{-a^2/2}\right). \end{aligned}$$

By a Chernoff Bound we obtain that, for any $t > 0$,

$$\begin{aligned} \mathbb{P}\left\{\sum_{i=1}^n (Z_i^2 - \nu_a) \mathbb{1}(|Z_i| \geq a) < -t\right\} &= \mathbb{P}\left\{-\sum_{i=1}^n (Z_i^2 - \nu_a) \mathbb{1}(|Z_i| \geq a) > t\right\} \\ &\leq \inf_{0 < \lambda \leq \frac{1}{2}} e^{-\lambda t} \left\{\mathbb{E}\left(e^{-\lambda X}\right)\right\}^p \\ &\leq \inf_{0 < \lambda \leq \frac{1}{2}} \exp\left(-\lambda t + 6\lambda^2 p e^{-a^2/2}\right) \\ &\leq \exp\left\{-\left(\frac{t^2 e^{a^2/2}}{24p} \wedge \frac{t}{4}\right)\right\}. \end{aligned}$$

Now take $t = 5 \left\{ \left(p e^{-a^2/2} x \right)^{1/2} + x \right\}$ to obtain the result. \square

The following Lemma is due to Birgé (2001).

Lemma 5.4 (Birgé 2001, Lemma 8.1). *Let $Y \sim \chi_p^2(\Psi)$ have a non-central Chi Square distribution with p degrees of freedom and non-centrality parameter $\Psi \geq 0$. Then, for any $x > 0$, we have that*

$$\mathbb{P}\left[Y \geq p + \Psi + 2\{x(p + 2\Psi)\}^{1/2} + 2x\right] \leq e^{-x},$$

and,

$$\mathbb{P}\left[Y \leq p + \Psi - 2\{x(p + 2\Psi)\}^{1/2}\right] \leq e^{-x},$$

Lemma 5.5. *Consider the model from Section 2, with one and only one changepoint η , and suppose $n \geq 3$ and $\sigma = 1$. Let $\mathcal{K} = \{i : \mu_{i,\eta+1} - \mu_{i,\eta} \neq 0\}$ denote the set of coordinates for which there is a change in mean, let $r(t)$ be defined as in (8), and let $h(t)$ be defined as in (10). Let the CUSUM transformation $T_{(s,e)}^v(\cdot)$ be defined as in (2), and for ease of notation, let $T^v(\cdot) = T_{(0,n]}^v(\cdot)$. Let $k =$*

$\|\mu_{\eta+1} - \mu_\eta\|_0$, and define $\beta_v = \sum_{i \in \mathcal{K}} \{T^\eta(\mu_{i,\cdot})^2 - T^v(\mu_{i,\cdot})^2\}$. Define the events

$$\begin{aligned} \mathcal{E}_1 &= \left\{ \forall 0 < v < n, \sum_{i \in \mathcal{K}} \{C^\eta(i)^2 - C^v(i)^2\} \geq \beta_v - 2(2\beta_v \log n)^{1/2} - 16r(k) \right\}, \\ \mathcal{E}_2 &= \left\{ \forall 0 < v < n, \forall t \in \mathcal{T}, \sum_{i \in [p] \setminus \mathcal{K}} \{C^v(i)^2 - \nu_{a(t)}\} \mathbb{1}\{|C^v(i)| > a(t)\} \leq 63r(t) \right\} \\ \mathcal{E}_3 &= \left\{ \forall 0 < v < n, \forall t \in \mathcal{T}, \sum_{i \in [p] \setminus \mathcal{K}} \{C^v(i)^2 - \nu_{a(t)}\} \mathbb{1}\{|C^v(i)| > a(t)\} \geq -35r(t) \right\} \\ \mathcal{E}_4 &= \left\{ \forall 0 < v < n, \forall t \in \mathcal{T}, t < (p \log n)^{1/2}; \right. \\ &\quad \left. \sum_{i=1}^p [\{C^v(i)^2 - \nu_{a(t)}\} \mathbb{1}\{|C^v(i)| > a(t)\} - C^v(i)^2 + 1] \leq 5h(p) + 63r(t) \right\} \end{aligned}$$

Then $\mathbb{P}(\mathcal{E}_1 \cap \mathcal{E}_2 \cap \mathcal{E}_3 \cap \mathcal{E}_4) \geq 1 - \frac{1}{n}$.

Proof. By a union bound it suffices to consider each event separately.

Step 1. We first show that $\mathbb{P}(\mathcal{E}_1^c) \leq \frac{1}{3n}$. As the CUSUM is a linear operation and $X = \mu + W$, we have for any $0 < v < n$ and $i \in [p]$ that $C^v(i) = T^v(\mu_{i,\cdot}) + T^v(W_{i,\cdot})$. Hence, for any v , we have that

$$\begin{aligned} \sum_{i \in \mathcal{K}} \{C^\eta(i)^2 - C^v(i)^2\} &= \beta_v + \sum_{i \in \mathcal{K}} \{T^\eta(W_{i,\cdot})^2 - T^v(W_{i,\cdot})^2\} \\ &\quad + 2 \sum_{i \in \mathcal{K}} \{T^\eta(W_{i,\cdot})T^\eta(\mu_{i,\cdot}) - T^v(W_{i,\cdot})T^v(\mu_{i,\cdot})\}. \end{aligned}$$

We construct high-probability bounds on the two last terms separately. For the first term, note that since $W_{i,j} \stackrel{\text{i.i.d.}}{\sim} \mathcal{N}(0, 1)$, for any fixed v we have $T^v(W_{i,\cdot}) \sim \mathcal{N}(0, 1)$ independently for all $i \in [p]$. Hence $\sum_{i \in \mathcal{K}} T^\eta(W_{i,\cdot})^2 \sim \chi_k^2$ and $\sum_{i \in \mathcal{K}} T^v(W_{i,\cdot})^2 \sim \chi_k^2$. By Lemma 5.4 and a union bound we therefore have that

$$\mathbb{P} \left[\sum_{i \in \mathcal{K}} \{T^\eta(W_{i,\cdot})^2 - T^v(W_{i,\cdot})^2\} \leq -4\{\log(9n^2)k\}^{1/2} - 2\log(9n^2) \right] \leq \frac{2}{9n^2}.$$

Using that $n \geq 3$ and the definition of $r(k)$, we obtain that

$$\mathbb{P} \left[\sum_{i \in \mathcal{K}} \{T^\eta(W_{i,\cdot})^2 - T^v(W_{i,\cdot})^2\} \leq -16r(k) \right] \leq \frac{2}{9n^2}. \quad (16)$$

To see this, consider first the case $k < (p \log n)^{1/2}$. Then $k \leq r(k)$ and $\log n \leq r(k)$, so $4\{\log(9n^2)k\}^{1/2} \leq 4\{4\log(n)k\}^{1/2} \leq 8r(k)$ and $2\log(9n^2) \leq 8\log n \leq 8r(k)$. For the case $k \geq (p \log n)^{1/2}$, we must have that $p \geq \log n$, and hence $4\{\log(9n^2)k\}^{1/2} \leq 8(p \log n)^{1/2} = 8r(k)$ and $2\log(9n^2) \leq 8\log(n) \leq 8(p \log n)^{1/2} = 8r(k)$.

For the second term, we make use of the fact that the CUSUM transformation $T^v(y)$ of any vector y can be expressed as an inner product. More precisely, define the n -dimensional vector $\Psi^v \in \mathbb{R}^n$ to have l th element given by

$$\Psi^v(l) = \begin{cases} \left(\frac{n-v}{nv}\right)^{1/2} & \text{for } l = 1, \dots, v, \\ -\left(\frac{v}{n(n-v)}\right)^{1/2} & \text{for } l = v+1, \dots, n. \end{cases}$$

Then for any vector $y \in \mathbb{R}^n$, we have that

$$T^v(y) = \langle y, \Psi^v \rangle,$$

see Baranowski et al. (2019). Hence, for any $i \in \mathcal{K}$,

$$\begin{aligned} T^\eta(\mu_{\cdot,i})T^\eta(W_{\cdot,i}) - T^v(\mu_{\cdot,i})T^v(W_{\cdot,i}) &= \langle \mu_{\cdot,i}, \Psi^\eta \rangle \langle W_{\cdot,i}, \Psi^\eta \rangle - \langle \mu_{\cdot,i}, \Psi^v \rangle \langle W_{\cdot,i}, \Psi^v \rangle \\ &= \langle W_{\cdot,i}, \langle \mu_{\cdot,i}, \Psi^\eta \rangle \Psi^\eta \rangle - \langle W_{\cdot,i}, \langle \mu_{\cdot,i}, \Psi^v \rangle \Psi^v \rangle \\ &= \langle W_{\cdot,i}, \langle \mu_{\cdot,i}, \Psi^\eta \rangle \Psi^\eta - \langle \mu_{\cdot,i}, \Psi^v \rangle \Psi^v \rangle. \end{aligned}$$

As $W_{\cdot,i} \stackrel{\text{i.i.d.}}{\sim} \mathbf{N}_n(0, I)$ for all $i \in \mathcal{K}$, we get that

$$T^\eta(\mu_{\cdot,i})T^\eta(W_{\cdot,i}) - T^v(\mu_{\cdot,i})T^v(W_{\cdot,i}) \stackrel{\text{i.i.d.}}{\sim} \mathbf{N}\left(0, \|\langle \mu_{\cdot,i}, \Psi^\eta \rangle \Psi^\eta - \langle \mu_{\cdot,i}, \Psi^v \rangle \Psi^v\|_2^2\right),$$

for $i \in \mathcal{K}$. By Lemma 5.11, we have that $\|\langle \mu_{\cdot,i}, \Psi^\eta \rangle \Psi^\eta - \langle \mu_{\cdot,i}, \Psi^v \rangle \Psi^v\|_2^2 = T^\eta(\mu_{\cdot,i})^2 - T^v(\mu_{\cdot,i})^2$. We therefore have that

$$\sum_{i \in \mathcal{K}} \{T^\eta(X_{i,\cdot})T^\eta(\mu_{i,\cdot}) - T^v(X_{i,\cdot})T^v(\mu_{i,\cdot})\} \sim \mathbf{N}(0, \beta_v).$$

By the standard Gaussian tail bound $\mathbb{P}(Z > t) \leq e^{-t^2/2}$ for $Z \sim \mathbf{N}(0, 1)$ and $t > 0$, we obtain

$$\mathbb{P}\left[\sum_{i \in \mathcal{K}} \{T^\eta(X_{i,\cdot})T^\eta(\mu_{i,\cdot}) - T^v(X_{i,\cdot})T^v(\mu_{i,\cdot})\} < -2(2\beta_v \log n)^{1/2}\right] \leq \frac{1}{9n^2}, \quad (17)$$

again using that $n \geq 3$. Combining (16) and (17) by a union bound, we have for any $0 < v < n$ that

$$\mathbb{P}\left[\sum_{i \in \mathcal{K}} \{C^\eta(i)^2 - C^v(i)^2\} \geq \beta_v - 2(2\beta_v \log n)^{1/2} - 16r(k)\right] \leq \frac{1}{3n^2}.$$

By another union bound (over v), we obtain that $\mathbb{P}(\mathcal{E}_1^c) \leq \frac{1}{3n}$.

Step 2. We now show that $\mathbb{P}(\mathcal{E}_2^c) \leq 1/6n$. Fix $0 < v < n$ and any $t \in \mathcal{T}$ such that $t \leq (p \log n)^{1/2}$. Fix $x_t > 0$, to be determined later. As $C^v(i) \stackrel{\text{i.i.d.}}{\sim} \mathbf{N}(0, 1)$ for all $i \in \mathcal{K}^c$, we have by Lemma 5.2 that

$$\sum_{i \in \mathcal{K}^c} \{C^v(i)^2 - \nu_{a(t)}\} \mathbb{1}\{|C^v(i)| > a(t)\} \leq 9 \left[\left\{ p e^{-a(t)^2/2} x_t \right\}^{1/2} + x_t \right] \quad (18)$$

with probability at least $1 - e^{-x_t}$. By a union bound, (18) holds for all $0 < v < n$ and $t \in \mathcal{T}$ such that $t \leq (p \log n)^{1/2}$, with probability at least $1 - n \sum_{t \in \mathcal{T} \setminus \{p\}} e^{-x_t}$. Now set $x_t = 6 \{p \log^2(n)/t^2 \wedge r(t)\}$. Then

$$\sum_{t \in \mathcal{T} \setminus \{p\}} e^{-x_t} \leq \sum_{t \in \mathcal{T} \setminus \{p\}} \exp\left\{-6 \frac{p \log^2(n)}{t^2}\right\} + \sum_{t \in \mathcal{T} \setminus \{p\}} \exp\{-6r(t)\}.$$

For the first sum, we have

$$\begin{aligned}
\sum_{t \in \mathcal{T} \setminus \{p\}} \exp \left\{ -6 \frac{p \log^2(n)}{t^2} \right\} &\leq \sum_{k=0}^{\infty} \exp \left\{ -6 \log(n) 4^k \right\} \\
&= \sum_{k=0}^{\infty} \left(\frac{1}{n^6} \right)^{4^k} \\
&\leq \frac{1}{n^6} + \frac{1}{n^6} \sum_{k=1}^{\infty} \left(\frac{1}{n^6} \right)^{3k} \\
&= \frac{1}{n^6} \left(1 + \frac{1}{n^{18} - 1} \right).
\end{aligned}$$

For the second sum, noting that $6r(t) = 6 \{t \log(ep \log n/t^2) \vee \log n\} \geq 3t \log(ep \log n/t^2) + 3 \log n$, we have

$$\begin{aligned}
\sum_{t \in \mathcal{T} \setminus \{p\}} \exp \{-6r(t)\} &\leq \frac{1}{n^3} \sum_{t \in \mathcal{T} \setminus \{p\}} \left(\frac{t^2}{ep \log n} \right)^{3t} \\
&\leq \frac{1}{n^3 e^3} \left(1 + \sum_{k=1}^{\infty} 4^{-3k} \right).
\end{aligned}$$

With our choice of x_t , using that $a^2(t) = 4 \log(ep \log n/t^2)$, we have that

$$\begin{aligned}
9 \left[\left\{ p e^{-a^2(t)/2} x_t \right\}^{1/2} + x_t \right] &= 9 \left[\left\{ p \frac{t^4}{e^2 p^2 \log^2 n} x_t \right\}^{1/2} + x_t \right] \\
&\leq 9 \left\{ \frac{t \sqrt{6}}{e} + 6r(t) \right\} \\
&\leq 63r(t),
\end{aligned}$$

where we used that $x_t \leq 6r(t)$ and $x_t \leq 6p \log^2(n)/t^2$, as well as the fact that $t \leq r(t)$ whenever $t \leq (p \log n)^{1/2}$. Hence, using that $n \geq 3$,

$$\begin{aligned}
&\mathbb{P} \left[\exists 0 < v < n, \exists t \in \mathcal{T}, t \leq (p \log n)^{1/2}; \sum_{i \in \mathcal{K}^c} \{C^v(i)^2 - \nu_{a(t)}\} \mathbb{1}\{|C^v(i)| > a(t)\} > 63r(t) \right] \\
&\leq \frac{1}{n^6} \left(1 + \frac{1}{n^{18} - 1} \right) + \frac{1}{n^3 e^3} \left(1 + \sum_{k=1}^{\infty} 4^{-3k} \right) \\
&\leq \frac{1}{18n^2}.
\end{aligned} \tag{19}$$

Now consider the case where $t = p$. If $p \leq (p \log n)^{1/2}$, then $a(p) > 0$ and similarly as above we have that

$$\begin{aligned}
&\mathbb{P} \left[\exists 0 < v < n, ; \sum_{i \in \mathcal{K}^c} \{C^v(i)^2 - \nu_{a(p)}\} \mathbb{1}\{|C^v(i)| > a(p)\} > 63r(p) \right] \\
&\leq \frac{1}{18n^2}.
\end{aligned} \tag{20}$$

If we instead have $p > (p \log n)^{1/2}$, in which case $a(p) = 0$ and $\nu_{a(p)} = 1$, then for any $0 < v < n$, we have

$$\sum_{i \in \mathcal{K}^c} \{C^v(i)^2 - \nu_{c(p)}\} \mathbb{1}\{|C^v(i)| > c(p)\} = \sum_{i \in \mathcal{K}^c} \{C^v(i)^2\} - p + k.$$

As $\sum_{i \in \mathcal{K}^c} C^v(i)^2 \sim \chi_{p-k}^2$, we obtain from Lemma 5.4 that

$$\sum_{i \in \mathcal{K}^c} \{C^v(i)^2\} - p + k > 2 \{p \log(12n^2)\}^{1/2} + 2 \log(12n^2),$$

with probability at most $1/(12n^2)$. Using that $n \geq 3$ and $r(p) \geq \log n$, we obtain by a union bound that

$$\mathbb{P} \left[\exists 0 < v < n ; \sum_{i \in \mathcal{K}^c} \{C^v(i)^2 - \nu_{c(p)}\} \mathbb{1}\{|C^v(i)| > c(p)\} > 15r(t) \right] \leq \frac{1}{12n}, \quad (21)$$

Combining (19), (20) and (21) by a union bound, we have that $\mathbb{P}(\mathcal{E}_2^c) \leq 1/(6n)$.

Step 3. We show that $\mathbb{P}(\mathcal{E}_3^c) \leq 1/6n$. Fix $0 < v < n$ and any $t \in \mathcal{T}$ such that $t \leq (p \log n)^{1/2}$. Fix $x_t > 0$, to be determined later. As $C^v(i) \stackrel{\text{i.i.d.}}{\sim} \mathcal{N}(0, 1)$ for all $i \in \mathcal{K}^c$, we have by Lemma 5.3 that

$$\sum_{i \in \mathcal{K}^c} \{C^v(i)^2 - \nu_{a(t)}\} \mathbb{1}\{|C^v(i)| > a(t)\} \geq -5 \left[\left\{ p e^{-a(t)^2/2} x_t \right\}^{1/2} + x_t \right] \quad (22)$$

with probability at least $1 - e^{-x_t}$. By a union bound, (22) holds for all $0 < v < n$ and $t \in \mathcal{T}$ such that $t \leq (p \log n)^{1/2}$, with probability at least $1 - n \sum_{t \in \mathcal{T} \setminus \{p\}} e^{-x_t}$. Now set $x_t = 6 \{p \log^2(n)/t^2 \wedge r(t)\}$. Similar to Step 2, we obtain that

$$\begin{aligned} & \mathbb{P} \left[\exists 0 < v < n, \exists t \in \mathcal{T}, t \leq (p \log n)^{1/2} ; \sum_{i \in \mathcal{K}^c} \{C^v(i)^2 - \nu_{a(t)}\} \mathbb{1}\{|C^v(i)| > a(t)\} < -35r(t) \right] \\ & \leq \frac{1}{18n^2}. \end{aligned}$$

Also similar to Step 2, we have that

$$\begin{aligned} & \mathbb{P} \left[\exists 0 < v < n ; \sum_{i \in \mathcal{K}^c} \{C^v(i)^2 - \nu_{a(p)}\} \mathbb{1}\{|C^v(i)| > a(p)\} < -35r(p) \right] \\ & \leq \frac{1}{12n^2}. \end{aligned}$$

It then follows that $\mathbb{P}(\mathcal{E}_3^c) \leq 1/(6n)$ by a union bound.

Step 4. Lastly we show that $\mathbb{P}(\mathcal{E}_4^c) \leq 1/(3n)$. Fix any $0 < v < n$ and $t \in \mathcal{T}$ such that $t < (p \log n)^{1/2}$. By Lemma 5.8 and Theorem 1.A.3(b) in Shaked and Shanthikumar (2007), we have that

$$\begin{aligned} & \sum_{i=1}^p [\{C^v(i)^2 - \nu_{a(t)}\} \mathbb{1}\{|C^v(i)| > a(t)\} - C^v(i)^2 + 1] \\ & \leq_{\text{st}} \sum_{i=i}^p [\{Y_i^2 - \nu_{a(t)}\} \mathbb{1}\{|Y_i| > a(t)\} - Y_i^2 + 1], \end{aligned}$$

where $Y_i \stackrel{\text{i.i.d.}}{\sim} \mathcal{N}(0, 1)$ for $i \in [p]$. Hence,

$$\begin{aligned} \mathbb{P}(\mathcal{E}_4^c) &\leq \sum_{0 < v < n} \sum_{t \in \mathcal{T} \setminus \{p\}} \mathbb{P} \left[\sum_{i=1}^p \{Y_i^2 - \nu_{a(t)}\} \mathbb{1}\{|Y_i| > a(t)\} \geq 63r(t) \right] \\ &\quad + \sum_{0 < v < n} \sum_{t \in \mathcal{T} \setminus \{p\}} \mathbb{P} \left\{ \sum_{i=1}^p \{Y_i^2 - 1\} \leq -5h(p) \right\} \\ &\leq \frac{1}{18n} + n \log_2(p) \mathbb{P} \left\{ \sum_{i=1}^p (Y_i^2 - 1) \leq -5h(p) \right\}, \end{aligned}$$

where we for the first sum used the same arguments as in Step 2. For the second sum, we have by Lemma 5.4 that

$$\mathbb{P} \left[\sum_{i=1}^p (Y_i^2 - 1) \leq -2p^{1/2} \{\log(6n^2) + \log \log_2 p\}^{1/2} \right] \leq \frac{1}{6n^2 \log_2 p}.$$

Now,

$$\begin{aligned} 2p^{1/2} \{\log(6n^2) + \log \log_2 p\}^{1/2} &\leq 2[6 \{\log n \vee \log \log(ep)\}]^{1/2} \\ &\leq 5h(p). \end{aligned}$$

Hence $\mathbb{P}(\mathcal{E}_4^c) \leq 1/(18n) + 1/(6n) \leq 1/(3n)$, and the proof is complete. \square

The following Lemma gives high-probability control over the score statistic $S_{\gamma, (s, e]}^v$ used as a test statistic.

Lemma 5.6. *Consider the model from Section 2, and assume $\sigma = 1$. Let $r(t)$ be defined as in (8). For any integer v such that $s < v < e$, let $T_{(s, e]}^b(\cdot)$ be defined as in (2), and define*

$$\beta_{(s, e]}^v = \sum_{i=1}^p T_{(s, e]}^v(\mu_{i, \cdot})^2,$$

and

$$k_{(s, e]} = \sum_{i=1}^p \mathbb{1} \left\{ T_{(s, e]}^v(\mu_{i, \cdot})^2 = 0 \right\}.$$

Note that if $\beta_{(s, e]}^v = 0$ for some v , then the open integer interval (s, e) contains no changepoint. Define the events

$$\begin{aligned} \mathcal{E}_5 &:= \left\{ \forall 0 \leq s < v < e \leq n, \beta_{(s, e]}^v = 0; S_{\gamma, (s, e]}^v < 0 \right\}, \\ \mathcal{E}_6 &:= \left\{ \forall 0 \leq s < v < e \leq n; S_{\gamma, (s, e]}^v \geq \beta_{(s, e]} - 8 \left\{ 2\beta_{(s, e]}^v r(k_{(s, e]}) \right\}^{1/2} - (\gamma + 106) r(k_{(s, e]}) \right\}. \end{aligned}$$

If $\gamma \geq 82$, then $\mathbb{P}(\mathcal{E}_5 \cap \mathcal{E}_6) \geq 1 - 1/n$.

Proof.

Step 1. We first show that $\mathbb{P}(\mathcal{E}_5^c) \leq 1/(2n)$. Consider any integer triple of s, e, v such that $0 \leq s < v < e \leq n$ and $\beta_{(s, e]}^v = 0$. Fix any $t \in \mathcal{T} \setminus \{p\}$ (the case $t = p$ is handled later), and fix $x_t > 0$,

to be specified later. As $\beta_{(s,e]}^v = 0$, the open integer interval (s, e) contains no changepoint, and thus $C_{(s,e]}^v(i) \stackrel{\text{i.i.d.}}{\sim} \mathbf{N}(0, 1)$ for all $i \in [p]$. By Lemma 5.2 we have that

$$\sum_{i=1}^p \left\{ C_{(s,e]}^v(i)^2 - \nu_{a(t)} \right\} \mathbb{1} \left\{ \left| C_{(s,e]}^v(i) \right| > a(t) \right\} \geq 9 \left[\left\{ p e^{-a(t)^2/2} x_t \right\}^{1/2} + x_t \right] \quad (23)$$

occurs with probability at most e^{-x_t} . Note that there are at most n^3 unique choices of the triple (s, e, v) . By a union bound, (23) holds for some $0 \leq s < v < e \leq n$ and some $t \in \mathcal{T} \setminus \{p\}$ with probability at most $n^3 \sum_{t \in \mathcal{T} \setminus \{p\}} e^{-x_t}$. Now set $x_t = 8 \left\{ \frac{p \log^2(n)}{t^2} \wedge r(t) \right\}$ for all t . Then,

$$\sum_{t \in \mathcal{T} \setminus \{p\}} e^{-x_t} \leq \sum_{t \in \mathcal{T} \setminus \{p\}} \exp \left\{ -8 \frac{p \log^2(n)}{t^2} \right\} + \sum_{t \in \mathcal{T} \setminus \{p\}} \exp \{-8r(t)\}.$$

For the first sum, we have

$$\begin{aligned} \sum_{t \in \mathcal{T} \setminus \{p\}} \exp \left\{ -8 \frac{p \log^2(n)}{t^2} \right\} &\leq \sum_{k=0}^{\infty} \exp \left\{ -8 \log(n) 4^k \right\} \\ &= \sum_{k=0}^{\infty} \left(\frac{1}{n^8} \right)^{4^k} \\ &\leq \frac{1}{n^8} + \frac{1}{n^8} \sum_{k=1}^{\infty} \left(\frac{1}{n^8} \right)^{3k} \\ &= \frac{1}{n^8} \left(1 + \frac{1}{n^{24} - 1} \right). \end{aligned}$$

For the second sum, noting that $8r(t) = 8 \left\{ t \log \left(\frac{ep \log n}{t^2} \right) \vee \log n \right\} \geq 4t \log \left(\frac{ep \log n}{t^2} \right) + 4 \log n$, we have

$$\begin{aligned} \sum_{t \in \mathcal{T} \setminus \{p\}} \exp \{-8r(t)\} &\leq \frac{1}{n^4} \sum_{t \in \mathcal{T} \setminus \{p\}} \left(\frac{t^2}{ep \log n} \right)^{4t} \\ &\leq \frac{1}{n^4 e^4} \left(1 + \sum_{k=1}^{\infty} 4^{-4k} \right). \end{aligned}$$

Hence, using that $n \geq 2$,

$$\begin{aligned} n^3 \sum_{t \in \mathcal{T} \setminus \{p\}} e^{-x_t} &\leq \frac{1}{n^5} \left(1 + \frac{1}{n^{24} - 1} \right) + \frac{1}{n e^4} \left(1 + \sum_{k=1}^{\infty} 4^{-4k} \right) \\ &\leq \frac{1}{10n}. \end{aligned}$$

With this choice of x_t , using that $a^2(t) = 4 \log \left(\frac{ep \log n}{t^2} \right)$, we have that

$$\begin{aligned} 9 \left[\left\{ p e^{-c^2(t)/2} x_t \right\}^{1/2} + x_t \right] &= 9 \left[\left\{ p \frac{t^4}{e^2 p^2 \log^2 n} x_t \right\}^{1/2} + x_t \right] \\ &\leq 9 \left\{ \frac{t \sqrt{8}}{e} + 8r(t) \right\} \\ &\leq 82r(t), \end{aligned}$$

where we used that $x_t \leq 8r(t)$ and $x_t \leq 8p \log^2(n)/t^2$, as well as the fact that $t \leq r(t)$ whenever $t \leq (p \log n)^{1/2}$. Hence,

$$\begin{aligned} & \mathbb{P} \left[\exists 0 \leq s < v < e \leq n, \exists t \in \mathcal{T} \setminus \{p\}; \sum_{i=1}^p \left\{ C_{(s,e]}^v(i)^2 - \nu_{a(t)} \right\} \mathbb{1} \left\{ |C_{(s,e]}^v(i)| > a(t) \right\} \geq 82r(t) \right] \\ & \leq \frac{1}{10n}. \end{aligned} \quad (24)$$

Now consider the case where $t = p$. If $p \leq (p \log n)^{1/2}$, then similarly as above we have that

$$\begin{aligned} & \mathbb{P} \left[\exists 0 \leq s < v < e \leq n, ; \sum_{i=1}^p \left\{ C_{(s,e]}^v(i)^2 - \nu_{a(p)} \right\} \mathbb{1} \left\{ |C_{(s,e]}^v(i)| > a(p) \right\} \geq 82r(p) \right] \\ & \leq \frac{1}{10n}. \end{aligned} \quad (25)$$

If we instead have $p > (p \log n)^{1/2}$ (in which case $a(p) = 0$ and $\nu_{a(p)} = 1$), then for any $0 \leq s < v < e \leq n$, we have

$$\sum_{i=1}^p \left\{ C_{(s,e]}^v(i)^2 - \nu_{c(p)} \right\} \mathbb{1} \left\{ |C_{(s,e]}^v(i)| > c(p) \right\} = \sum_{i=1}^p C_{(s,e]}^v(i)^2 - p.$$

As $\sum_{i=1}^p C_{(s,e]}^v(i)^2 \sim \chi_p^2$, we obtain from Lemma 5.4 that

$$\sum_{i=1}^p \left\{ C_{(s,e]}^v(i)^2 \right\} - p \geq 2 \left\{ p \log(4n^4) \right\}^{1/2} + 2 \log(4n^4),$$

occurs with probability at most $1/(4n^4)$. Using that $n \geq 2$ and $r(p) \geq \log n$, we obtain by a union bound that

$$\begin{aligned} & \mathbb{P} \left[\exists 0 \leq s < v < e \leq n; \sum_{i=1}^p \left\{ C_{(s,e]}^v(i)^2 - \nu_{c(p)} \right\} \mathbb{1} \left\{ |C_{(s,e]}^v(i)| > c(p) \right\} \geq 17r(t) \right] \\ & \leq \frac{1}{4n}, \end{aligned} \quad (26)$$

Combining (24), (25) and (26) by a union bound, and using that $\gamma \geq 82$, we get that $\mathbb{P}(\mathcal{E}_5^c) \leq 1/(2n)$.

Step 2. Now we show that $\mathbb{P}(\mathcal{E}_6^c) \leq 1/(2n)$. Consider any $0 \leq s < v < e \leq n$. Without loss of generality, assume that $T_{(s,e]}^v(\mu_{1,\cdot})^2 \geq T_{(s,e]}^v(\mu_{2,\cdot})^2 \geq \dots \geq T_{(s,e]}^v(\mu_{p,\cdot})^2$. Let z denote the smallest integer in \mathcal{T} no smaller than $k_{(s,e]}$, where we suppress the dependence of z on s, e in the notation. For $z \leq (p \log n)^{1/2}$, observe that

$$\begin{aligned} & \sum_{i=1}^p \left\{ C_{(s,e]}^v(i)^2 - \nu_{a(z)} \right\} \mathbb{1} \left\{ |C_{(s,e]}^v(i)| > a(z) \right\} \\ & \geq \sum_{i=1}^{k_{(s,e]}} \left\{ C_{(s,e]}^v(i)^2 - \nu_{a(z)} \right\} + \sum_{i=k_{(s,e]}+1}^p \left\{ C_{(s,e]}^v(i)^2 - \nu_{a(z)} \right\} \mathbb{1} \left\{ |C_{(s,e]}^v(i)| > a(z) \right\}. \end{aligned} \quad (27)$$

We lower bound the two sums separately. For each $i \in [p]$ we have that $C_{(s,e]}^v = T_{(s,e]}^v(\mu_{i,\cdot}) + T_{(s,e]}^v(W_{i,\cdot}) \stackrel{\text{ind}}{\sim} N(T_{(s,e]}^v(\mu_{i,\cdot}), 1)$. Let $x_t = 8 \{p \log^2(n)/t^2 \wedge r(t)\}$ for all $t \in [p]$, as in Step 1.

For the first sum, noting that $\sum_{i=1}^{k_{(s,e]}} C_{(s,e]}^v(i)^2 \sim \chi_{k_{(s,e]}}^2(\beta_{(s,e]}^v)$ (a non-central Chi Square distribution with $k_{(s,e]}$ degrees of freedom and non-centrality parameter $\beta_{(s,e]}^v$), we have by Lemma 5.4 that

$$\begin{aligned} & \mathbb{P} \left[\sum_{i=1}^{k_{(s,e]}} \left\{ C_{(s,e]}^v(i)^2 - \nu_{a(z)} \right\} < k_{(s,e]} - k_{(s,e]}\nu_{a(z)} + \beta_{(s,e]}^v - 2 \left\{ x_z \left(z + 2\beta_{(s,e]}^v \right) \right\}^{1/2} \right] \\ & \leq e^{-x_z}. \end{aligned}$$

Note that, since $k_{(s,e]} \leq z \leq (p \log n)^{1/2}$, we have $z \leq r(z)$ and $k_{(s,e]} \leq r(k_{(s,e]})$. Moreover, by Lemma 5.1, we have $\nu_{a(z)}^2 \leq 2 + a^2(z) \leq 2 + a^2(k_{(s,e]})$, where we for the last inequality used that $z \geq k_{(s,e]}$ and that $t \mapsto a^2(t)$ is decreasing. Since $z \leq 2k_{(s,e]}$, it also holds that $r(z) \leq 2r(k_{(s,e]})$. Hence,

$$\mathbb{P} \left[\sum_{i=1}^{k_{(s,e]}} \left\{ C_{(s,e]}^v(i)^2 - \nu_{a(z)} \right\} < \beta_{(s,e]}^v - 8 \left\{ 2\beta_{(s,e]}^v r(k_{(s,e]}) \right\} - 14r(k_{(s,e]}) \right] \leq e^{-x_z}.$$

For the second sum, we obtain from Lemma 5.3 that

$$\begin{aligned} & \mathbb{P} \left[\sum_{i=k_{(s,e]}+1}^p \left\{ C_{(s,e]}^v(i)^2 - \nu_{a(z)} \right\} \mathbb{1} \left\{ |C_{(s,e]}^v(i)| > a(z) \right\} \leq -5 \left[\left\{ p e^{-b^2(z)/2} x_z \right\}^{1/2} + x_z \right] \right] \\ & \leq e^{-x_t}. \end{aligned}$$

By the definition of x_z , we have that

$$\begin{aligned} 5 \left[\left\{ p e^{-b^2(z)/2} x_z \right\}^{1/2} + x_z \right] & \leq 46r(z) \\ & \leq 92r(k_{(s,e]}). \end{aligned}$$

By a union bound over the two sums in (27), we have that

$$\begin{aligned} & \sum_{i=1}^p \left\{ C_{(s,e]}^v(i)^2 - \nu_{a(z)} \right\} \mathbb{1} \left\{ |C_{(s,e]}^v(i)| > a(z) \right\} \\ & < \beta_{(s,e]}^v - 8 \left\{ 2\beta_{(s,e]}^v r(k_{(s,e]}) \right\}^{1/2} - 106r(k_{(s,e]}) \end{aligned} \quad (28)$$

occurs with probability at most $2e^{-x_t}$.

Now suppose that $z > (p \log n)^{1/2}$. Then,

$$\sum_{i=1}^p \left\{ C_{(s,e]}^v(i)^2 - \nu_{a(z)} \right\} \mathbb{1} \left\{ |C_{(s,e]}^v(i)| > a(z) \right\} = \sum_{i=1}^p \left\{ C_{(s,e]}^v(i)^2 \right\} - p.$$

Using that $\sum_{i=1}^p C_{(s,e]}^v(i)^2 \sim \chi_p^2(\beta_{(s,e]}^v)$, we have by Lemma 5.4 that

$$\sum_{i=1}^p \left\{ C_{(s,e]}^v(i)^2 \right\} - p < \beta_{(s,e]}^v - 2 \left\{ \log(4n^4)(p + 2\beta_{(s,e]}^v) \right\}^{1/2}$$

occurs with probability at most $1/(4n^4)$. In particular, since $\log n \leq r(t)$ for all t , we have $r(z) = r(\sqrt{(p \log n)}) \leq 2r(k_{(s,e)})$ and $n \geq 2$, this implies that (28) occurs probability at most $1/(4n^4)$ whenever $z \geq (p \log n)^{1/2}$. By a union bound over $0 \leq s < v < e \leq n$, we obtain that

$$\begin{aligned} \mathbb{P}(\mathcal{E}_6^c) &\leq n^3 \left(\frac{1}{4n^4} + 2 \sum_{t \in \mathcal{T} \setminus \{p\}} e^{-xt} \right) \\ &\leq \frac{1}{4n} + \frac{1}{5n} \\ &\leq \frac{1}{2n}, \end{aligned}$$

where we used the same approach as in Step 1 to bound $\sum_{t \in \mathcal{T} \setminus \{p\}} e^{-xt}$. The proof is complete. \square

Lemma 5.7. *Let \mathcal{M} denote the collection of seeded intervals generated by Algorithm 4 with parameters $\alpha \in (1, 2]$ and $K \geq 2$. Then for all real numbers $h > 0$ such that $h \leq n/2$, and all integers η such that $3h/2 \vee 1 \leq \eta \leq n - (3h/2 \vee 1)$, there exists integers $l \geq 1$ and v such that the following holds.*

(P1) $(v - l, v + l] \in \mathcal{M}$;

(P2) $h/2 \leq l \leq h \vee 1$;

(P3) $|v - \eta| \leq l/K \leq l/2$.

In particular, $(v - l, v + l] \subseteq (\eta - (3/2h \vee 1), \eta + (3/2h \vee 1))$.

Proof. Define the recursive sequence $(l_j)_{j \in \mathbb{N}}$ by $l_1 = 1$, and $l_{j+1} = \max\{l_j + 1, \lfloor \alpha l_j \rfloor\}$ for $j \in \mathbb{N}$. Let $H = \max\{j \in \mathbb{N} : l_j \leq n/2\}$. Formally, the set \mathcal{M} of seeded intervals generated by Algorithm 4 is given by

$$\mathcal{S} = \bigcup_{l \in \{l_1, \dots, l_H\}} \mathcal{I}_l,$$

where

$$\begin{aligned} \mathcal{I}_l &= \{(n - 2l, n]\} \cup \bigcup_{i=0}^{\lfloor \frac{n-2l}{s_l} \rfloor} \{(is_l, is_l + 2l]\}, \\ s_l &= \max\left\{1, \left\lfloor \frac{l}{K} \right\rfloor\right\}. \end{aligned}$$

Note that, for any $j \in [H - 1]$, it holds that $l_{j+1}/l_j \leq \max\{2, \alpha\} = 2$. Hence, there must exist an integer $j \in [H]$ such that $h/2 \leq l_j \leq h \vee 1$. Moreover, by the definition of \mathcal{I}_{l_j} , there must exist an integer v such that $|v - \eta| \leq \lfloor l_j/K \rfloor \leq l_j/2$ and $(v - l_j, v + l_j] \in \mathcal{I}_{l_j}$. This proves the first three claims. For the last claim, note that

$$\begin{aligned} v - l_j &= v - \eta + \eta - l_j \\ &\geq -\lfloor l_j/K \rfloor + \eta - l_j \\ &\geq \eta - (3/2h \vee 1). \end{aligned}$$

Similarly, we have that $v + l_j \leq \eta + (3/2h \vee 1)$. \square

Lemma 5.8. Let $Y \sim N(\theta, 1)$, $\theta \in \mathbb{R}$, $a > 0$ and $\nu_a = \mathbb{E}(Y^2 \mid |Y| \geq a)$. Let $A = (Y^2 - \nu_a) \mathbb{1}(|Y| \geq a)$ and $B = Y^2 - 1$. Then $A - B$ is stochastically decreasing in $|\theta|$.

Proof. It is equivalent to show that $B - A$ is stochastically increasing in $|\theta|$. Note first that Y^2 has a Chi Square distribution with non-centrality parameter θ^2 , which is stochastically increasing in $|\theta|$. Further, we have that $B - A = f(Y^2)$, where the function f is given by

$$f(x) = \begin{cases} x - 1, & \text{if } x < a^2 \\ \nu_a - 1, & \text{otherwise.} \end{cases}$$

Since $\nu_a \geq a^2$, f is an increasing function. By Shaked and Shanthikumar (2007, Theorem 1.A.3(a)), $B - A$ must be stochastically increasing in $|\theta|$. \square

Lemma 5.9. Let \mathcal{M} denote the set of candidate intervals generated from Algorithm 4 with fixed input parameters $\alpha > 1$, $K > 1$ and $n \in \mathbb{N}$. Then the number of distinct triples of integers s, e, v such that $(s, e] \in \mathcal{M}$ and $s < v < e$ is of order $\mathcal{O}(n \log n)$.

Proof. Let α and K be given, and define the recursive sequence $(l_j)_{j \in \mathbb{N}}$ by $l_1 = 1$, and $l_{j+1} = \max(l_j + 1, \lfloor \alpha l_j \rfloor)$ for $j \in \mathbb{N}$. Let $H = \sup\{j \in \mathbb{N} : l_j \leq n/2\}$. Formally, the set \mathcal{M} of seeded intervals generated by Algorithm 4 is given by

$$\mathcal{S} = \bigcup_{l \in \{l_1, \dots, l_H\}} \mathcal{I}_l,$$

where

$$\mathcal{I}_l = \{(n - 2l, n]\} \cup \bigcup_{i=0}^{\lfloor \frac{n-2l}{s_l} \rfloor} \{(is_l, is_l + 2l]\},$$

and

$$s_l = \max\left\{1, \left\lfloor \frac{l}{K} \right\rfloor\right\}.$$

For any $(s, e] \in \mathcal{I}_l$, there are precisely $2l - 1 < 2l$ integers v such that $s < e < v$. Hence, the number N of distinct triples of integers s, e, v such that $(s, e] \in \mathcal{M}$ and $s < v < e$ therefore satisfies

$$N < \sum_{l \in \{l_1, \dots, l_H\}} 2l |\mathcal{I}_l|.$$

For all $l < K$, we have that $|\mathcal{I}_l| \leq n$, and so $2l |\mathcal{I}_l| \leq 2ln < 2Kn$. For $l \geq K$ we have that $\lfloor l/K \rfloor \geq l/(2K)$, and so $2l |\mathcal{I}_l| \leq 4Kn$. Therefore,

$$\begin{aligned} N &< \sum_{l \in \{l_1, \dots, l_H\}} 4Kn \\ &= 4HKn. \end{aligned}$$

Noting that $H \leq \lceil \frac{1}{\alpha-1} \rceil + \log_\alpha n$, we thus get

$$\begin{aligned} N &< 4 \left(\lceil \frac{1}{\alpha-1} \rceil + \log_\alpha n \right) Kn \\ &= \mathcal{O}(n \log n), \end{aligned}$$

which gives the desired result. \square

In the following we restate some useful Lemmas from Baranowski et al. (2019).

Lemma 5.10 (Baranowski et al. 2019, Lemma 2).

Consider the model from Section 2, assuming that $p = 1$. Let the CUSUM transformation $T_{(s,e]}^v(\cdot)$ be defined as in (2). Suppose $s < e$ are such that $\eta_{j-1} \leq s < \eta_j < e \leq \eta_{j+1}$ for some $j \in [J]$. Then,

$$\max_{s < v < e} T_{(s,e]}^v(\mu)^2 = T_{(s,e]}^{\eta_j}(\mu)^2 \begin{cases} \geq \frac{1}{2} \delta \theta_j^2 \\ \leq \delta \theta_j^2. \end{cases}$$

Given an $n \in \mathbb{N}$ and any integer $0 < v < n$, define the n -dimensional vector $\Psi^v \in \mathbb{R}^n$ to have l th element given by

$$\Psi^v(l) = \begin{cases} \left(\frac{n-v}{nv}\right)^{1/2}, & \text{for } l = 1, \dots, v, \\ -\left(\frac{v}{n(n-v)}\right)^{1/2}, & \text{for } l = v+1, \dots, n. \end{cases}$$

Lemma 5.11 (Baranowski et al. 2019, Lemma 4). Consider the model from Section 2, assuming that $p = 1$. Let the CUSUM transformation $T_{(s,e]}^v(\cdot)$ be defined as in (2). Pick any interval $(s, e] \subset (0, n]$ such that the open integer interval (s, e) contains precisely one changepoint η_j . Pick any integer v such that $s < v < e$. Define $\rho = |\eta_j - v|$, $\delta_L = \eta_j - s$, and $\delta_R = e - \eta_j$. Then,

$$\left\| \Psi_{(s,e]}^{\eta_j} \langle \mu, \Psi_{(s,e]}^{\eta_j} \rangle - \Psi_{(s,e]}^v \langle \mu, \Psi_{(s,e]}^v \rangle \right\|_2 = T_{(s,e]}^{\eta_j}(\mu)^2 - T_{(s,e]}^v(\mu)^2.$$

Moreover,

- (1) for any $\eta_j \leq v < e$, $T_{(s,e]}^{\eta_j}(\mu)^2 - T_{(s,e]}^v(\mu)^2 = \frac{\rho \delta_L}{\rho + \delta_L} \theta_j^2$;
- (2) for any $s < v \leq \eta_j$, $T_{(s,e]}^{\eta_j}(\mu)^2 - T_{(s,e]}^v(\mu)^2 = \frac{\rho \delta_R}{\rho + \delta_R} \theta_j^2$.